MECHANISMS OF CYTOSKELETAL DYSREGULATION IN THE KIDNEY PROXIMAL TUBULE DURING ATP DEPLETION AND ISCHEMIA

Hao Zhang

Submitted to the faculty of the University Graduate School
in partial fulfillment of the requirements
for the degree
Doctor of Philosophy
in the Department of Biochemistry and Molecular Biology,
Indiana University

August 2009

Accepted by the Faculty of Indiana University, in partial
fulfillment of the requirements for the degree of Doctor of Philosophy.

_____

Simon J. Atkinson Ph.D., Chair

_____

Maureen A. Harrington Ph.D.

Doctoral Committee

_____

April 22, 2009

James A. Marrs Ph.D.

_____

Lawrence A. Quilliam Ph.D.

DEDICATION

I would like to dedicate this dissertation to my dearest parents, Zhang Zhaomei and Peng Sihua. They teach me how to be a respectable person in every aspect of my life. Their teaching helped me to overcome every major obstacle in my life. This dissertation is also dedicated to my dearest brother, Zhang Hong. Without his support and encouragement at every difficult moment in my life, I would not have been able to finish all the hard work for this dissertation and achieve a doctorate degree.

ACKNOWLEDGEMENTS

I would like to thank my academic advisor, Dr. Simon J. Atkinson. His mentoring and his patience with my study and research work will be remembered and cherished for the rest of my life.

I would like to thank the other members of my doctoral committee, Dr. Maureen A. Harrington, Dr. James A. Marrs, Dr. Lawrence A. Quilliam. They gave me all the invaluable advice and support throughout my graduate education.

I would also like to thank the other members of our lab, Nahid Akhtar and Dr. Mark A. Hallett. They gave me so much precious assistance in my research work. Dr. Mark A. Hallett has given me numerous advice on my research work from day to day.

ABSTRACT

Hao Zhang

Mechanisms of Cytoskeletal Dysregulation in the Kidney Proximal Tubule During ATP Depletion and Ischemia

Knowledge of the molecular and cellular mechanisms of ischemic injury is necessary for understanding acute kidney injury and devising optimal treatment regimens. The cortical actin cytoskeleton in the proximal tubule epithelial cells of the kidney nephron, playing an important role in both the establishment and maintenance of cell polarity, is drastically disrupted by the onset of ischemia. We found that in LLC-PK cells (a porcine kidney proximal tubule epithelial cell line), cortactin, an important regulator of actin assembly and organization, translocated from the cell cortex to the cytoplasmic regions upon ischemia/ATP-depletion. Meanwhile both the tyrosine phosphorylation level of cortactin and cortactin's interaction with either F-actin or the actin nucleator Arp2/3 complex were down-regulated upon ischemia/ATP-depletion or inhibition of Src kinase activity. These results suggest that tyrosine phosphorylation plays an important role in regulating cortactin's cellular function and localization in the scenario of kidney ischemia. The Rho GTPase signaling pathways is also a critical mediator of the effects of ATP depletion and ischemia on the actin cytoskeleton, but the mechanism by which ATP depletion leads to altered RhoA and Rac1 activity is unknown. We propose that ischemia and ATP depletion result in activation of AMP-activated protein kinase (AMPK) and that this affects Rho GTPase activity and cytoskeletal organization (possibly via TSC1/2

complex and/or mTOR complex). We found that AMPK was rapidly activated (≤ 5 minutes) by ATP depletion in S3 epithelial cells derived from the proximal tubule in mouse kidney, and there was a corresponding decrease in RhoA and Rac1 activity. During graded ATP-depletion, we found intermediate levels of AMPK activity at the intermediate ATP levels, and that the activity of RhoA and Rac1 activity correlated inversely with the activity of AMPK. Activation of AMPK using two different drugs suppressed RhoA activity, and also led to morphological changes of stress fibers. In addition, the inhibition of AMPK activation partially rescued the disruption of stress fibers caused by ATP-depletion. This evidence supports our hypothesis that the activation of AMPK is upstream of the signaling pathways that eventually lead to RhoA inactivation and cytoskeletal dysregulation during ATP-depletion.

Simon J. Atkinson Ph.D., Chair

TABLE OF CONTENTS

LIST OF FIGURES

LIST OF ABBREVIATIONS

ADP: Adenosine 5’-Diphosphate

AICAR: 5-Aminoimidazole-4-Carboxamide Ribonucleoside

AMP: Adenosine 5’-Monophosphate

AMPK: AMP-activated Protein Kinase

ARI: Acute Renal Injury

ATP: Adenosine 5’-Triphosphate

BSA: Bovine Serum Albumin

DMEM: Dulbecco’s Modified Eagle’s Medium

DMSO: Dimethyl Sulfoxide

ER: Endoplasmic Reticulum

FBS: Fetal Bovine Serum

FITC: Fluorescein Isothiocyanate

GAP: GTPase Activating Protein

GDI: Guanine Nucleotide Dissociation Inhibitor

GDP: Guanosine 5’-Diphosphate

GED: GTPase Effector Domain

GEF: Guanine Nucleotide Exchange Factor

GMP: Guanosine 5’-Monophosphate

GTP: Guanosine 5’-Triphosphate

mTOR: Mammalian Target of Rapamycin

NTA: Amino Terminal Acidic Domain

PBS: Phosphate Buffered Saline

PH: Pleckstrin Homology

PKD: Protein Kinase D

PRD: Proline Rich Domain

SDS: Sodium Dodecyl Sulfate

SDS-PAGE: Sodium Dodecyl Sulfate Polyacrylamide Gel Electrophoresis

TSC: Tuberous Sclerosis Complex

ZMP: 5-Aminoimidazole-4-Carboxamide-1-β-D-Dibofuranosyl 5’-Monophosphate

CHAPTER I

Introduction

Cellular injuries during ischemia

Ischemic acute renal injury (ARI) remains the leading cause of renal failure in adults [1]. Understanding the cellular consequences of ischemic injury is necessary for devising optimal treatment regimens for ARI.

The basic structural and functional unit of the kidney is the nephron. The glomerulus of the nephron delivers a plasma ultra-filtrate to the proximal tubule, which selectively secretes and reabsorbs a variety of substances in the process of making urine. The proximal tubule of the nephron reabsorbs about 60% of the ultrafiltrate delivered from the glomerulus before passing the filtrate on sequentially to the descending limb, loop and ascending limb of Henle, the distal tubule and finally the collecting duct [2]. The proximal tubule epithelium is the most susceptible to low oxygen tension among all the tissues of the nephron. After an ischemic insult, some cells of the proximal tubule epithelium lose polarity, become necrotic or undergo apoptosis. The damaged cells slough-off into the lumen forming an intratubular cast. With recovery, some of the remaining epithelia depolarize, divide, migrate to vacant locations along the tubule and repolarize into functional epithelium [3-6].

The epithelial cells lining the proximal tubule lumen possess highly polarized apical (facing the urinary lumen) and basolateral surface membrane domains that have distinctly different lipid and protein compositions [7]. The main structures of the apical

membrane domain include the terminal web and the brush border, and the brush border can be divided into microvilli. Within each microvillus are 20-30 longitudinally oriented, polarized actin microfilaments that extend into, and are stabilized in the terminal web region by interaction with different proteins. There is a dense meshwork of actin and associated proteins as well as intermediate filaments in the terminal web. These meshwork structures are oriented primarily perpendicular to the microvilli [8, 9].

The proximal tubule has a high rate of endocytic activity at the apical membrane. There are different kinds of receptors enriched at the apical membrane [10-12]. Sodium (Na^+) reabsorption is one of the key functions of the proximal tubule. Such sodium reabsorption is dependent upon both the polarized delivery of specific carrier proteins such as the Na^+ transporter and the Na^+-dependent cotransporter to the apical membrane and the localization of the Na^+, K^+-ATPase to the basolateral membrane [13, 14]. Many receptors on the apical membrane are in a constant process of endocytosis/internalization and/or eventually being recycled back to the apical surface [15, 16]. The actin and microtubule cytoskeleton play critical roles for efficient and accurate targeting and delivery of these receptors in their recycling pathways [10, 17-19]. The basolateral membrane is structurally separated from the apical by junctional complexes which are critical for establishing and maintaining structural and functional cell polarity, as well as for the formation of a protein channel between the adjacent cells for the passage of low molecular weight proteins [13, 20]. The basal portion of the cells is attached to the substratum via hemidesmosomes mediated by integrins. Focal adhesions are also present on the basal surface membrane and help anchoring cells to the substratum [13, 21].

The apical and basolateral membrane polarity is critical for the normal filtration function of the proximal tubule, and the loss of such a membrane polarity is the hallmark

Figure 1. Cellular injuries in proximal tubule epithelia after ischemia

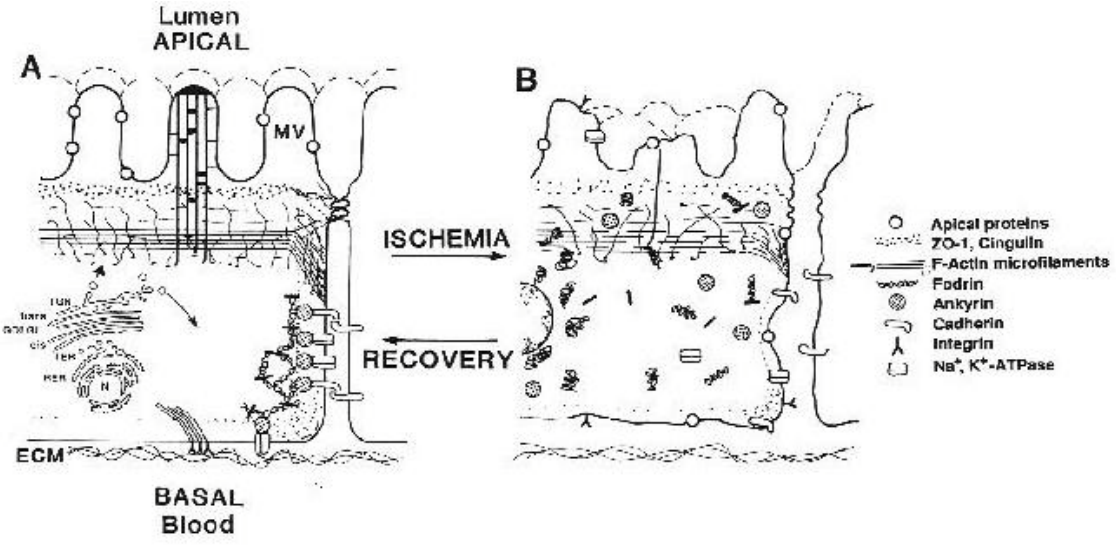

Fig. 1. During ischemia multiple cellular injuries including actin cytoskeleton disruption occur in proximal tubule epithelial cells (see text for details). Adapted from Wagner *et al.* 1999 *Pediatric Nephrology* 13(2):163-170

of cellular injury caused by ischemia [22-24] (Fig. 1). The onset of ischemia rapidly induces distinctive and rapid disruption of microvilli of apical brush border in proximal tubule epithelia, with the extent of such disruptions being dependent on the severity of ischemia [5, 25]. During microvilli disruptions induced by ischemia, the microvillar actin core disassembles [26, 27]. Meanwhile, either concurrently or subsequently, microvillar membranes either internalize into the cell's cytosol or are shed into the tubule lumen as blebs [5]. In parallel with apical membrane structural changes, basolateral membrane changes also occur during ischemia. One example is that many surface

basolateral membrane proteins will be untethered or redistributed, contributing to the loss of cell-substrate and cell-cell adhesion [28-31]. Meanwhile the junctional complexes in proximal tubule epithelial cells are also disrupted by ischemia, which contributes to the loss of cell polarity [32, 33].

The cortical actin cytoskeleton plays a critical role in terms of establishing and maintaining the apical and basolateral membrane polarity, therefore its disruption to a significant extent precedes the membrane changes during ischemia [26, 27, 34]. During kidney ischemia there are two fundamental components of the actin cytoskeletal alterations that are observed; the first is the breakdown of actin filament-containing structures including microvillar actin bundles and stress fibers, with the actin they contain being re-distributed to other regions of the cell [26, 35]; the second is the unregulated polymerization of G-actin (unpolymerized actin monomers) so that the net fraction of F-actin increases with ischemia and ATP depletion and the monomer pool necessary for maintenance of normal dynamic actin structures is depleted [35, 36]. This global dysregulation of the cytoskeleton in the setting of increased F-actin implies a complex effect that not only impinges directly on the biochemistry of actin polymerization, but also affects higher order assembly of actin filaments into structures such as bundles and stress fibers. The most likely explanation for the latter effects is that signaling pathways regulating the actin cytoskeleton are affected by ATP depletion and ischemia, so that the mechanisms that normally integrate actin function become the mediators of its dysregulation instead. Therefore the study of these upstream signaling pathways regulating the actin cytoskeleton is particularly important for us to understand the molecular mechanisms of kidney ischemic injury.

On the other hand, ischemic injury also disrupts the localization of apical and basolateral membrane components, for example the normally basolateral Na^+, K^+-ATPase translocates to the apical membrane, apical leucine aminopeptidase to the basolateral membrane, while ischemia duration-dependent alterations in apical and basolateral membrane lipids also occur [22, 35, 37, 38]. The correct targeting of protein components of the apical and basolateral membranes to surface membrane destinations after synthesis at ER, modification at and transportation from Golgi; as well as their recycling from surface membrane in clathrin-coated vesicles by endocytosis and then recycling back to the original surface membrane domains, or transcytosis to particular surface membrane domains for enrichment; all these processes are very important for establishing and maintaining apical and basolateral membrane polarity, and also important for the proper filtration function of the proximal tubule, therefore they could be disrupted by ischemia too [13, 39, 40]. Investigating the regulation of proteins that play important roles in these processes mentioned above will certainly advance our knowledge of ischemic acute renal failure and consequently assist our search for optimal treatments.

CHAPTER II

Decrease of Cortactin Tyrosine Phosphorylation during ATP-Depletion in a Cell Culture Model of Ischemic Renal Injury and Its Effect on Cortactin's Cellular Function

1. Introduction

Cortactin

Cortactin is an 80/85kDa (both vertebrate and invertebrate cortactin migrate as a doublet separated by 5kDa upon SDS-PAGE) protein expressed in all types of eukaryotic cells. It contributes to the epithelial cell phenotype as an important regulator of actin assembly and organization [41]. Cortactin was initially discovered in *v-Src*-transformed chicken embryo cells as a tyrosine phosphorylation substrate of Src, and it co-localized with F-actin in the peripheral extensions of normal cells and podosomes (rosettes) after *v-Src* transformation [42]. It was later discovered to bind F-actin directly and was enriched in cortical structures such as membrane ruffles and lamellipodia in different adherent cell types [43]. So far cortactin has been discovered to localize to dynamic actin cytoskeleton at multiple cellular locations and to be involved in many kinds of cellular functions. It localizes to growth cones of cultured neurons [44]; it was found to associate with endosomal vesicles in fibroblast cells [45], and its overexpression was found to enhance the motility of fibroblasts [46]; it binds directly and co-localizes with *Drosophila* cell-cell tight junction component ZO-1 [47]; it is recruited to cell-cell adherens junctions in response to homophilic E-cadherin ligation and inhibition of cortactin activity perturbs

both cell morphology and junctional accumulation of cadherin in polarized MDCK epithelial cells [48]. In addition to regulating the actin cytoskeleton, cortactin is also a component of clathrin-coated pits and inhibition of its activity disrupts both clathrin-dependent and clathrin-independent receptor-mediated endocytosis [49-51]; it was also found to localize to the Golgi apparatus and play an important role in post-Golgi transport [52]. On the other hand, cortactin and/or its triggering of actin polymerization were found to be important to the invasion of pathogens in different cell types [53, 54]. Meanwhile the human homologue of cortactin, the EMS1 gene, its amplification and overexpression were found in human carcinomas [55, 56]; overexpression of cortactin was also found to enhance significantly bone metastasis of breast cancer cells [57], and it was also found to be essential for the formation of invadopodia and subsequent extracellular matrix degradation in metastatic cancer cells [58, 59]. Therefore cortactin is also a protein of great interest to oncologists. Finally in immunohistochemistry study cortactin was found to stain the brush border / terminal web region of human kidney [60].

The N-terminal region of cortactin's total length of approximately 90 amino acids is designated the amino terminal acidic domain (NTA) (Fig. 2). It binds directly with Arp2/3 complex, the actin nucleator. Following the NTA domain are six and a half tandem copies of a 37 amino acid repeat. The tandem repeat four is necessary for cortactin to bind F-actin stably [61]. Cortactin binds with both F-actin and Arp2/3 complex by itself or in synergy with other actin nucleation promotion factors, for example N-WASP, and subsequently stimulates Arp2/3 complex's actin nucleation activity which initiates the "branching-out" from the side of existing F-actin filament to build up an actin network [62, 63]. The tandem repeats are followed by an α-helical

domain of approximately 50 amino acids, which is a less well-conserved region rich in proline, serine and threonine residues, and then finally a C-terminal SH3 domain. The SH3 domain of cortactin binds with multiple partners, for example the proline-rich domain of dynamin-II [64]; N-WASP and WASP [65]; WIP (WASP-interacting protein) which is involved in filopodia formation [66].

Figure 2. Cortactin structural domains

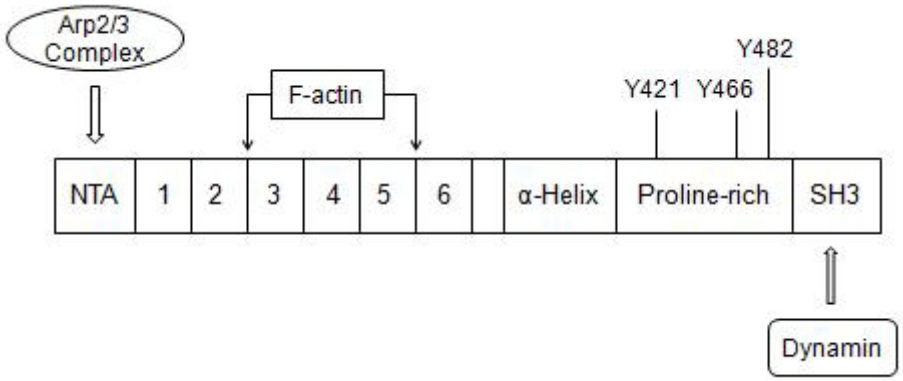

Fig. 2. The structural domains of cortactin and the interactions of cortactin with other proteins at different domains (see text for details).

Cortactin has always been considered as an important regulator of the actin cytoskeleton, and has been found to participate in multiple cellular functions, although our knowledge of regulatory mechanisms controlling its activity and localization is still very incomplete and sometimes even contradictory. One mechanism that is of great interest to investigators is the phosphorylation of cortactin at multiple sites by different kinases including Src. Three tyrosine residues, Tyr-421, 466 and 482, have been identified as the target phosphorylation sites of Src [67]. Cortactin was also reported to

be tyrosine-phosphorylated by Fyn/Fer kinase [68, 69]; meanwhile, Syk, another Src family kinase, also binds with and tyrosine-phosphorylates cortactin in platelets upon thrombopoietin stimulation [70]. Two serine residues (Ser-405, Ser-418) in the proline-rich domain are phosphorylated by Erks *in vitro* and possibly also *in vivo* in HEK 293 cells treated with epidermal growth factor [71]. In addition to the phosphorylation sites mentioned above, 17 new sites were reported recently in a study using mass spectrometry [72]. Most recently cortactin was reported to be an *in vivo* substrate of protein kinase D (PKD) on Ser298 and Ser348, although no effect was found on cortactin's cellular function and localization by PKD phosphorylation on these target sites yet [73].

Extensive studies have been done on tyrosine-phosphorylation of cortactin and its functional consequences, although we still do not know how tyrosine-phosphorylation regulates cortactin's function exactly. It was reported that tyrosine-phosphorylated cortactin is enriched in lamellipodia of fibroblasts [74], and yet cortactin's translocation to the cell periphery does not depend on tyrosine phosphorylation in COS7 cells [75]; tyrosine phosphorylation of cortactin has been shown to be important to migration of endothelial cells [67], while an *in vitro* assay shows that it down-regulates cortactin's actin-filament cross-linking ability [76]; tyrosine phosphorylation terminates cortactin's activation of N-WASP and WASP [65], on the other hand, it was also reported that in the presence of the adaptor protein Nck, the tyrosine phosphorylation of cortactin by Src greatly enhanced Arp2/3 complex-mediated actin polymerization *in vitro*, which was further enhanced by the addition of N-WASP and WIP (WASP-interacting protein) [77]. Phosphorylation of cortactin by Src was found to be important for podosome formation in osteoclasts [78], and is essential for the functional invadopodia formation in fibroblast

cells and human melanoma cells [79, 80]. Cortactin's tyrosine phosphorylation was also reported to be involved in the regulation of endocytosis and ion channels [81-83], and src-mediated phosphorylation of cortactin enhances its association with GTPase dynamin-2 as shown by *in vitro* study. Cortactin's phosphorylation on Tyr421 has been shown to be important to N-cadherin-mediated intercellular adhesion strength [84], and Fer-dependent tyrosine phosphorylation of cortactin promotes N-cadherin's mobility and enhances N-cadherin-mediated intercellular adhesion strength [85]. During ischemia, tight junction integrity is compromised and intercellular adhesion strength is reduced [86], and N-cadherin expression is reduced during ischemia and proteolytic fragments appear [87], but the fate of cortactin during ischemia and with recovery is unknown yet.

Therefore we were interested in determining whether the tyrosine phosphorylation of cortactin changed during kidney ischemia, and whether this change affected cortactin's cellular localization and its interactions with other proteins, and finally how these changes were related to the global actin cytoskeleton dysregulation during kidney ischemia.

Dynamin

The SH-3 domain at the C-terminus of cortactin can bind with the proline-rich domain of multiple partners, one of which is dynamin [64]. Co-localizing with cortactin and/or actin structures at multiple cellular locations *in vivo*, dynamin influences actin nucleation by purified Arp2/3 complex and cortactin *in vitro* in a biphasic manner [49, 52, 64, 88, 89]. Dynamin, a 100kDa GTPase, is an essential component of vesicle formation in receptor-mediated endocytosis, caveolae internalization and also vesicle traffic in and

out of the Golgi [90, 91]. Among the three major isoforms of dynamin, dynamin-II is the only one that is ubiquitously expressed in different mammalian cells [90]. Dynamin was initially discovered and presumed to be a mechanochemical enzyme mediating interaction between microtubules [92]. Since the discovery that the protein encoded by the gene shibire in *Drosophila*, whose mutant impairs vesicular traffic in endocytosis, is dynamin's homologue [93], as well as that the amino acid sequence of dynamin contains a GTP-binding domain [94], one of the major focuses of dynamin research has been its function in endocytosis as a GTPase by acting either like a pinching-force generating molecular motor during GTP hydrolysis or a traditional regulatory GTPase working on downstream effectors (and which mechanism is true is still to be determined).

Dynamin's critical role in endocytosis was confirmed by expressing its mutant with GTP-binding domain being either defective or deleted in different cell lines. The expression of such mutants significantly blocked receptor-mediated endocytosis via clathrin-coated pits [95-97]. Later on, dynamin was found to be involved in multiple aspects of intracellular transport. Dynamin was found to localize on caveolae and its GTPase activity was critical to caveolae-mediated endocytosis in both endothelial and epithelial cells [98, 99]. Dynamin-II (the ubiquitously expressed isoform) is enriched on phagosomes, and overexpression of its GTP-binding defective mutant inhibits particle internalization in macrophages [100]. Dynamin-II was first found to localize on trans-Golgi network in HepG2 cells [101], later on it was found that dynamin antibodies strongly labeled the Golgi complex in cultured fibroblasts and melanocytes [102]; overexpression of dynamin-I GTP-binding defective mutant was found to inhibit endosome to Golgi transport [103], while overexpression of the similar mutant of

dynamin-II disrupted Golgi structure and also inhibited protein secretion from the trans-Golgi to the plasma membrane in epithelial cells [104, 105]. Dynamin is also involved in regulation of the actin cytoskeleton. Dynamin was found to translocate from the cytoplasmic regions to membrane ruffles at the leading edge of fibroblasts upon growth factor stimulation, while overexpression of a dynamin-II mutant, which had the proline-rich domain (which binds to SH3 domain of cortactin) truncated, in Clone 9 rat hepatocyte cells changed the cell shape from being discoid into being peculiarly elongated or moon-shaped [64]; dynamin was also reported to be important for lamellipodia formation and cell spreading [106]. Dynamin was found to localize on and play an important role for the formation of highly dynamic actin-containing adhesion structures, podosomes, in Rous sarcoma virus (RSV)-transformed fibroblasts and osteoclasts [107], while in invasive tumor cells dynamin also localizes in invadopodia and is essential for the degradation of extracellular matrix [108].

The three isoforms of dynamin all share the same domain structure (Fig. 3). The N-terminus of dynamin is the GTP hydrolysis domain followed by a middle domain which lacks sequence homology to any known structural motif [90]. After the middle domain is the PH (Pleckstrin Homology) domain. The PH domain of dynamin favors binding to PI(4,5)P2, which is crucial for dynamin's membrane localization and also enhances its GTPase activity [109]. The PH domain is followed by the GTPase effector domain (GED). GED is the GAP (GTPase activating protein) for dynamin itself. Phospholipase D was identified to be another GAP for dynamin, and phospholipase D's GAP function for dynamin is important for EGFR endocytosis in HEK 293 cells [110].

The C-terminus of dynamin is the PRD (proline-rich domain) which mediates the binding with multiple partners including cortactin.

Figure 3. Dynamin structural domains

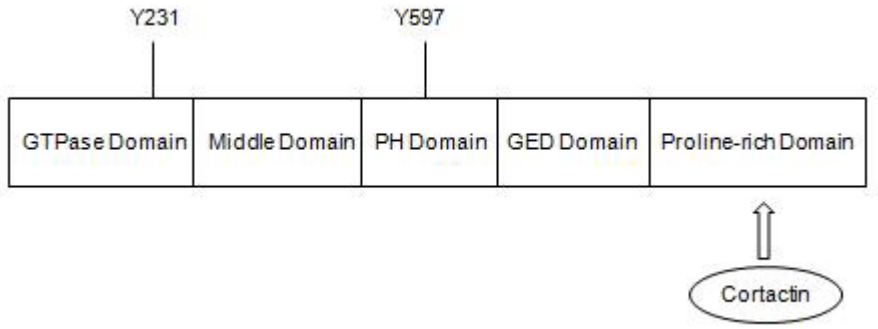

Fig. 3. The structural domains of dynamin and the interaction of dynamin with cortactin (see text for details).

One of dynamin's special features is its self-assembly by oligomerization which significantly stimulates its GTPase activity [111]. Under low salt conditions and without either any underlying support or the presence of any nucleotide, purified recombinant dynamin was found to assemble spontaneously *in vitro* into rings and stacks of interconnected rings, which were comparable in dimension to the "collars" observed at the necks of invaginated coated pits that accumulated at synaptic terminals in shibire flies (which have paralysis associated with the block of endocytosis) [112]; similar rings and spirals of dynamin also formed under physiological salt conditions when beryllium fluoride (or aluminum fluoride) and GDP (or GTPγS) were added into purified recombinant dynamin [113]. Purified recombinant dynamin was also demonstrated to bind to anionic phospholipid bilayers in the absence of other proteins or guanine

nucleotide to form helical tubular structure, and the addition of GTP caused constriction of such dynamin tubules and formation of numerous small vesicles [114]. Meanwhile it has also been demonstrated that strong binding of dynamin PH domain to lipid membranes requires self-assembly of dynamin by oligomerization [115]. GED has been confirmed to be essential for dynamin self-assembly which is critical for GED's GAP activity and therefore GTP hydrolysis by dynamin [116].

Like cortactin, dynamin also directly binds with Src kinase [117]. Src-mediated tyrosine-phosphorylation of dynamin has been found to be important for both receptor-mediated and non-receptor-mediated endocytosis in different cell lines [118-120]. The major tyrosine phosphorylation sites of dynamin by either Src or possibly other kinases *in vivo* have been identified to be Tyr-231 in the GTPase domain and Tyr-597 in PH domain for both dynamin-I and dynamin-II [118, 120]. Tyrosine phosphorylation of dynamin by Src was found to stimulate dynamin-I's GTPase activity significantly and also enhance its self-assembly *in vitro*, while for mutant Y231F/Y597F of dynamin-I, such stimulation and enhancement were significantly repressed [121]. Src-induced tyrosine-phosphorylation of dynamin-II, which plays an important role for caveolae-mediated endocytosis in endothelial cells, has also been shown to promote its translocation from the cytosol to the membrane *in vivo* [120].

Study outline

In this study, our initial observation was that cortactin translocated from the cell cortex to the cytoplasmic region of kidney proximal tubule epithelial cells in an ATP-depletion model of ischemia. This translocation was reversed after the cells were placed

in normal growth medium and allowed to recover. We then studied the tyrosine phosphorylation status of cortactin in both normal growth conditions and ATP-depletion conditions. We found that coincident with ATP-depletion, the tyrosine phosphorylation level of cortactin decreased. Cortactin's binding to F-actin and the actin nucleator Arp2/3 complex was also weakened as indicated by co-immunoprecipitation experiments. In addition we propose that cortactin's direct binding with dynamin-II is important for the localization of cortactin and dynamin-II to target membrane locations, such as the cytoplasmic membrane regions, or the Golgi membranes, in order to exert their proper functions in endocytosis and protein secretion from Golgi. During ischemia, dynamin-II's tyrosine phosphorylation level decreases, the same as cortactin. Tyrosine-dephosphorylation of both cortactin and dynamin-II impairs their binding with each other. Such decrease of tyrosine-phosphorylation and subsequent dissociation between dynamin-II and cortactin down-regulate oligomerization and self-assembly of dynamin-II. As a result of these events, dynamin-II's binding with membrane lipids is disrupted. Consequently both dynamin-II and cortactin translocate from membrane locations to cytosol, which further contributes to the disruption of endocytosis and protein-secretion from Golgi, and consequently to the structural and functional degenerations in kidney proximal tubule epithelial cells experiencing ATP-depletion/ischemia. We studied the possible localization of cortactin at trans-Golgi network in kidney proximal tubule epithelial cells under both normal growth conditions and ischemic conditions. We also studied the tyrosine-phosphorylation status of dynamin-II before and after ATP-depletion, in addition to the possible interaction changes between cortactin and dynamin-II after ATP-depletion.

2. Materials and Methods

Cell culture. LLC-PK1 porcine proximal tubule cells [American Type Culture Collection (ATCC), Manassas, VA] were maintained in 1:1 DMEM/F-12 (SIGMA-Aldrich Corp.) medium containing 10% fetal bovine serum (FBS), 100IU/ml penicillin, 100µg/ml streptomycin at 37ºC in a humidified atmosphere of 5% CO_2. For ATP-depletion, cells were incubated in depleted DMEM (medium without amino acids, glucose, serum, and antibiotics) and 100nM antimycin A (SIGMA-Aldrich Corp.). If recovery of these cells was required, they were rinsed with depleted DMEM and incubated in 1:1 DMEM/F-12 (SIGMA-Aldrich Corp.) medium containing 10% FBS, 100IU/ml penicillin, and 100µg/ml streptomycin. For Src kinase inhibition, cells were incubated for 45 minutes in 1:1 DMEM/F-12 (SIGMA-Aldrich Corp.) medium containing 10% FBS, 100IU/ml penicillin, 100µg/ml streptomycin, supplemented with 50µM Src kinase inhibitor PP2 (10mM solution in DMSO, Calbiochem) (or 0.5% DMSO as control of PP2).

Cell lysis and immunoprecipitation. LLC-PK1 cells were grown in 10cm cell culture dishes until reaching 100% confluence and then kept for 3 to 4 days. The buffer (50mM Tris-HCl pH8.0, 150mM NaCl, 1% Triton-X100, 0.5% Sodium Deoxycholate, 0.1% SDS) containing 2mM Na_3VO_4 and protease inhibitors (1:500 dilution of the protease inhibitors cocktail from SIGMA-Aldrich Corp. P8340) was used for cell lysis. Before cell lysis, the LLC-PK1 cells in 10cm dish were washed with ice-cold PBS (supplemented with 1mM Na_3VO_4) for once, and then 1ml ice-cold lysis buffer was added into each dish. After 5 minutes incubation on ice, the cells were scraped off the dish surface. The lysis buffer

containing cells was then incubated at 4ºC on a rotator for 15 minutes, and then centrifuged at 16,000 x g for 10 minutes at 4ºC to remove the insoluble fraction. This supernatant was used for immunoprecipitation. For cortactin immunoprecipitation, 6µg of mouse monoclonal cortactin antibody (clone 4F11, Upstate Biotechnology, Inc.) was added to 500µl of cell lysate and incubated on a rotator at 4ºC for 4 hours. Meanwhile, 40µl protein A-agarose beads (50% slurry, SIGMA-Aldrich Corp.) were incubated with 12µg rabbit anti-mouse IgG (Jackson ImmunoResearch) at 4ºC on a rotator for 2 hours. After incubation with the cortactin antibody, the cell lysate was added to the protein A-agarose beads and then incubated on a rotator at 4ºC for 2 hours. To immunoprecipitate dynamin-II, 6µg of rabbit polyclonal dynamin-II antibody (Genetex, Inc.) was added to 500µl of cell lysate and incubated on a rotator at 4ºC for 4 hours, and then 40µl protein A-agarose beads (50% slurry, SIGMA-Aldrich Corp.) were added into the cell lysate and incubated on a rotator for 2 hours; after the incubation the protein A-agarose beads were washed with the lysis buffer for twice and with PBS for once, and then 50µl SDS sample buffer (50mM Tris-HCl pH6.8, 2% SDS, 10% glycerol, 5% β-mercaptoethanol, 6M urea, 2mM EGTA, 0.01% bromophenol blue) was added and heated in a heating block at 80ºC for 10 minutes. The supernatant was then collected for SDS-PAGE.

Antibodies and western blotting. Western blotting was carried out with standard procedures. The primary antibodies included mouse monoclonal cortactin antibody (clone 4F11, Upstate Biotechnology, Inc.), rabbit polyclonal cortactin antibody (H-191, Santa Cruz Biotechnology), rabbit polyclonal anti-Cortactin (pY^{421}) phospho-specific antibody (Biosource), rabbit polyclonal anti-Cortactin (pY^{466}) phospho-specific antibody

(SIGMA-Aldrich Corp.), rabbit polyclonal anti-Cortactin (pY^{486}) phospho-specific antibody (Chemicon, Australia), biotin-conjugated mouse monoclonal phosphotyrosine antibody (4G10, Upstate Biotechnology, Inc.), rabbit polyclonal p34-Arc antibody (Upstate Biotechnology, Inc.), mouse monoclonal actin antibody (Chemicon International), rabbit polyclonal dynamin-II antibody (Genetex, Inc.). The secondary antibodies included peroxidase-conjugated goat anti-mouse (Jackson ImmunoResearch), peroxidase-conjugated donkey anti-rabbit (GE Healthcare). Peroxidase-conjugated streptavidin (Upstate Biotechnology, Inc.) was used for the detection of biotin-conjugated mouse monoclonal phosphotyrosine antibody (4G10, Upstate Biotechnology, Inc.).

Immunofluorescence microscopy. LLC-PK1 cells were grown on 10x10 mm coverslips in 35 mm cell culture dishes until reaching 100% confluence and then kept for 3 to 4 days. The cells on coverslips were fixed with 3.7% paraformaldehyde in PBS for 10 minutes at room temperature and permeabilized with 0.05% Triton X-100 in PBS for 5 minutes. The coverslips were blocked in blocking buffer (PBS containing 10% goat serum and 0.2% BSA) at room temperature for 30 minutes. Primary antibody incubation, with 5μg/ml mouse monoclonal cortactin antibody (clone 4F11, Upstate Biotechnology, Inc.) and/or goat polyclonal TGN38 antibody (Santa Cruz Biotechnology), was done for 1 hour. After brief washing in PBS, the coverslips were then incubated in blocking buffer containing fluorescein isothiocyanate-conjugated donkey anti-mouse IgG (1:100 dilution, Jackson Immunoresearch) and/or cy5-conjugated donkey anti-goat IgG (1:50 dilution, Jackson Immunoresearch), and 0.1 μg/ml rhodamine-phalloidin (Molecular Probes) for 1 hour. After brief washing in PBS, the coverslips were mounted with DABCO mounting media

(10% 1,4-diazabicyclo-[2,2,2]-octane, 50% glycerol, 2% sodium azide, 1xPBS) on glass slides. The fluorescent images were collected with a Zeiss UV LSM-510 confocal microscope system.

3. Results

ATP-depletion and cortactin localization

Kidney proximal tubule cells exhibit aggregated F-actin during oxidative stress. We examined what actin regulatory proteins might be associated with these structures. In LLC-PK1 cells under normal growth conditions, we found relatively stronger localization of cortactin at the cell cortex compared with the cytoplasmic regions, using immunofluorsence staining (Fig. 4A). F-actin was labeled with rhodamine-conjugated phalloidin, and cortactin was labeled with fluorescein isothiocyanate (FITC). The staining of cortactin appeared as small puncta throughout the cytoplasm and it exhibited stronger staining patterns at the cell cortex. Actin staining was in stress fibers (not shown) and at the cell cortex. Cortactin and actin showed colocalization at the cell cortex (merged images). However, after a 90 minute treatment with 100nM antimycin A in depleted DMEM to induce ATP-depletion, we found that LLC-PK1 cells exhibited much stronger localization of cortactin in the cytoplasmic regions while there was less cortactin localized at the cell cortex (Fig. 4B). Cortactin staining appeared in large aggregates in the cytoplasm colocalizing with actin (merged images). Stress fibers were reduced (not shown) and actin staining at the cell cortex was increased. After 90 minutes of ATP-depletion, we returned the LLC-PK1 cells to normal growth conditions. After a subsequent 60 minutes of recovery, we found that even though the localization of cortactin at the cell cortex was not completely recovered, the large aggregates of cortactin and actin had disappeared from the cytoplasmic regions (Fig. 4C).

Figure 4. Cortactin localization pattern changes upon ischemia/ATP-depletion in LLC-PK1 cells

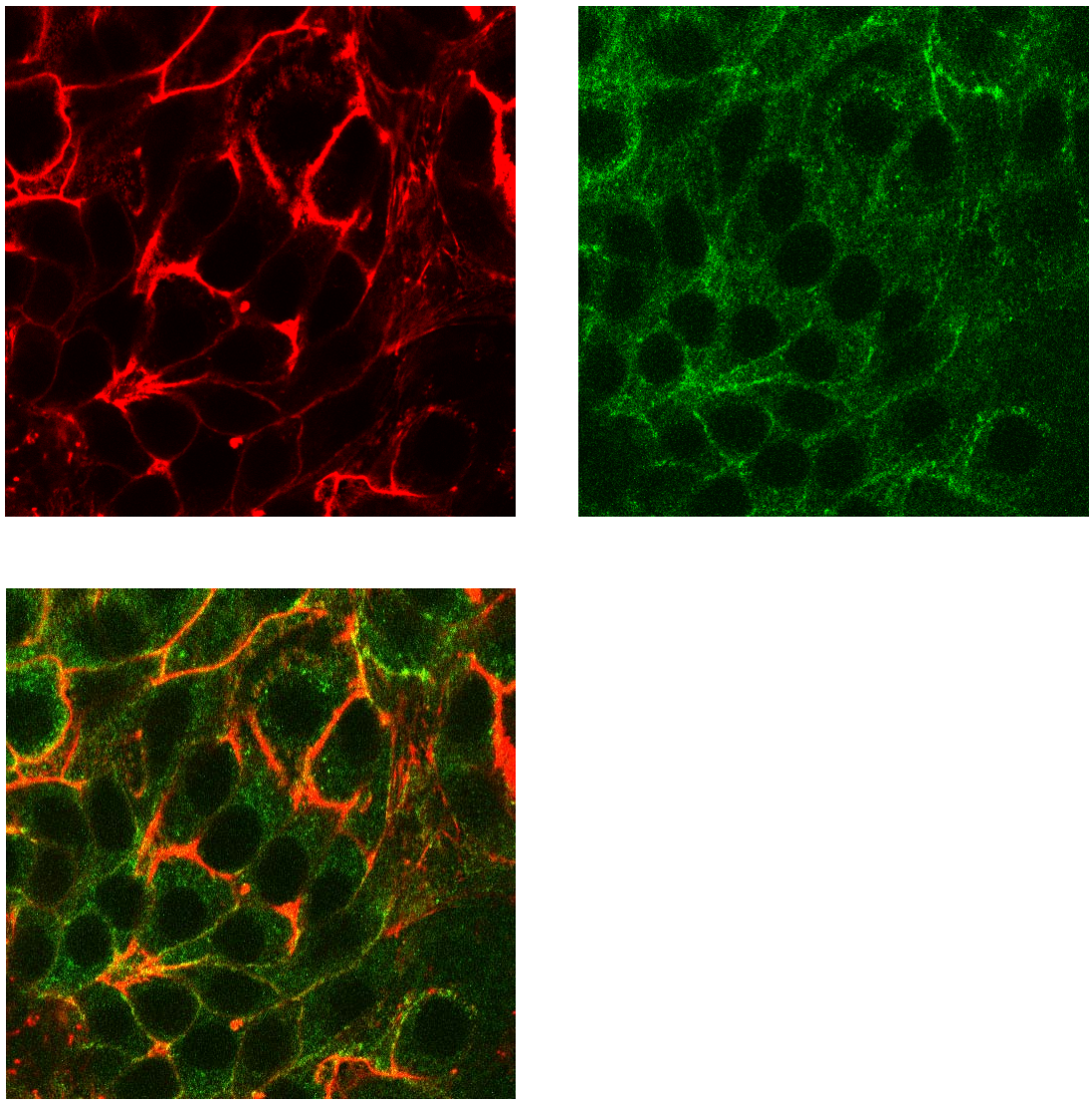

A. Control LLC-PK1 cells before ATP-depletion

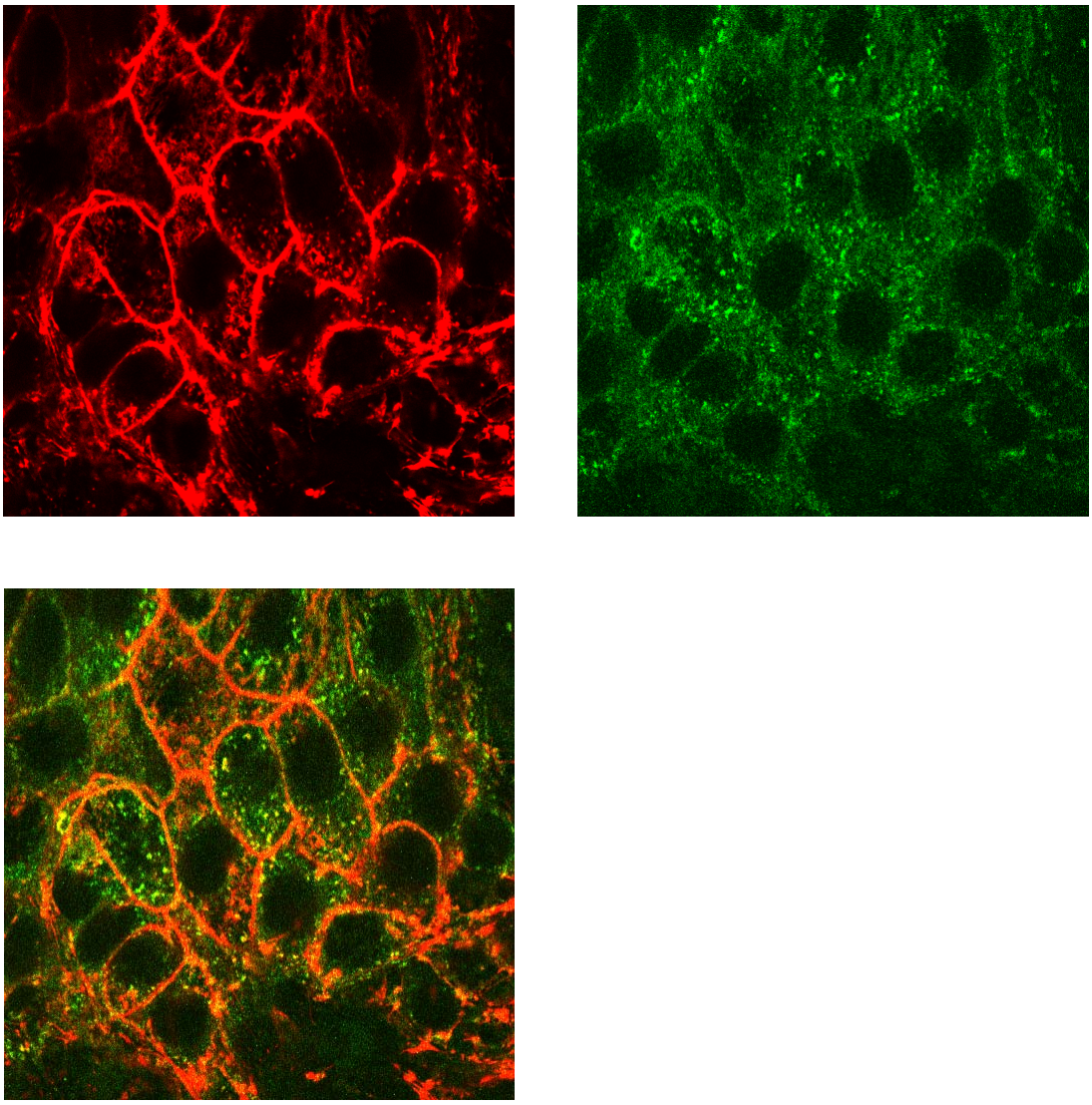

B. LLC-PK1 cells after 90 minutes ATP-depletion

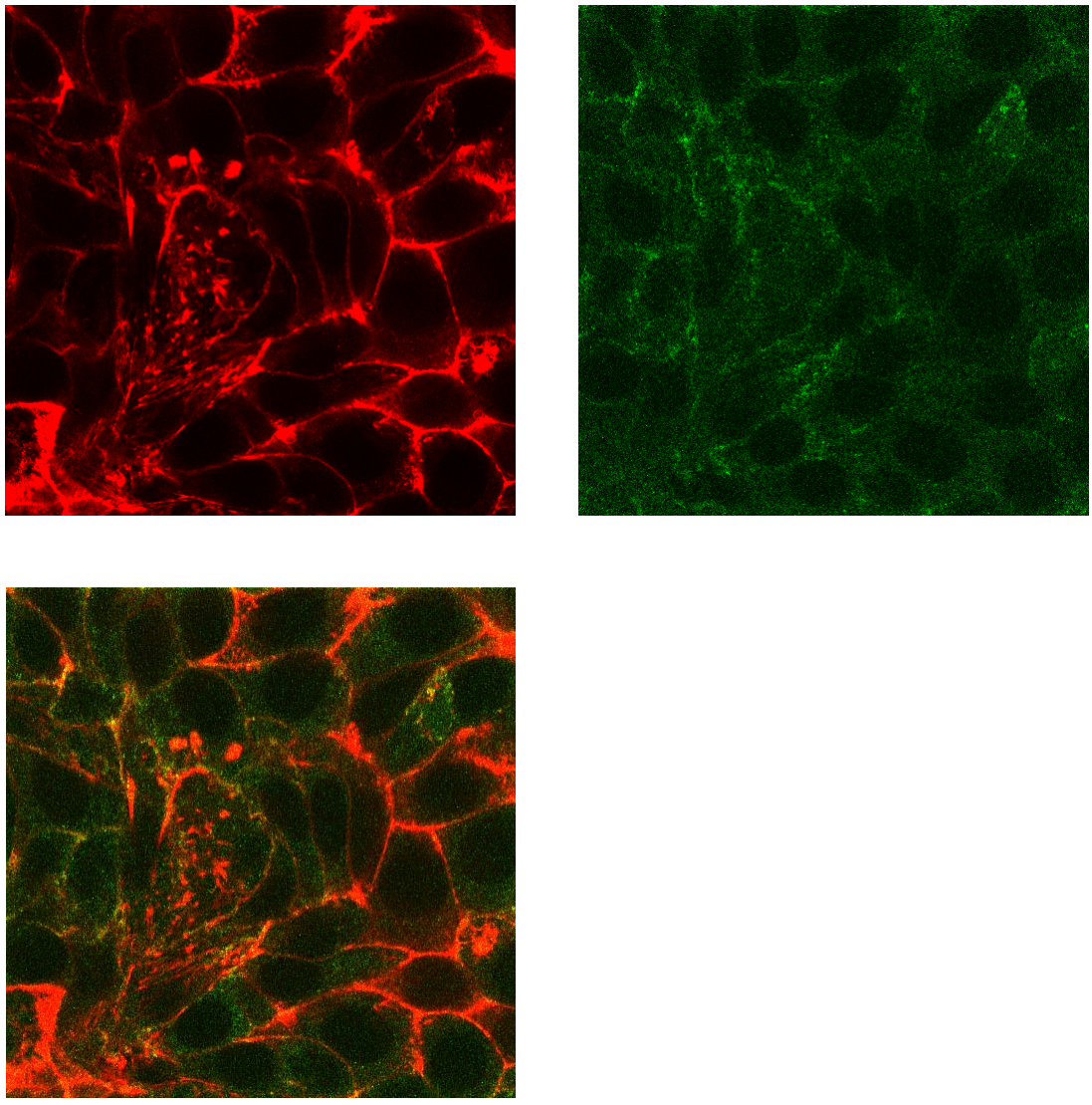

C. LLC-PK1 cells after 90 minutes ATP-depletion followed by 60 minutes recovery

Fig. 4. F-actin was labeled with rhodamine-phalloidin (red); cortactin was labeled with primary antibody against cortactin and then FITC-conjugated secondary antibody (green). In each group of images, the top left one shows only the image from red channel, the top

right one shows only the image from green channel, and the bottom left one shows the images combined from both red and green channels.

[A] LLC-PK1 cells under normal growth conditions. Cortactin exhibited distinct localization at the cell cortex and its localization in cytoplasmic regions was at a relatively low level.

[B] LLC-PK1 cells after 90 minutes of ATP-depletion with the treatment of 100nM antimycin-A in depleted DMEM. Compared with cells under normal growth conditions, cortactin exhibited much stronger localization at the cytoplasmic regions while there was less cortactin localized at the cell cortex in ATP-depleted cells. F-actin formed aggregates in cytoplasmic regions with cortactin colocalization.

[C] LLC-PK1 cells after 90 minutes of ATP-depletion and then 60 minutes recovery back in normal growth conditions. Although the localization of cortactin at the cell cortex was not yet recovered back to the level before ATP-depletion, the aggregates of cortactin and actin disappeared from the cytoplasm.

Cortactin was previously reported to localize to Golgi apparatus, and to play an important role in post-Golgi transport [52]. Considering the importance of post-Golgi protein transport to the establishment and maintenance of cytoplasmic membrane dipolarity in kidney proximal tubule cells, we decided to investigate whether cortactin also localized to Golgi apparatus in LLC-PK1 cells, and whether this possible localization was affected by ATP-depletion. In immunofluorescence experiments, we stained the LLC-PK1 cells with cortactin antibody and an antibody against the trans-Golgi marker TGN38 either under normal growth conditions or after 90 minutes ATP-

depletion; however we failed to observe colocalization of cortactin and TGN38 under both conditions (Fig. 5).

Figure 5. No cortactin localization at trans-Golgi was observed in LLC-PK1 cells

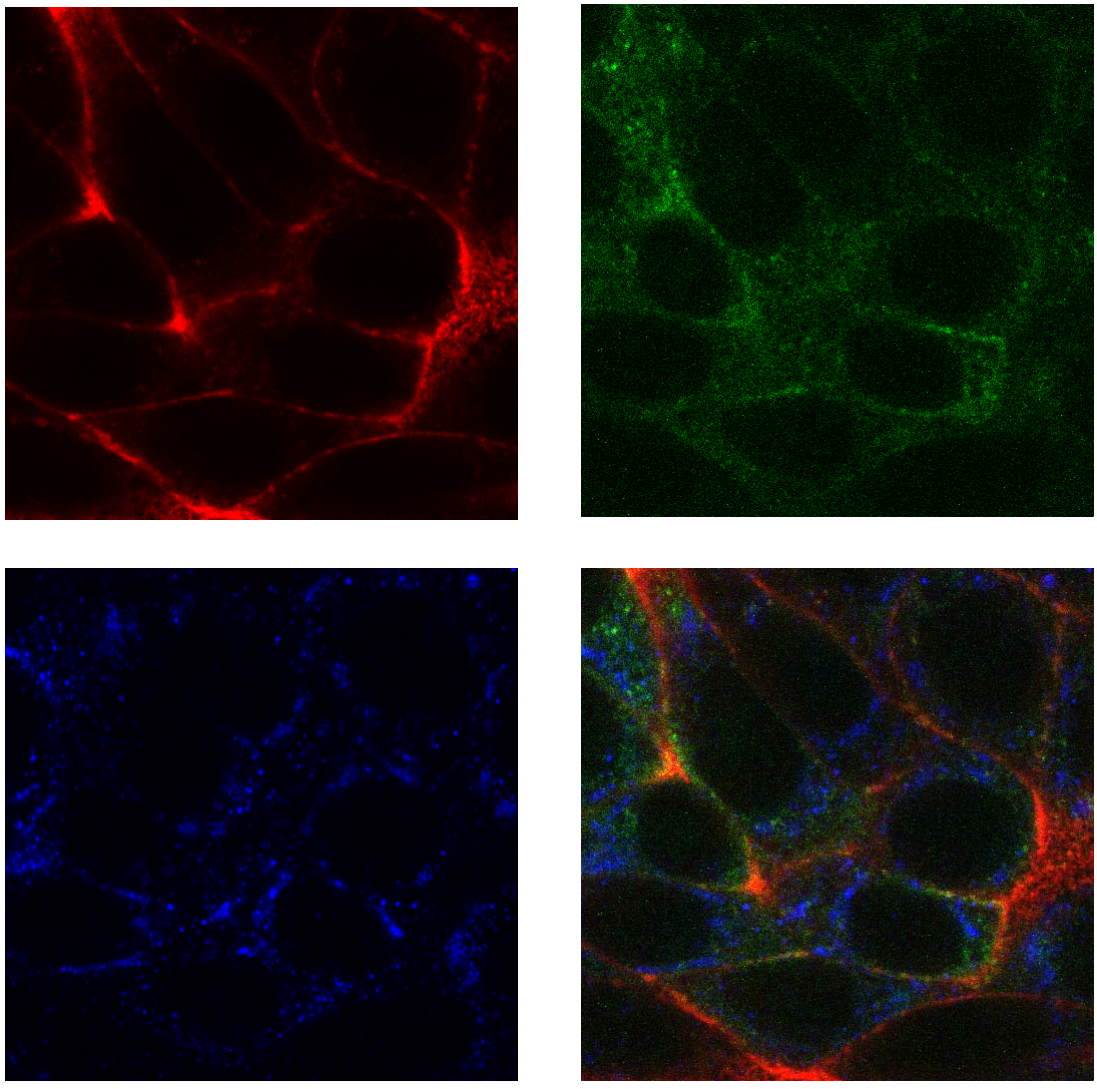

10 µm

A. LLC-PK1 cells under normal growth conditions

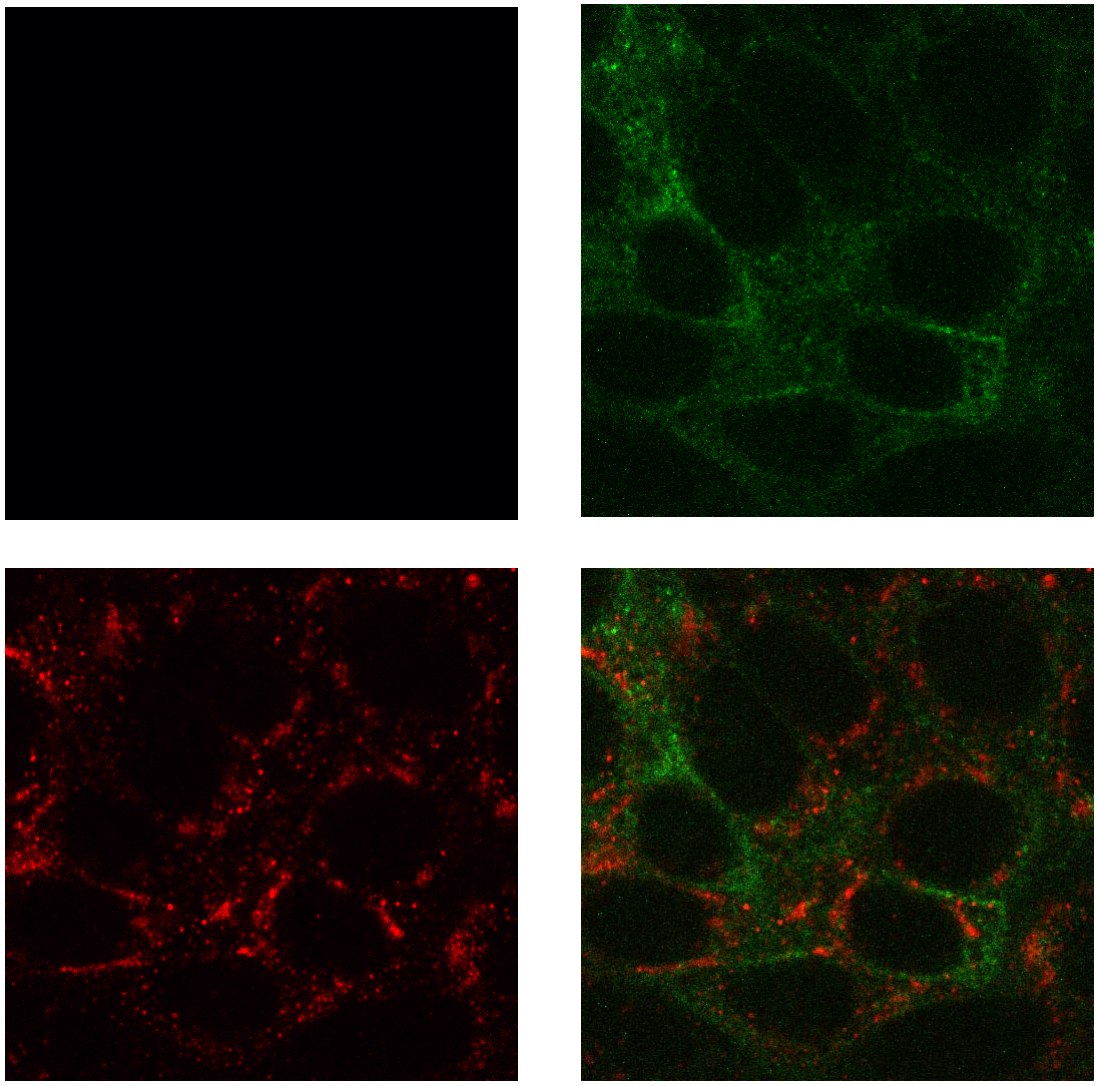

10 µm

B. LLC-PK1 cells under normal growth conditions

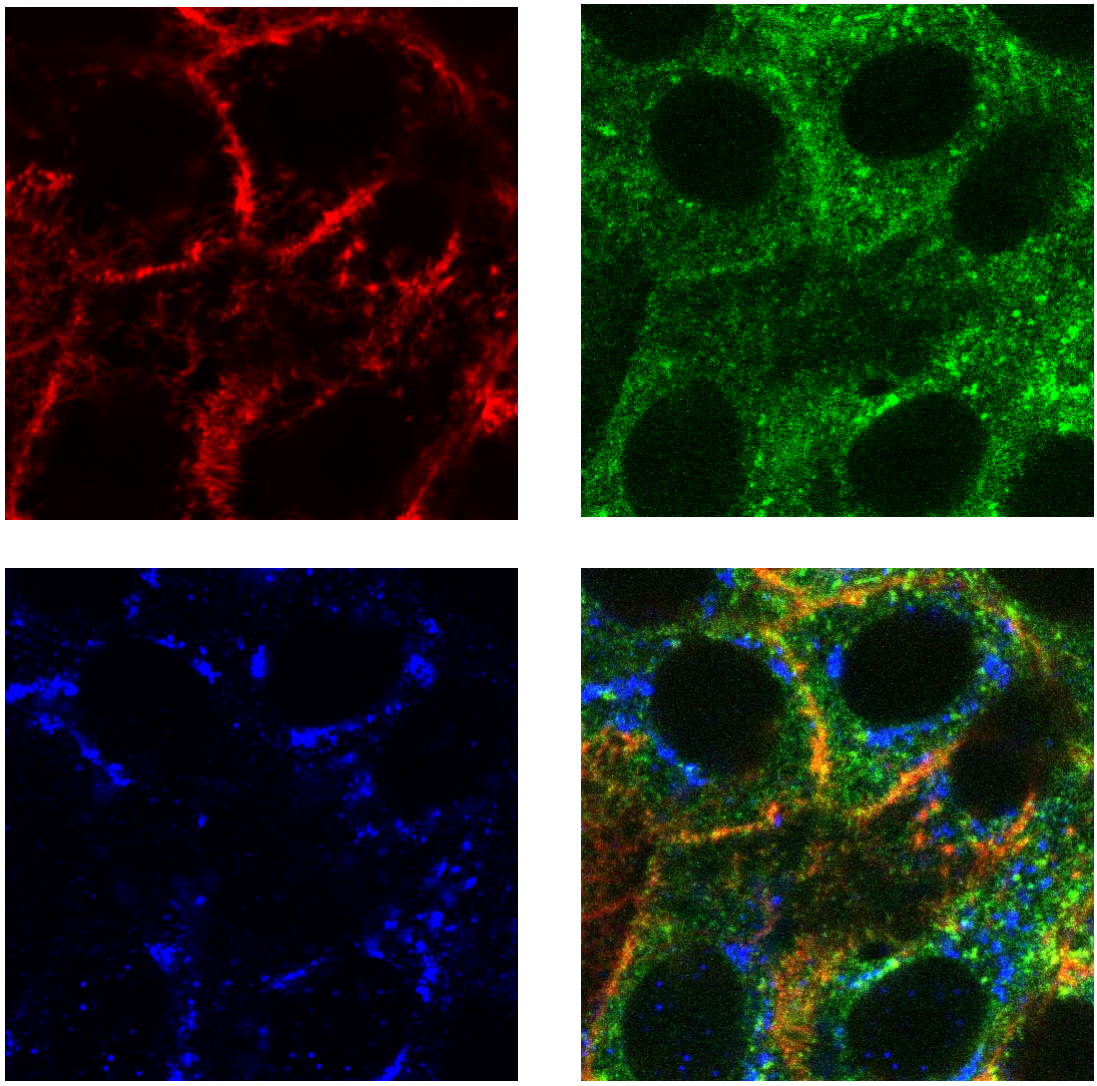

10 µm

C. LLC-PK1 cells after 90 minutes ATP-depletion

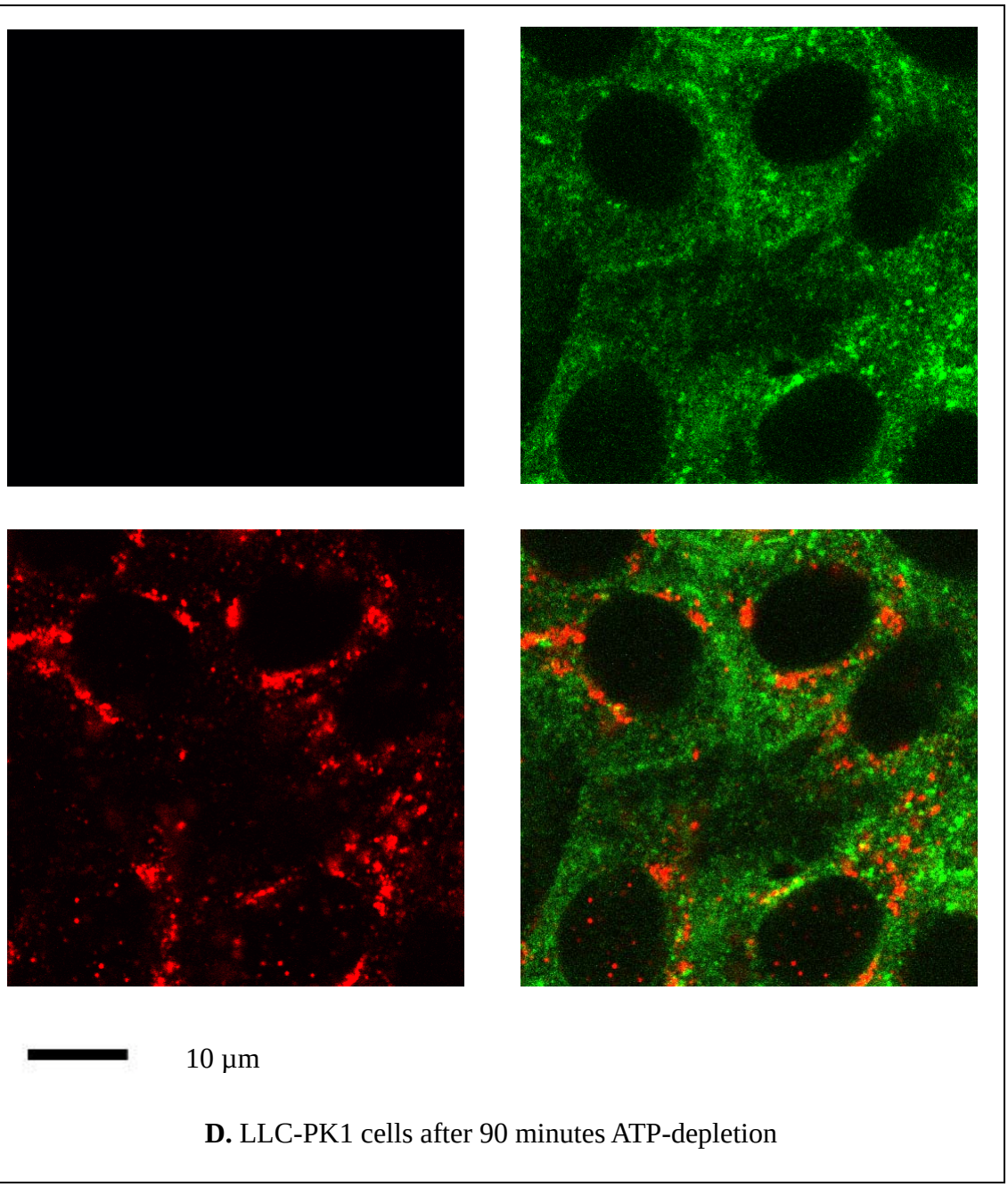

D. LLC-PK1 cells after 90 minutes ATP-depletion

Fig. 5. F-actin was labeled with rhodamine-phalloidin (red); cortactin was labeled with primary antibody against cortactin and then FITC-conjugated secondary antibody (green); trans-Golgi marker TGN38 was labeled with primary antibody against TGN38 and then Cy5-conjugated secondary antibody (blue).

[A, B] The same immunofluorescence images of LLC-PK1 cells under normal growth conditions. In B, the rhodamine (red) signal of F-actin was removed and the cy5 (blue) signal of TGN38 was shown as green for better viewing purpose. No cortactin colocalization with TGN38 at trans-Golgi was observed.

[C, D] The same immunofluorescence images of LLC-PK1 cells after 90 minutes of ATP-depletion with the treatment of 100nM antimycin-A in depleted DMEM. In D, the rhodamine (red) signal of F-actin was removed and the cy5 (blue) signal of TGN38 was shown as green for better viewing purpose. No cortactin colocalization with TGN38 at trans-Golgi was observed.

The tyrosine phosphorylation level of cortactin decreases in LLC-PK1 cells upon ATP-depletion and Src kinase inhibition

After observing the translocation of cortactin from the cell cortex to the cytoplasmic regions in LLC-PK1 cells upon ATP-depletion, we investigated whether there was a correlation with its tyrosine phosphorylation level. LLC-PK1 cells were lysed under normal growth conditions or after 90 minutes of ATP-depletion. Cortactin antibody was then used for immunoprecipitation with the lysate. Three tyrosine residues, Y421, Y466 and Y482 of cortactin have been identified as the major phosphorylation sites of Src kinase. We used phospho-specific antibodies to each one of these three tyrosine residues of cortactin to probe the western blot of the cortactin immunoprecipitation product. We found that the tyrosine phosphorylation level of all three tyrosine residues (Y421, Y466 and Y482) of cortactin decreased upon ATP-depletion (top panels of Fig. 6A-C). In addition, we also treated LLC-PK1 with 50 μM

Src kinase inhibitor PP2 under normal growth conditions for 45 minutes. We found that compared with the control LLC-PK1 cells, the cells treated with PP2 also showed reduced tyrosine phosphorylation (top panels of Fig. 6A-C). The lower panels (Fig. 6A-C) show the quantification of the western blots normalized to their respective control. The cortactin immunoprecipitate was also probed with a non-specific phospho-tyrosine antibody (Fig. 6D). No tyrosine-phosphorylated cortactin was detected after ATP depletion or Src kinase inhibition (PP2) treatment.

Figure 6. Tyrosine phosphorylation level of cortactin in LLC-PK1 cells decreases upon ATP-depletion and Src kinase inhibition

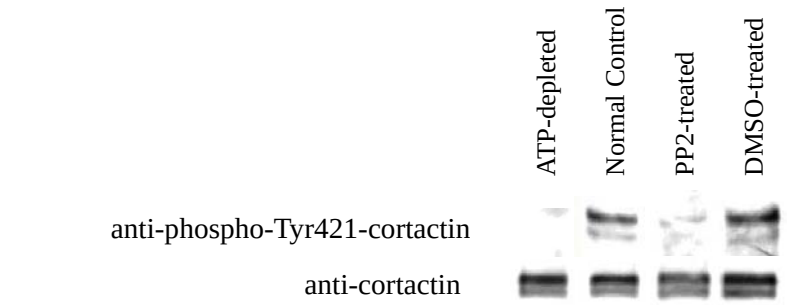

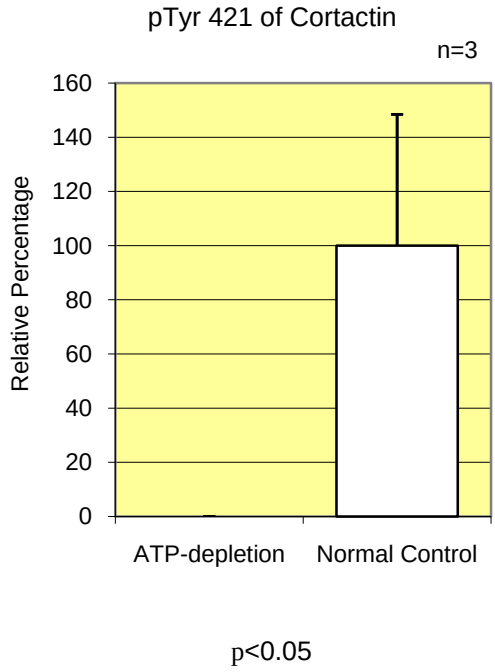

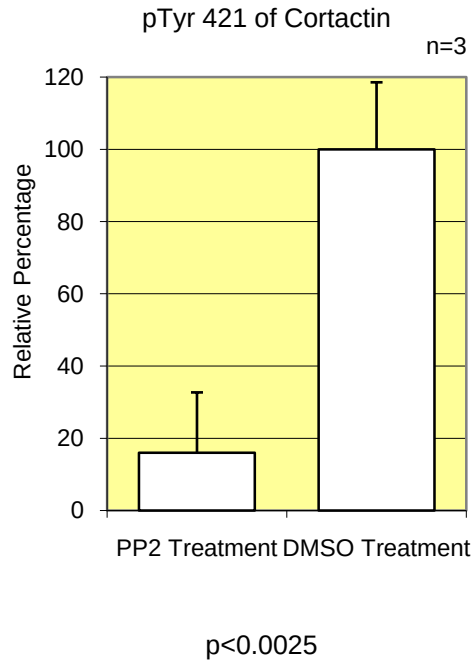

p<0.05

p<0.0025

A. Phosphorylation of Tyr421 residue of cortactin

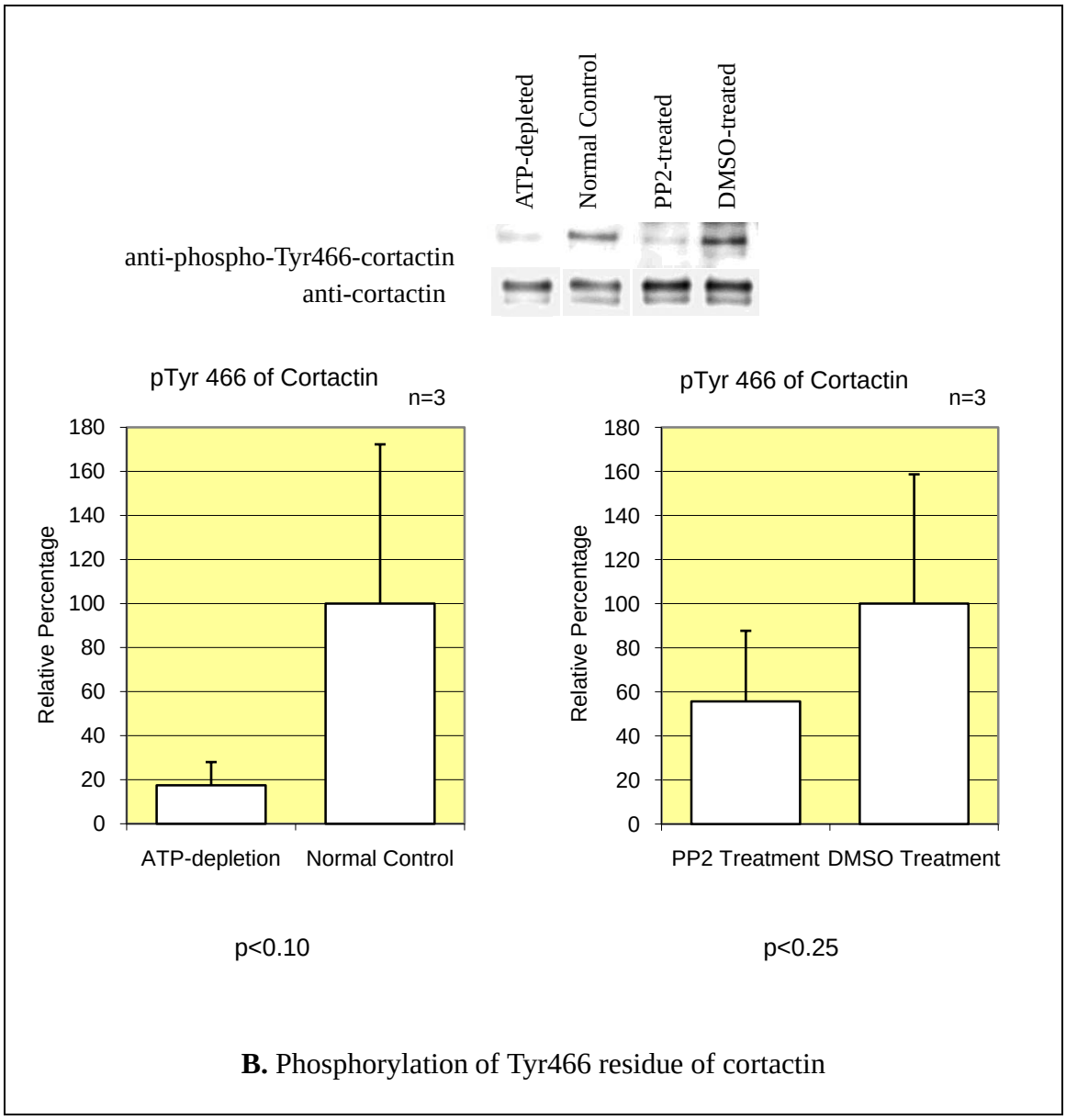

B. Phosphorylation of Tyr466 residue of cortactin

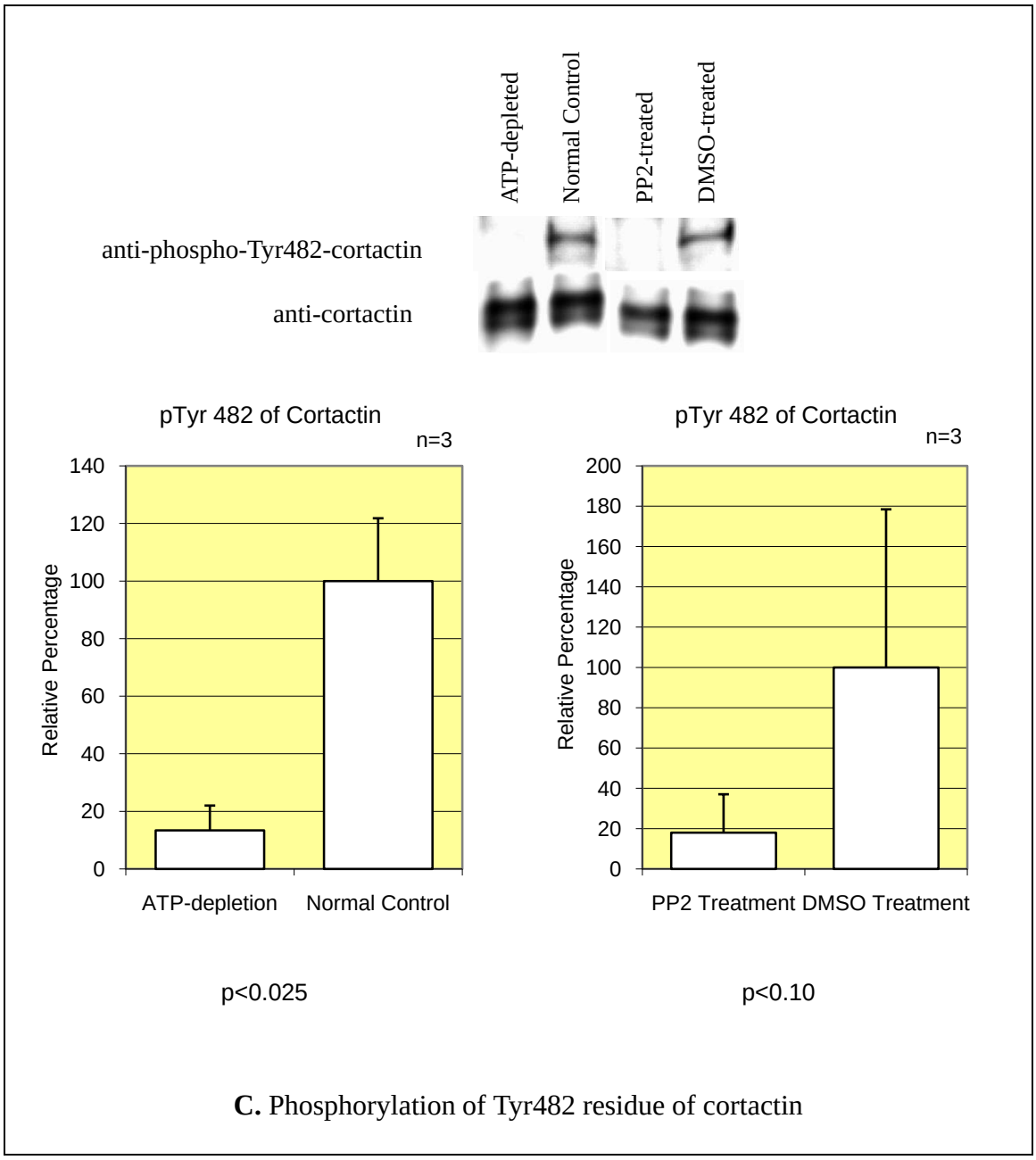

C. Phosphorylation of Tyr482 residue of cortactin

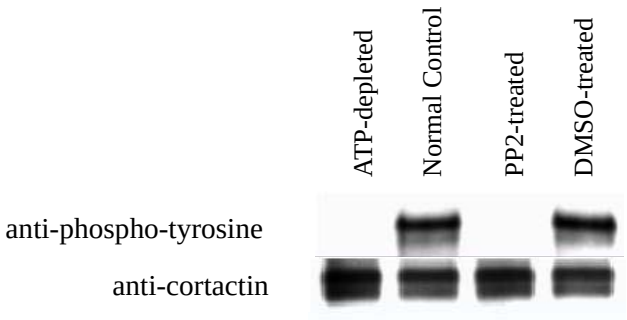

D. Tyrosine phosphorylation of cortactin

Fig. 6. After either ATP-depletion or Src kinase inhibition with 50 μM PP2 treatment, cortactin was immunoprecipitated from LLC-PK1 cell lysate and then western-blotted with specific antibodies against each of the three phospho-tyrosine residues, the target sites of Src kinase, which are pTyr421 (Fig. 6A), pTyr466 (Fig. 6B), pTyr482 (Fig. 6C), and also with the general phospho-tyrosine antibody (Fig. 6D). For Src kinase inhibition with 50 μM PP2 treatment, LLC-PK1 cells were also treated with 0.5% DMSO separately as the respective control. In each single experiment, the phosphorylation level of Tyr421, Tyr466 or Tyr482 after ATP-depletion is presented as the percentage compared with the sample of normal control, and the phosphorylation level of Tyr421, Tyr466 or Tyr482 after PP2 treatment is presented as the percentage compared with the sample after DMSO treatment. The error bars in the columns of normal control and DMSO treatment show the standard deviation of the phosphorylation level of Tyr421, Tyr466 or Tyr482 around the respective average of three experiment repeats.

Cortactin's interaction with F-actin and Arp2/3 complex

Since we found that the tyrosine phosphorylation level of cortactin decreased upon either ATP-depletion or Src kinase inhibition, we decided to investigate whether there were also functional changes of cortactin. Cortactin has many protein targets *in vivo*, and among the interactions with those multiple binding partners, the direct binding with F-actin and actin nucleation factor Arp2/3 complex are possibly the most extensively studied and also the most critical for cortactin to regulate actin cytoskeleton. We were able to co-immunoprecipitate both actin and Arp2/3 complex with cortactin. Western-blotting using the actin (top panel of Fig. 7A) antibody and Arc-p34 (an Arp2/3 complex component) (top panel of Fig. 7B) antibody showed decreases in co-immunoprecipitation of actin and Arp2/3 complex with cortactin when LLC-PK1 cells were subject to ATP-depletion or Src kinase inhibition. These results indicate that tyrosine phosphorylation of cortactin is related to its binding with F-actin and actin nucleator Arp2/3 complex. Quantifications of the western blots normalized to their respective control are shown in Fig. 7A and Fig. 7B in the lower panels.

Figure 7. Cortactin's interactions with F-actin and Arp2/3 complex decrease in LLC-PK1 cells upon ATP-depletion and Src kinase inhibition

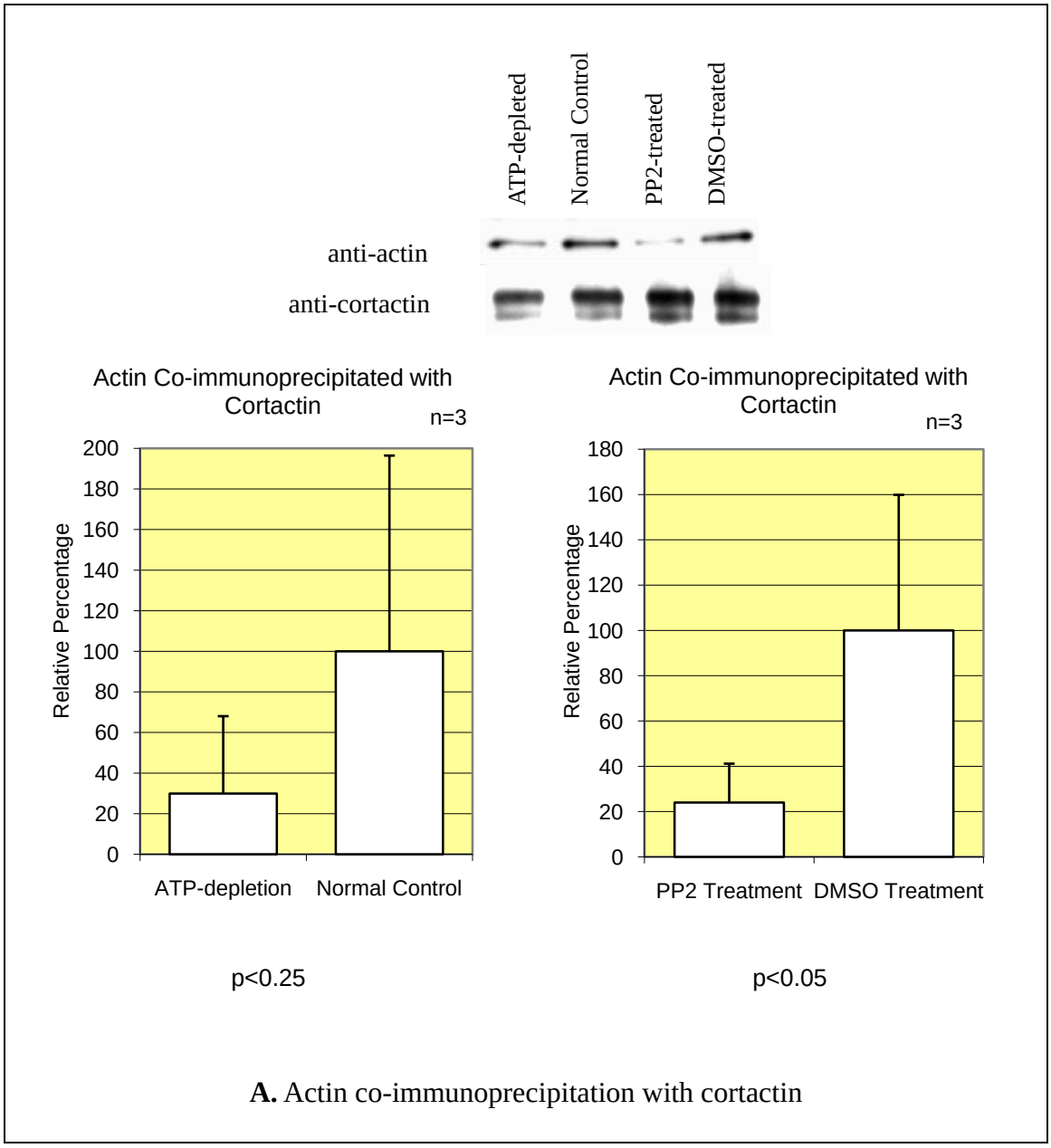

A. Actin co-immunoprecipitation with cortactin

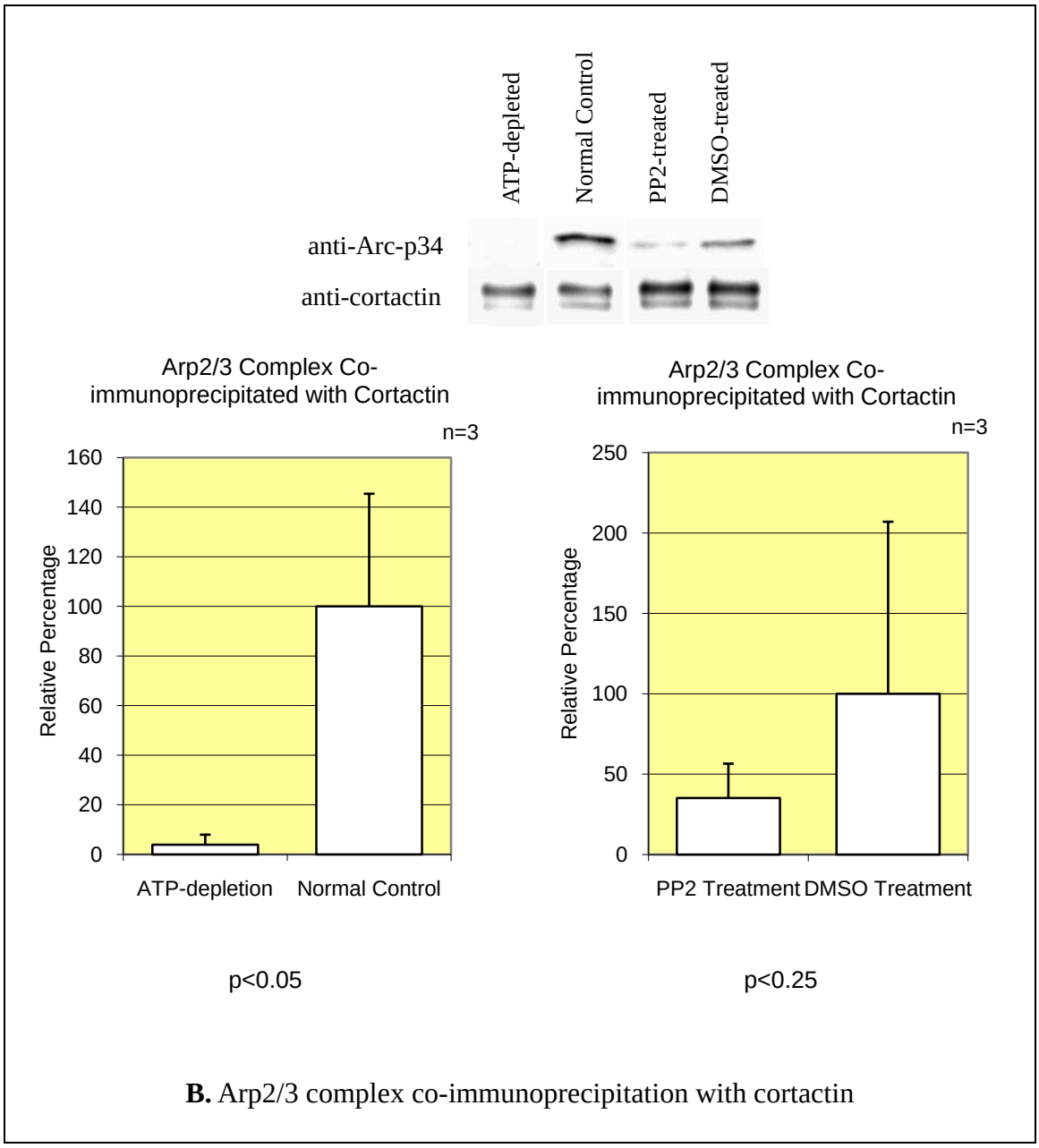

B. Arp2/3 complex co-immunoprecipitation with cortactin

Fig. 7. After either ATP-depletion or Src kinase inhibition with 50 µM PP2 treatment, cortactin was immunoprecipitated from LLC-PK1 cell lysate and then western-blotted with antibody against actin (Fig. 7A) or Arc-p34, a component of Arp2/3 complex (Fig. 7B). For Src kinase inhibition with 50 µM PP2 treatment, LLC-PK1 cells were also treated with 0.5% DMSO separately as the control. In each single experiment, the

amount of actin or Arp2/3 complex co-immunoprecipitated with cortactin after ATP-depletion is presented as the percentage compared with the sample of normal control, and the amount of actin or Arp2/3 complex co-immunoprecipitated with cortactin after PP2 treatment is presented as the percentage compared with the sample after DMSO treatment. The error bars in the columns of normal control and DMSO treatment show the standard deviation of the amount of actin or Arp2/3 complex co-immunoprecipitated with cortactin around the respective average of three experiment repeats.

Tyrosine phosphorylation level of dynamin-II decreases in LLC-PK1 cells upon ATP-depletion and Src kinase inhibition

The SH-3 domain at the C-terminus of cortactin binds with proline-rich domain of multiple partners *in vivo*, one of which is dynamin [64]. Dynamin co-localizes with cortactin and/or actin structures at multiple cellular locations *in vivo* [49, 52, 64, 88, 89]. Like cortactin, dynamin also directly binds with Src kinase [117]. Src-induced tyrosine-phosphorylation of dynamin-II has been shown to promote its translocation from cytosol to membrane *in vivo* [120]. We investigated if tyrosine phosphorylation level of dynamin-II was also affected by ATP-depletion in LLC-PK1 cells. Using phospho-tyrosine antibody to western-blot the immunoprecipitated dynamin-II from LLC-PK1 cell lysate, we found that the tyrosine-phosphorylation level of dynamin-II decreased after either ATP-depletion or Src kinase inhibition with PP2 treatment (Fig. 8A). Considering the importance of both cortactin and dynamin-II to endocytosis and post-Golgi transport and their direct *in vivo* binding, we investigated if their direct binding was affected by ATP-depletion and the changes of their tyrosine phosphorylation level. When we

immunoprecipitated cortactin, we were unable to detect dynamin-II in the immunoprecipitated protein complex; however when we immunoprecipitated dynamin-II, we detected the co-immunoprecipitated cortactin. Contrary to our initial expectations, the western-blotting results did not show major changes of cortactin co-immunoprecipitation with dynamin-II after either ATP-depletion or Src kinase inhibition with PP2 treatment (Fig. 8B). The data suggests that there is no major change of cortactin and dynamin-II interaction *in vivo* in LLC-PK1 cells after those treatments.

Figure 8. ATP-depletion or Src kinase inhibition leads to the decrease of the dynamin-II tyrosine phosphorylation level but does not affect the interaction between cortactin and dynamin-II

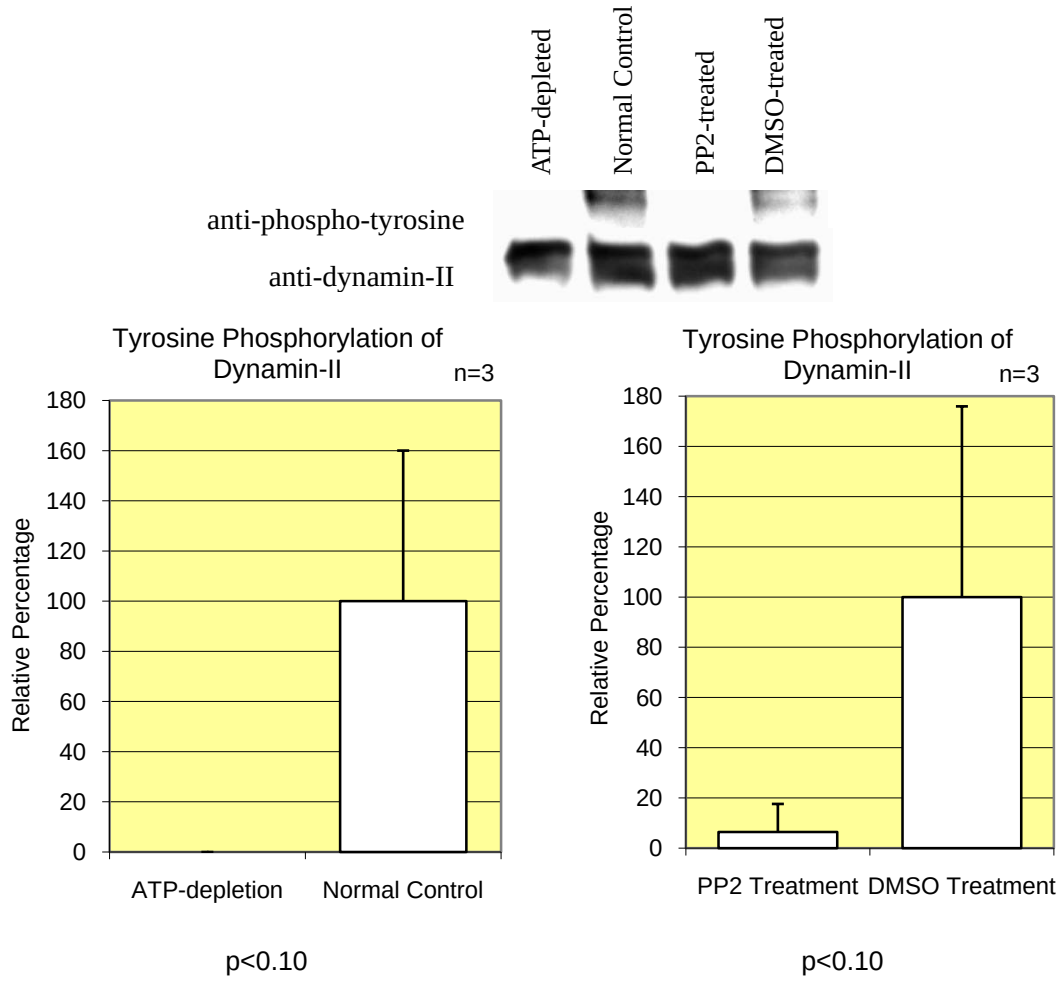

A. Tyrosine phosphorylation of dynamin-II

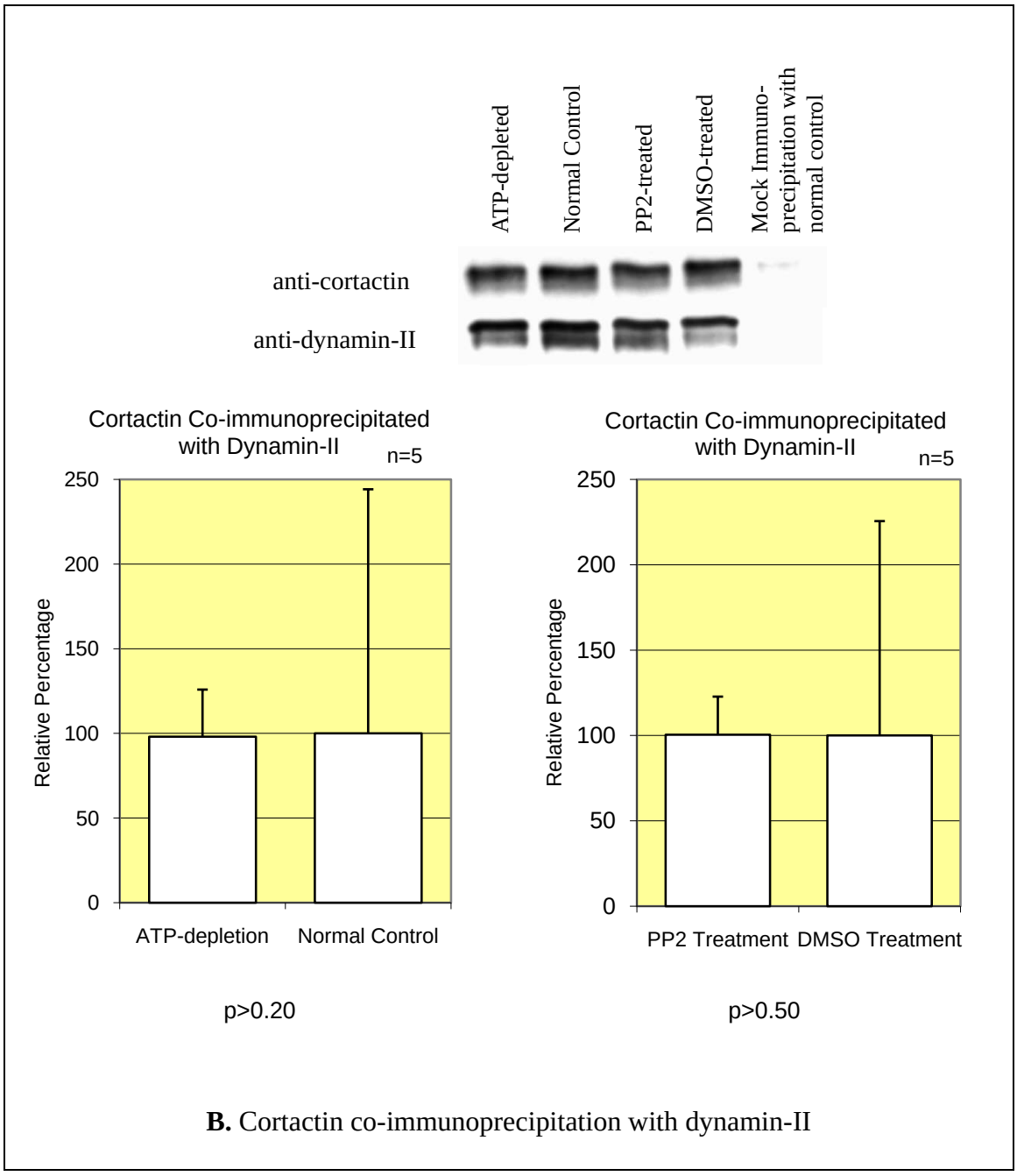

B. Cortactin co-immunoprecipitation with dynamin-II

Fig. 8. After either ATP-depletion or Src kinase inhibition with 50 µM PP2 treatment, dynamin-II was immunoprecipitated from LLC-PK1 cell lysate and then western-blotted with biotin-conjugated phospho-tyrosine antibody (Fig. 8A) or cortactin antibody (Fig. 8B). For Src kinase inhibition with 50 µM PP2 treatment, LLC-PK1 cells were also

treated with 0.5% DMSO separately as the control. In each single experiment, the tyrosine phosphorylation level of dynamin-II after ATP-depletion is presented as the percentage compared with the sample of normal control, and the tyrosine phosphorylation level of dynamin-II after PP2 treatment is presented as the percentage compared with the sample after DMSO treatment. The error bars in the columns of normal control and DMSO treatment show the standard deviation of the tyrosine phosphorylation level of dynamin-II around the respective average of three experiment repeats. In each single experiment, the amount of cortactin co-immunoprecipitated with dynamin-II after ATP-depletion is presented as the percentage compared with the sample of normal control, and the amount of cortactin co-immunoprecipitated with dynamin-II after PP2 treatment is presented as the percentage compared with the sample after DMSO treatment. The error bars in the columns of normal control and DMSO treatment show the standard deviation of the amount of cortactin co-immunoprecipitated with dynamin-II around the respective average of five experiment repeats.

4. Discussion

The epithelial cells lining the proximal tubule of the nephron are particularly susceptible to ischemic renal injury. The disruption of the actin cytoskeleton in proximal tubules begins at a very early stage of ARI. The actin cytoskeleton is also responsible for the establishment and maintenance of epithelial cell polarity. Therefore, the study of actin cytoskeleton regulators, in particular the changes of their function during renal ischemia, is vital to the understanding of the pathological etiology of ARI. In this study, we used an *in vitro* cell culture system to model ischemia by incubation with antimycin A in a substrate depleted medium, resulting in ATP depletion. We observed actin aggregates in LLC-PK1 cells upon ATP-depletion. We also found that with ATP depletion cortactin translocated from the cell cortex to the cytoplasmic regions and colocalized in actin aggregates. Cytoplasmic actin aggregates resulting from ATP depletion were first reported by Hinshaw *et al.* [122]. More recently, F-actin aggregates were found to form merely by disrupting F-actin filament dynamics with jasplakinolide, and cortactin was found in these aggregates [79]. It has been suggested that the formation of actin aggregates during ATP depletion is beneficial to the cell; for example the actin turnover uses up to 50% of the ATP in neurons while the actin aggregates formed in neurons during ATP stress are less dynamic and consume much less ATP [123]. In kidney ischemia, conservation of ATP by actin aggregate formation may allow the epithelium to cope with low oxygen tension for longer than it would otherwise. After LLC-PK1 cells were returned to normal growth conditions for one hour, cortactin/actin aggregates disappeared.

Post-translational modification of proteins by kinase phosphorylation is an important regulatory mechanism. Protein phosphorylation generally decreases significantly during ischemia [124]. However, not all proteins become dephosphorylated. For example, AMPK (AMP-activated protein kinase) becomes phosphorylated during ischemia [125]. With this in mind, we decided to test whether the tyrosine phosphorylation of cortactin changed during ATP depletion. The immunoprecipitation and western blotting results showed that the tyrosine phosphorylation level of cortactin decreased during ATP-depletion. In addition the phosphorylation level of cortactin on Y421, Y466 and Y482 residues also appeared to decrease when the cells were subject to Src kinase inhibition. Although the decrease of Y466 and Y482 phosphorylation after Src kinase inhibition was not statistically significant (as shown by the one-sided p value in t-test), that could be due to the small number of experiment repeats. Meanwhile, when we probed the cortactin immunoprecipitate with the general phospho-tyrosine antibody in western-blotting analysis, there was no tyrosine-phosphorylated cortactin detected after either ATP-depletion or Src kinase inhibition, which proved that the overall tyrosine phosphorylation of cortactin decreased upon ATP-depletion or Src kinase inhibition.

We were also interested in finding out whether cortactin's interaction with its targets of regulation changed in parallel with the decrease of its tyrosine phosphorylation level. To investigate these interactions, we immunoprecipitated cortactin from normal control and ATP depleted cells and probed for Arc-p34, a protein component of the Arp2/3 complex, as well as for actin. In both cases there appeared to be a decrease in terms of their interactions with cortactin in ATP-depleted LLC-PK1 cells and cells treated

with Src kinase inhibitor. Once again the small number of experiment repeats might have contributed to the fact that some of the results were not statistically significant.

Many studies have been published on how tyrosine phosphorylation affects cortactin's cellular function. One major conclusion is that tyrosine phosphorylation regulates cortactin's targeting to the cell cortex [74, 84, 85]. Our study shows that this relationship also exists in kidney epithelial cells. Meanwhile, during ATP depletion the decrease of cortactin tyrosine phosphorylation also happens in parallel with the redistribution of cortactin from the cortex to cytoplasmic aggregates containing actin. Our previous study shows in LLC-PK1 cells, the F-actin content increases while G-actin monomer content decrease after ATP-depletion, in comparison with normal growth conditions [36]. Previously it was reported that in CHO cells F-actin depolymerization induced by LB (latrunculin-B) led to Fyn/Fer kinase-mediated tyrosine phosphorylation of cortactin at the same target sites as Src kinase, and in LB-treated cells tyrosine-phosphorylated cortactin predominantly distributed in cytoplasmic regions; on the other hand the F-actin polymerization induced by jasplakinolide and the concomitant actin-cortactin clustering reduce cortactin tyrosine phosphorylation [69]. In our study we observed an increase of F-actin content in cytoplasmic regions in LLC-PK1 cells after ATP-depletion and also observed cortactin translocating from cell cortical region to cytoplasmic regions and colocalizing with the F-actin aggregates at cytoplasmic regions; therefore it is possible that such an increase of F-actin content in cytoplasmic regions of LLC-PK1 cells after ATP-depletion inhibits the tyrosine phosphorylation of cortactin by Fyn/Fer kinases, which further contributes to the overall decrease of cortactin tyrosine phosphorylation.

The cortical actin cytoskeleton plays a critical role in establishing and maintaining the apical and basolateral membrane polarity, and its disruption to a significant extent precedes the membrane changes during ischemia. Ischemic injury also disrupts the localization of apical and basolateral membrane components. The correct targeting of protein components of the apical and basolateral membranes to surface membrane destinations after synthesis at the ER, modification at and transportation from Golgi; as well as their recycling from the surface membrane in clathrin-coated vesicles by endocytosis and then recycling back to the original surface membrane domains, or transcytosis to particular surface membrane domains for enrichment; all these processes are very important for establishing and maintaining apical and basolateral membrane polarity, and also important for the proper filtration function of the proximal tubule; therefore they could be disrupted by ischemia [13, 39, 40]. Cortactin, along with its direct binding partner dynamin, have been reported to be important for receptor-mediated endocytosis and post-Golgi transport [49-52]. We speculated that during ischemia/ATP-depletion in kidney epithelial cells, the changes of cortactin's tyrosine phosphorylation level and its localization pattern also affected its normal function in endocytosis and post-Golgi transports. However by immunofluorescence microscopy, we failed to detect the colocalization of cortactin with *trans*-Golgi protein TGN38 in both normal control and ATP-depleted LLC-PK1 cells, even though such a colocalization was previously reported in different types of cells [52]. Recently it was reported that receptor-mediated endocytosis involved tyrosine phosphorylation of cortactin, and src-mediated phosphorylation of cortactin enhanced its association with dynamin-II as shown by *in vitro* study [83]. We detected endogenous cortactin in the protein complexes from

dynamin-II immunoprecipitation with LLC-PK1 cell lysate, but the western-blotting results did not show any major change of interaction between cortactin and dynamin-II when the LLC-PK1 cells were subject to ATP-depletion or Src kinase inhibition. Therefore, whether in kidney epithelial cells the ATP-depletion disrupts cortactin's normal function in post-Golgi transports and endocytosis through the decrease of its tyrosine phosphorylation level, and whether these functional disruptions of cortactin further contribute to the ischemic cellular injury, these questions remain to be answered by further investigations.

5. Summary

Cortactin, an important regulator of actin assembly and organization, plays an important role in endocytosis and post-Golgi transport. One mechanism controlling cortactin's cellular activity and localization is the phosphorylation of several tyrosine residues located within the proline-rich domain of cortactin by different kinases including Src. Using LLC-PK1 cells (a porcine kidney proximal tubule epithelial cell line) as a cell culture model of renal ischemia, we found that cortactin translocated from the cell cortex to the cytoplasmic regions upon ATP-depletion. Even though cortactin was previously reported to localize on trans-Golgi network, we were unable to detect the colocalization of cortactin and the trans-Golgi marker TGN38 in LLC-PK1 cells under either normal growth conditions or ATP-depletion. Meanwhile the overall tyrosine phosphorylation level of cortactin as well as on each of the three target sites (Y421/466/482) of Src family kinases decreases in LLC-PK1 cells upon ATP-depletion or inhibition of Src kinase activity. In addition, co-immunoprecipitation assays indicate that cortactin's *in vivo* interaction with F-actin and the actin nucleator Arp2/3 complex is also weakened upon ATP-depletion or inhibition of Src kinase activity. Dynamin-II, a GTPase with a critical role in multiple cellular functions including endocytosis, vesicle traffic in and out of the Golgi, directly binds with cortactin and is also a regulator of dynamic actin cytoskeleton structures. We found that the overall tyrosine phosphorylation level of dynamin-II decreased in LLC-PK1 cells upon ATP-depletion or inhibition of Src kinase activity. Previously it was reported that src-mediated phosphorylation of cortactin enhanced its association with dynamin-II, but in our study the co-immunoprecipitation assays did not show any major change of interaction between cortactin and dynamin-II interaction when

LLC-PK1 cells were subject to ATP-depletion or Src kinase inhibition. These results suggest that tyrosine phosphorylation plays an important role in regulating cortactin's cellular function and localization in the scenario of kidney ischemia. Further studies could be done on how cortactin's tyrosine phosphorylation affects its interactions with proteins other than dynamin-II, and how these interactions subsequently affects actin cytoskeleton and the apical/basolateral membrane dipolarity in kidney proximal tubule epithelia. These studies will significantly assist us with better understanding of the mechanisms by which the actin cytoskeleton dysregulation, a critical feature of cellular injury caused by kidney ischemia, occurs.

CHAPTER III

AMP-Activated Protein Kinase is an Upstream Regulator of Rho GTPases Activity and Cytoskeletal Organization during ATP-Depletion in a Cell Culture Model of Ischemic Renal Injury

1. Introduction

Rho GTPases and renal ischemia

The Rho family of small GTPases in eukaryotic cells, encompassing more than 20 members of intracellular signaling molecules, directly interact with numerous proteins and are involved in the regulation of multiple cellular functions and processes including cell cycle control, cell morphogenesis, cell migration, apoptosis and so on [126]. In terms of biochemical functions, the Rho family GTPases regulate enzymatic activities, affect gene expression, in addition to controlling the actin and microtubule cytoskeleton, which has been the most extensively studied so far. Other than several "atypical" members which are predominantly GTP-bound, the majority of Rho GTPases switch between the GTP-bound active state and the GDP-bound inactive state. When bound to GTP, Rho GTPases interact and activate downstream effectors to regulate multiple cellular processes. Regulated by upstream signaling pathways, a large family of GTPase-activating proteins (GAP) significantly stimulate the GTPase activity of Rho proteins (which is usually low) to catalyze the hydrolysis of GTP into GDP. By promoting the release of GDP from and the binding of GTP to Rho proteins, another large number of guanine nucleotide-exchange factors (GEFs) activate them. A relatively small number of

Figure 9. Rho GTPase functional cycle

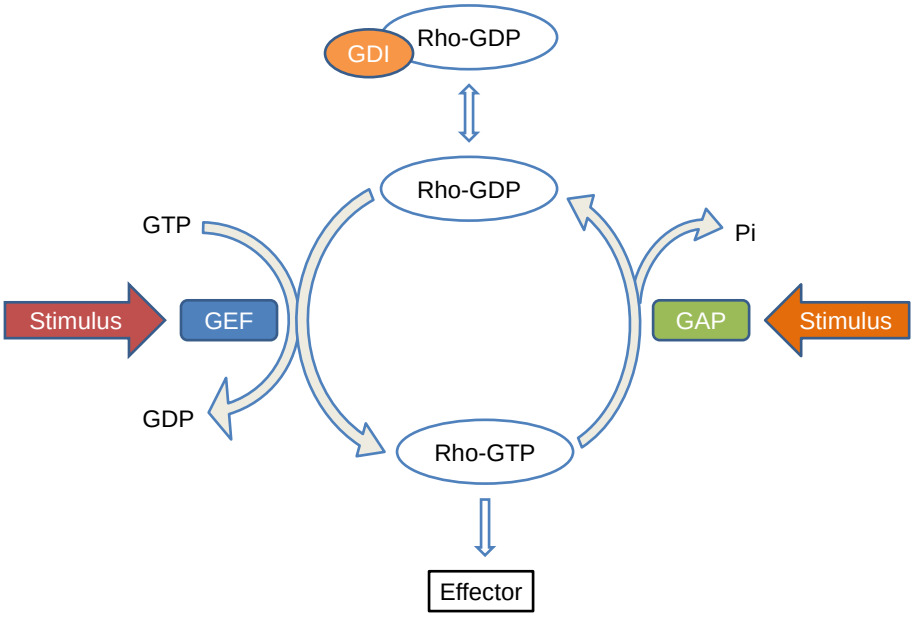

Fig. 9. The majority of Rho family GTPases cycle between the inactive GDP-bound form and the active GTP-bound form (see text for details).

guanine nucleotide-dissociation inhibitors (GDIs) bind to C-terminal prenyl groups on some GDP-bound Rho proteins, thereby sequestering them in the cytoplasm away from the upstream regulators and downstream targets [127] (Fig. 9). Among all the Rho family GTPases, Rho, Rac and Cdc42 are so far the best-understood ones. In terms of regulating the actin cytoskeleton, it is commonly agreed that the activation of Rho, Rac and Cdc42 regulates the assembly of actin-myosin filaments (stress fibers) and associated cell-substrate focal adhesion complexes, the actin filament meshwork at the cell periphery to produce protrusive lamellipodia and membrane ruffles, and the highly dynamic

finger-like actin-rich protrusions known as filopodia which are important for cells to sense the environment, respectively.

The apical and basal membrane dipolarity is critical for the normal function of epithelial cells. The homophilic interactions among E-cadherin, which produce stable cell-cell adherens junctions through the further recruitment of intracellular proteins and the actin cytoskeleton, are necessary for the establishment of cell polarity. Rho, Rac and Cdc42 are all implicated in adherens junction assembly. In addition the claudin-mediated tight junctions assembled apically to adherens junctions are also needed for cell polarity establishment, and for this process Cdc42 is considered to be a regulator [126]. Rho and Rac are involved in signaling from the extracellular environment for the establishment of epithelial cell polarity, and finally Cdc42 is required for vesicle trafficking to reinforce membrane polarity [128]. In previous research conducted in our lab, we found that in kidney epithelial cells the activity of Rac and RhoA but not Cdc42 significantly and also very quickly decreased with ATP-depletion [129]. On the other hand certain aspects of the cytoskeleton disruptions exhibited in the cell culture model of kidney ischemia can be reversed by manipulating RhoA activity [130-132]. Our research has established that Rho GTPases signaling is very important to the process through which the energy and ATP level decrease leads to actin cytoskeleton dysregulation during kidney ischemia, and the next step of our study will be to elucidate how the GTPase signaling is affected during ATP-depletion. We propose that the AMP-activated protein kinase (AMPK), whose regulation and activity acts as an ultrasensitive system for monitoring cellular energy change in all eukaryotic cells, which was also found to be important for the maintenance of epithelial cell polarity [133-135], works upstream of Rho GTPases

signaling when Rho GTPase activity changes quickly as a response to the decrease of energy and ATP level upon kidney ischemia.

AMP-activated protein kinase

AMPK was initially identified as a mammalian protein kinase that phosphorylates and inactivates enzymes of lipid synthesis, for example acetyl-CoA carboxylase, and this is still considered to be one of the major cellular functions of AMPK [136]. Mammalian AMPK is highly sensitive to the cellular AMP/ATP ratio and is primarily activated by metabolic stresses that either disrupt the synthesis of ATP or stimulate the consumption of ATP.

Figure 10. The regulation of AMPK by energy level

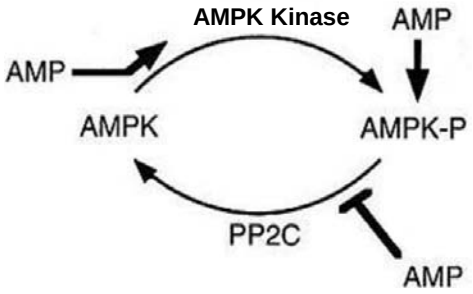

Fig. 10. The Thr172 phosphorylation and kinase activity of AMPK are regulated by ATP and AMP levels (see text for details).

AMPK exists as a hetero-trimeric complex composed of catalytic α subunit and scaffolding β subunit and regulatory γ subunit. The binding of AMP to the γ subunit stimulates the kinase activity of the α subunit, and also promotes the phosphorylation of

Thr172 residue in the kinase domain of the α subunit by upstream kinases, such as tumor suppressor LKB1 and calmodulin-dependent protein kinase kinase β. The phosphorylation of Thr172 residue is essential for the kinase activity of AMPK, and also is frequently studied as an indicator of AMPK activity [137]. Meanwhile AMP inhibits the dephosphorylation of Thr172 in the α subunit, and this effect of AMP is antagonized by high concentration of ATP [138, 139] (Fig. 10). That is the mechanism by which AMPK works as an energy sensor.

Since the discovery of AMPK, it has been extensively studied in terms of its regulation of glucose uptake, gene transcription, cell growth and proliferation, and most recently its regulation of the establishment and maintenance of cell polarity. For the regulation of cell growth and proliferation, one of the downstream targets of AMPK is mammalian target of rapamycin (mTOR) complex (Fig. 11), a critical integrator of both intracellular and extracellular signals leading to cell growth and survival [140]. AMPK directly phosphorylates TSC2 (tuberous sclerosis complex) protein which forms a heterodimer protein complex with TSC1 *in vivo* [141]. The phosphorylation of TSC2 by AMPK stimulates its GAP (GTPase activating protein) function on downstream effectors, one of which is Rheb protein [142]. Rheb has a low basal level of GTPase activity and has been identified as a regulator of the mTOR complex 1. Both GDP-bound and GTP-bound Rheb bind directly with mTOR complex 1, but only the GTP-bound Rheb stimulates mTOR complex 1 activity [143]. AMPK was recently found to phosphorylate directly one of the components of mTOR complex 1, Raptor, on two well-conserved serine residues, and this phosphorylation is required for the inhibition of mTOR complex 1 induced by energy stress [144].

Figure 11. From AMPK activation to actin cytoskeleton dysregulation

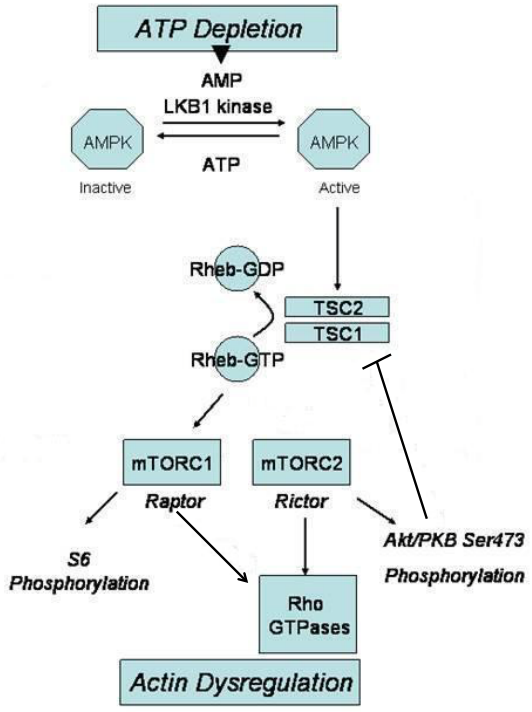

Fig. 11. We propose that AMPK acts as a sensor of energy and ATP level decrease in kidney ischemia and depresses the activity of signaling pathways through TSC1/2, Rheb GTPase and mTOR kinase in mTOR complexes, leading to disrupted Rho GTPase activity and eventually cytoskeletal dysregulation (see text for details).

mTOR complex

The TOR1 and TOR2 genes were initially identified in the study of yeast cell cycle arrest caused by immunosuppressive drug rapamycin [145, 146]. Subsequently the TOR genes were also discovered in higher eukaryotes, including mammals. Since then mTOR has been extensively studied because of its essential role in cell growth and its

involvement in human tumorigenesis. The mTOR kinase is an atypical serine/threonine protein kinase with a predicated molecular weight of 290 kDa, and *in vivo* it exists within even bigger protein complexes. Two major protein complexes containing mTOR, which are termed mTOR complex 1 and mTOR complex 2, have been identified so far [147]. The mTOR complex 1 has been identified as an important regulator of protein synthesis. The active mTOR complex 1 binds to the eIF3 (eukaryotic initiation factor 3) and phosphorylates the S6K1 and 4EBP1 that are bound to eIF3 under basal conditions. The phosphorylation of S6K1 and 4EBP1 eventually leads to the stimulation of protein translation [148]. The mTOR complex 1 is composed of mTOR, Raptor and mLST8, and is sensitive to rapamycin inhibition. So far, four components, mTOR, Rictor, Sin1 and mLST8 have been identified in mTOR complex 2, which is generally considered to be insensitive to rapamycin, although there is data suggesting that prolonged rapamycin treatment inhibits the assembly of mTOR complex 2 and also affects its downstream signaling [149]. Unlike mTOR complex 1, the major cellular function of mTOR complex 2 has been identified as the control of actin cytoskeleton and it is suggested to work at the upstream of Rho GTPases [150, 151]. In our previous research, we also found that when either mTOR or Rictor protein expression was knocked down with siRNA in renal epithelial cells, the RhoA activity decreased in parallel.

Although the study of mTOR complex 1 had been historically focused on its regulation of cell growth and proliferation, recent research showed that it was also involved in the regulation of actin cytoskeleton. In different types of human tumor cells, rapamycin treatment was found to inhibit type I insulin growth factor-stimulated cell motility by preventing F-actin reorganization and inhibiting the phosphorylation of focal

adhesion proteins. The inhibitory effect of cell motility by rapamycin was found to be mediated through the inhibition of the kinase activity of mTOR complex 1. Meanwhile the disruption of either mTOR complex 1 or mTOR complex 2 by knocking down protein expression of either Raptor or Rictor with shRNA inhibited cell motility [152,153].

Study outline

Previously AMPK was found to be activated *in vivo* by acute renal ischemia in animal model (induced by cross-clamping the renal pedicle in the rat) [154]. In our study we also found that AMPK was activated after 30 minutes ATP-depletion in an *in vitro* model of ischemic injury in cultured renal epithelial cells (mouse S3 cell line). Our unpublished study showed that ATP-depletion decreased the phosphorylation of mTOR at the Ser2448 (which is considered to be the indicator of overall mTOR kinase activity level [155]). Therefore we propose that AMPK acts as a sensor of energy and ATP level decrease in kidney ischemia and depresses the activity of signaling pathways through TSC1/2, Rheb GTPase and mTOR kinase in mTOR complex, leading to disrupted Rho GTPase activity and eventually cytoskeletal dysregulation.

To test this hypothesis we used S3 epithelial cells derived from the proximal tubule in mouse kidney in a cell culture model of renal ischemia using antimycin A and substrate depletion to induce ATP depletion. In this study we used the phosphorylation of Thr172 of the AMPK α-subunit as a measure of AMPK activation, and also utilized pull-down assays of GTP-bound RhoA and Rac1 to measure the GTPase activity of RhoA and Rac1 proteins. We found that AMPK was rapidly activated ($\leq$5 minutes) by ATP depletion from the low basal activity level in normal control S3 cells, and there was a

corresponding decrease in RhoA and Rac1 activity. We used graded concentrations of glucose in substrate-depleted growth medium containing antimycin A to achieve intermediate levels of ATP depletion, confirmed by HPLC analysis. We found intermediate levels of AMPK activity at these intermediate ATP levels. We also found that the GTPase activity of RhoA and Rac1 correlated inversely with the activity of AMPK. AICAR (5-aminoimidazole-4-carboxamide ribonucleoside) and the anti-diabetic drug metformin are two cell-permeable reagents that have been found to activate AMPK and are widely used in studies of AMPK [156-158]. We found that the activation of AMPK using AICAR or metformin suppressed RhoA (but not Rac1) activity, consistent with our hypothesis; meanwhile after either metformin or AICAR treatment the stress fibers of S3 cells exhibited morphological changes. Compound C, a cell-permeable small molecule chemical, is a selective, ATP-competitive inhibitor of AMPK [158, 159]. We found that treating S3 cells with compound C continuously before and during ATP-depletion partially inhibited the activation of AMPK caused by ATP-depletion, and also partially rescued the disruptions of stress fibers caused by ATP-depletion. But we did not detect a significant change of RhoA and Rac1 activity when AMPK activation during ATP-depletion was partially inhibited by compound C. Therefore our data support the hypothesis that the activation of AMPK is at the upstream of the signaling pathways downregulating RhoA activity during ATP depletion that eventually leads to actin cytoskeletal disruption.

2. Materials and Methods

Cell culture and ATP-depletion. The S3 cells were originally derived from a transgenic mouse carrying the large T antigen of the SV40 virus. They were initially isolated by microdissection of the S3 segment of the proximal tubule from this mouse. We chose this cell line instead of the LLC-PK cells due to the better availability of murine reagents and also because the proximal tubule S3 segment is particularly susceptible to ischemic injury and cytoskeletal disruption. The S3 cells were maintained in S1 medium containing 7% fetal bovine serum (FBS), 100IU/ml penicillin, 100µg/ml streptomycin at 37ºC in a humidified atmosphere of 38% O_2 and 5% CO_2. For ATP-depletion, cells were incubated in depleted DMEM (medium without amino acids, glucose, serum, and antibiotics) with 100nM antimycin A (SIGMA-Aldrich Corp.) for 30 minutes. For graded ATP-depletion, the depleted DMEM was supplemented with both 100nM antimycin A and different concentrations of glucose (500mg/L, 1000mg/L, 1500mg/L and 2000mg/L respectively).

AMPK activation and inhibition. For AMPK activation with either AICAR (EMD Chemicals Inc.) or metformin (SIGMA-Aldrich Corp.), S3 cells were treated with regular growth medium supplemented with either 2mM AICAR for 90 minutes or 10mM metformin for 4 hours before cell lysis or fixation with 3.7% paraformaldehyde. For AMPK inhibition with compound C (EMD Chemicals Inc.), S3 cells were treated with regular growth medium supplemented with 100µM compound C for 4 hours before 30 minutes ATP-depletion, and the medium during ATP-depletion was also supplemented with 100µM compound C. For control purpose, the compound C was replaced with 1% DMSO and all the other conditions were the same.

Cell lysis and Rho GTPases pull-down assay. S3 cells were grown in 35mm cell culture dishes until reaching 100% confluence and then kept for 3 to 4 days with daily feeding of fresh growth medium. The lysis buffer (25mM Tris-HCl pH7.5, 150mM potassium acetate, 5mM EDTA, 5mM EGTA, 10mM DL-Dithiothreitol, 10% glycerol, 1% Triton-X100, 60mM Octyl-β-D-Glucopyranoside) supplemented with 10mM NaF, protease inhibitors (1:200 dilution of the protease inhibitor cocktail from SIGMA-Aldrich Corp. P8340) and phosphatase inhibitors (1:100 dilution of the phosphatase inhibitor cocktail 1 from SIGMA-Aldrich Corp. P2850), was used for cell lysis. Before cell lysis, the S3 cells in 35mm dish were washed with ice-cold PBS for once, and then 150µl ice-cold lysis buffer was added into each dish. After 10 minutes incubation on ice, the cells were scraped off the dish surface. The lysis buffer containing cells was then centrifuged at 10,000 x g for 1 minute at 4ºC to remove the insoluble fractions. The supernatant was the cell lysate used for total proteins precipitation or Rho GTPases pull-down assay. Acetone was used for the total proteins precipitation from the cell lysate of S3 cells. For Rho GTPases pull-down assay, 20µl cell lysate (for RhoA pull-down) or 35µl cell lysate (for Rac1 pull-down) was added into 30µl glutathione-agarose beads that were either pre-bound with recombinant GST fusion protein containing the RhoA binding domain of Rho kinase (which only binds the GTP-bound form of RhoA), or pre-bound with recombinant GST fusion protein containing the CRIB (GTPase binding-domain) of PAK kinase (which binds the GTP-bound form of Rac and Cdc42). After 1 hour incubation on a rotator at 4ºC, the beads were then washed for three times with washing buffer (25mM Tris-HCl pH7.5, 150mM potassium acetate, 5mM EDTA, 5mM EGTA, 10mM DL-Dithiothreitol, 10% glycerol). After the washing, 50µl SDS sample buffer (50mM Tris-

HCl pH6.8, 2% SDS, 10% glycerol, 5% β-mercaptoethanol, 6M urea, 2mM EGTA, and 0.01% bromophenol blue) was added into the beads and then the beads were heated on a heating block at 80ºC for 10 minutes. The supernatant was then collected for SDS-PAGE.

Antibodies and western blotting. Western blotting was carried out with standard procedures. The primary antibodies included rabbit monoclonal phospho-AMPKα (pThr172) antibody (Cell Signaling Technology, #2535), rabbit polyclonal AMPKα antibody (Cell Signaling Technology, #2532), rabbit polyclonal RhoA antibody (Santa Cruz Biotechnology, Inc., SC-179), mouse monoclonal RhoA antibody (Santa Cruz Biotechnology, Inc., SC-418), and mouse monoclonal Rac1 antibody (Millipore Corp., clone 23A8). The secondary antibodies included peroxidase-conjugated sheep anti-mouse (GE Healthcare), peroxidase-conjugated donkey anti-rabbit (GE Healthcare).

Expression of GST-fusion proteins for Rho GTPases pulldown assay. LB plates containing carbenicillin were streaked with the glycerol stock of E-coli cells expressing the GST-fusion proteins. A single colony was picked from the LB plate and was inoculated into each of the 4 flasks of 100ml LB medium containing carbenicillin for overnight growth on shaker at 37ºC and 250 rpm. The overnight cultures were transferred into 4 flasks of 1 litre LB medium for 2 hours growth on shaker at 37ºC and 250 rpm, and then the GST-fusion proteins expression was induced with 1mM IPTG for 3 hours. The cells were collected by centrifugation at 5,000 x g for 15 minutes at 4ºC. The cell pellets were resuspended with buffer A (50mM Tris-HCl pH7.5, 50mM potassium acetate, 5mM $MgSO_4$, 10mM DL-Dithiothreitol, 10% glycerol, 50μM BHT) that was

supplemented with protease inhibitors (1:100 dilution of the protease inhibitor cocktail from SIGMA-Aldrich Corp. P8340). The cells were lysed with a French press for twice and then centrifuged for 10 minutes at 10,000 x g and 4ºC. The supernatant was collected and added into 2ml of glutathione agarose beads (50% slurry, SIGMA-Aldrich Corp.) that was pre-washed with buffer A once. The beads were incubated at 4ºC for 1 hour on a rotator and then washed with buffer B (same recipe as buffer A except 150mM potassium acetate) for twice followed by washing with buffer C (same recipe as buffer A except 500mM potassium acetate) for twice. The beads were then washed with buffer D (25mM Tris-HCl pH7.5, 1mM $MgSO_4$, 1mM DL-Dithiothreitol, 10% glycerol, 50µM BHT) for twice and kept in buffer D as 50% slurry. The beads were aliquoted and stored in liquid nitrogen for future Rho GTPases pull-down assays.

F-actin labeling and microscopy. S3 cells were grown on 10x10mm coverslips in 35 mm cell culture dishes until 80-90% confluence. The cells on coverslips were fixed with 3.7% paraformaldehyde in PBS for 10 minutes at room temperature and then permeabilized with 0.05% Triton X-100 in PBS for 5 minutes. The coverslips were blocked in blocking buffer (PBS containing 10% goat serum and 0.2% BSA) at room temperature for 30 minutes and then incubated in the same blocking buffer supplemented with 0.1µg/ml rhodamine-phalloidin (Molecular Probes) for 1 hour to label the F-actin. After brief washing in PBS, the coverslips were mounted with DABCO mounting media (10% 1,4-diazabicyclo-[2,2,2]-octane, 50% glycerol, 2% sodium azide, 1x PBS) on glass slides. The fluorescent images were collected with a Zeiss UV LSM-510 confocal microscope system.

3. Results

ATP-depletion rapidly activates AMPK

In our previous study, we found that AMPK was activated after 30 minutes of ATP-depletion in S3 cells as indicated by the significant increase of Thr172 phosphorylation level of AMPK α subunit from the very low basal level under normal growth conditions. Since we knew that the activity of RhoA and Rac1 decreased very rapidly with ATP-depletion, we investigated whether AMPK was also activated by ATP-deletion rapidly. We ATP-depleted S3 cells in a time course from 5 up to 90 minutes. We found that after only 5 minutes ATP-depletion, the phosphorylation of Thr172 already reached the highest level and then stayed at the plateau during the entire time course, which indicated that AMPK was strongly activated within only 5 minutes ATP-depletion. The result of a typical experiment is shown in Fig. 12.

RhoA and Rac1 activity correlates inversely with the activity of AMPK at different levels of ATP-depletion

Since ATP-depletion was achieved by nutrient depletion in growth media combined with antimycin A treatment, we wanted to determine whether it was the energy and ATP level decrease in S3 cells that activated AMPK or it was the drug effect of antimycin A instead. To achieve that purpose, we added different amounts of glucose into the media (0mg/L to 2,000mg/L) during ATP-depletion. The intermediate levels of ATP-depletion were confirmed by HPLC measurements of nucleotide concentrations in the acetonitrile extracts of S3 cells. With the increase of glucose concentrations, the ATP and GTP levels increased (only ATP results are shown here) while the AMP level and

Figure 12. AMPK activity during time course of ATP-depletion

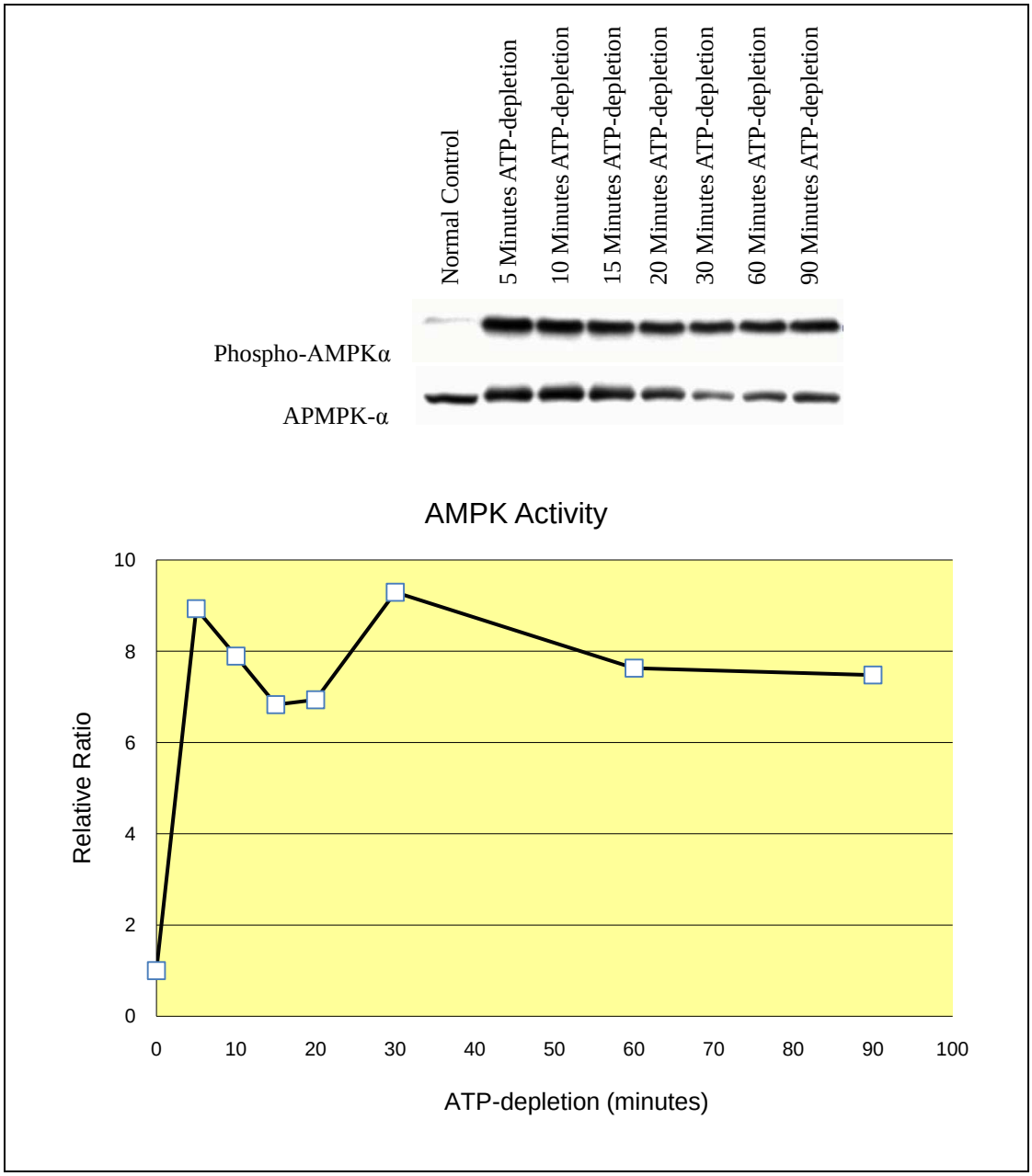

Fig. 12. AMPK was rapidly activated by ATP-depletion (≤ 5 minutes). The activity of AMPK in S3 cells was measured with the antibody against the phospho-Thr172 of AMPK α subunit, and normalized against the total AMPK.

AMP/ATP ratio decreased (Fig. 13). At these intermediate levels of ATP-depletion, AMPK exhibited intermediate levels of activity as indicated by the intermediate phosphorylation levels of Thr172 of the AMPK α subunit (Fig. 14). We also measured the RhoA and Rac1 activity separately at these intermediate levels of ATP-depletion as well as under the regular ATP-depletion and normal growth conditions by the widely-employed method of "pulling-down" the fraction of RhoA or Rac1 protein that was in the active, GTP-bound state from the lysate of S3 cells. After normalizing the amount of GTP-bound RhoA/Rac1 protein to the total RhoA/Rac1 protein in the lysate of S3 cells, we were able to compare the activity of RhoA/Rac1 under different conditions. We found that at the intermediate levels of ATP-depletion, RhoA and Rac1 also exhibited intermediate levels of GTPase activity, which was higher than after ATP-depletion without glucose supplementation, and lower than under normal growth conditions (Fig. 15A-B). These results show that the AMPK activity is inversely co-related with the energy and ATP level in S3 cells during ATP-depletion, and also inversely co-related with the GTPase activity of RhoA and Rac1. The results also indicate that AMPK activity and RhoA/Rac1 activation are not affected by antimycin A treatment per se, but rather by cellular ATP levels.

Figure 13. Nucleotide concentrations in S3 cells upon graded ATP-depletion

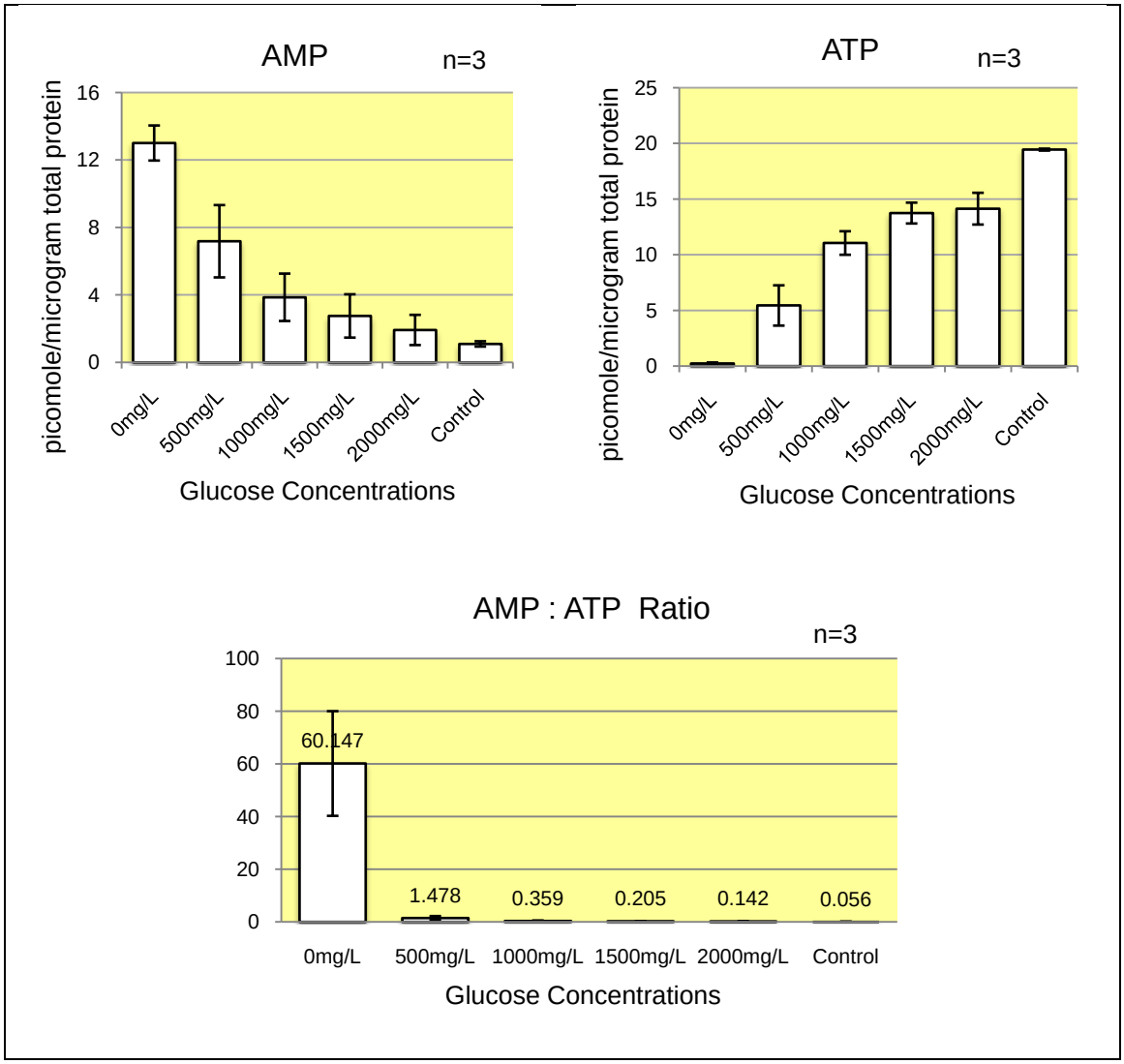

Fig. 13. Graded ATP-depletion was achieved by adding graded concentrations of glucose into the nutrient-depleted growth media containing 100nM antimycin A. Nucleotide concentrations were measured by HPLC in the acetonitrile extracts of S3 cells.

Figure 14. AMPK activity upon graded ATP-depletion

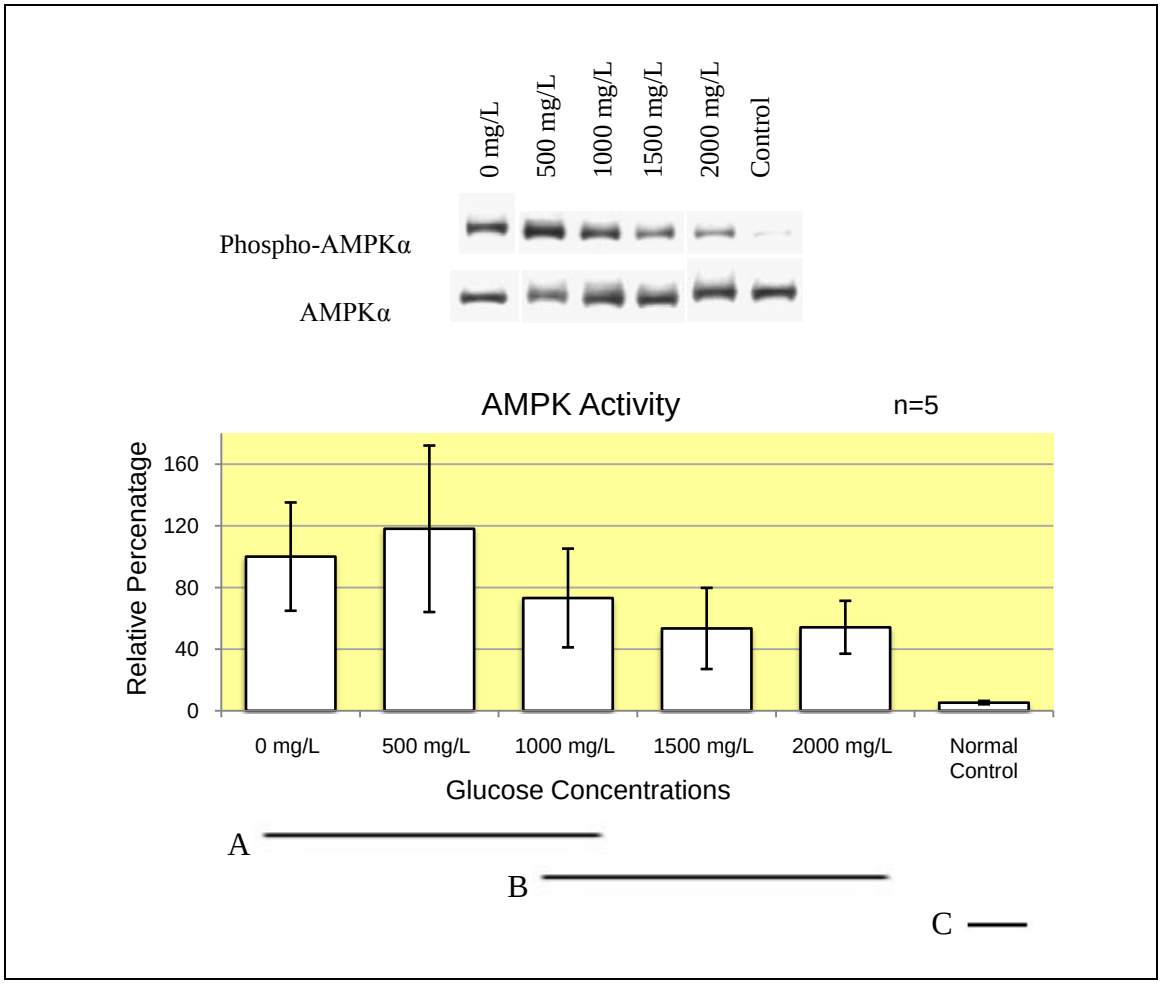

Fig. 14. AMPK exhibited intermediate levels of activity at intermediate ATP levels upon graded ATP-depletion. The activity of AMPK in S3 cells lysate was measured with the specific antibody against the phospho-Thr172 of AMPK α subunit, and normalized against the total AMPK. ATP depletion was done for 30 minutes. In each single experiment, the activity of AMPK in all the other samples are presented as percentages compared with the sample of regular ATP-depletion with 0mg/L glucose. The error bar in the column of ATP-depletion with 0mg/L glucose shows the standard deviation of AMPK

activity around the average of 5 experiment repeats. The underlines (A, B, and C) are used to group samples. The data values of samples in different groups are significantly different from each other by statistical analysis (two-way ANOVA).

Figure 15. RhoA and Rac1 activity upon graded ATP-depletion

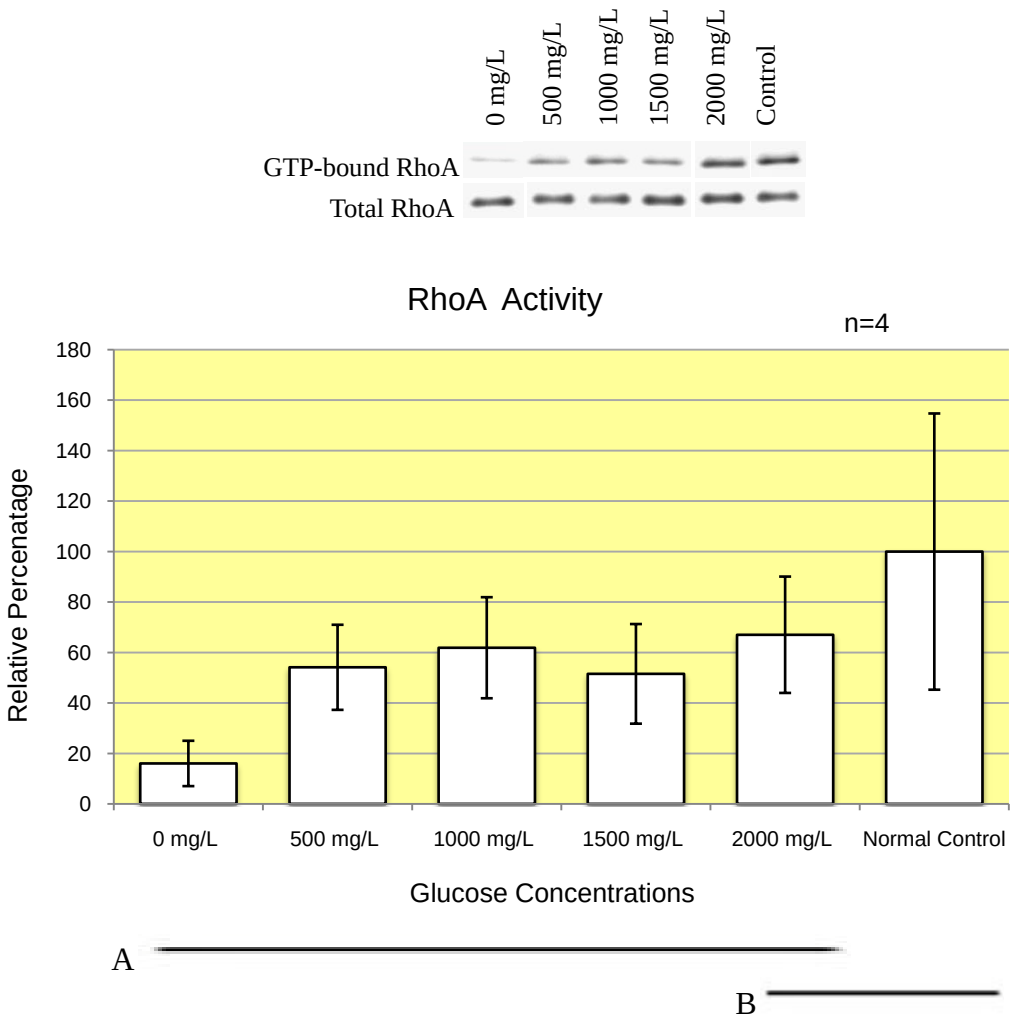

Fig. 15A. RhoA activity upon graded ATP-depletion

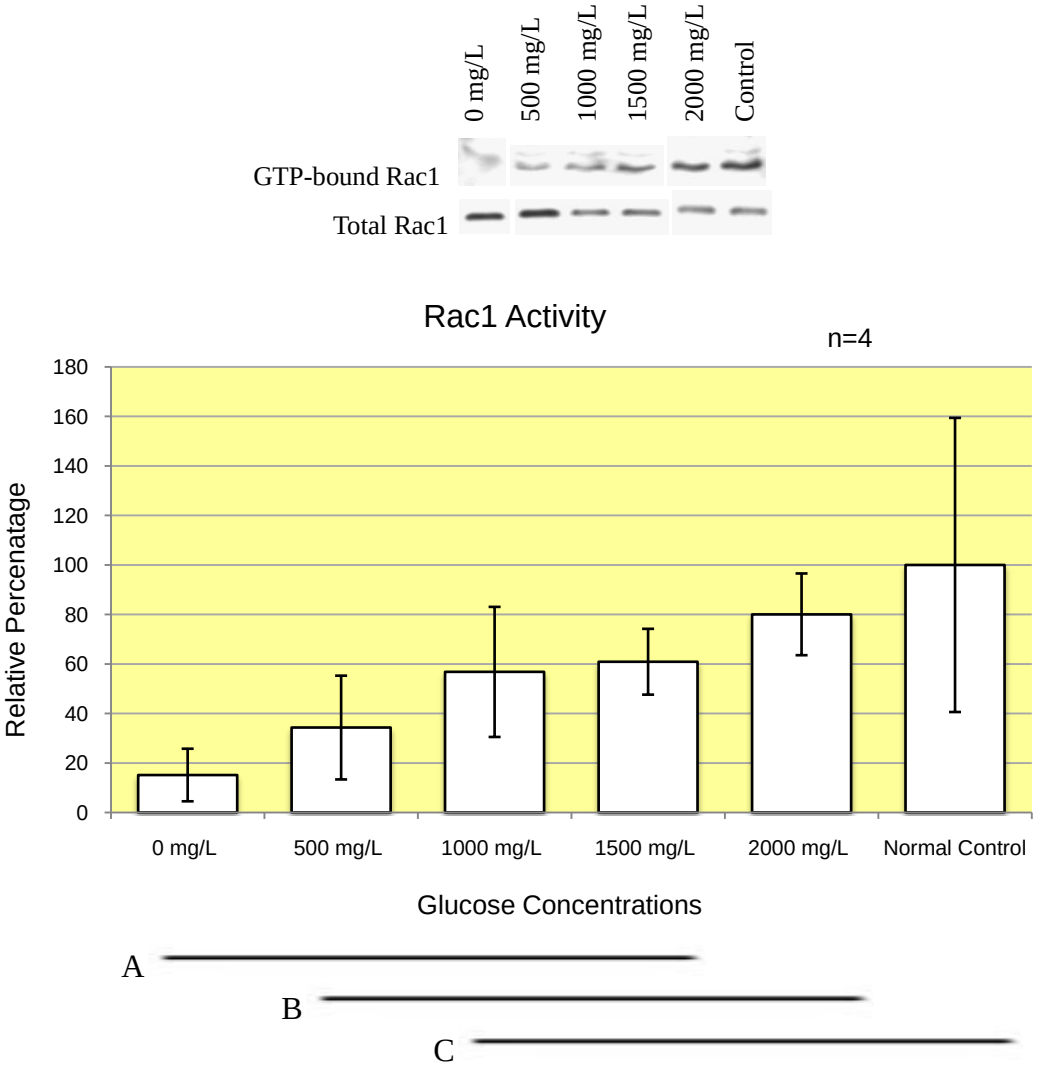

Fig. 15B. Rac1 activity upon graded ATP-depletion

Fig. 15. RhoA and Rac1 exhibited intermediate levels of activity at intermediate ATP levels upon graded ATP-depletion. The active GTP-bound RhoA was pulled-down from the lysate of S3 cells using glutathione-agarose beads pre-bound with recombinant GST fusion protein containing the RhoA binding domain of Rho kinase (which only binds the GTP-bound form of RhoA), measured with RhoA antibody, and then normalized against the total RhoA in the lysate of S3 cells. The active GTP-bound Rac1 was pulled-down

from the lysate of S3 cells using glutathione-agarose beads pre-bound with recombinant GST fusion protein containing the CRIB (GTPase binding-domain) of PAK kinase (which binds the GTP-bound form of Rac and Cdc42), measured with Rac1 antibody, and then normalized against the total Rac1 in the lysate of S3 cells. ATP depletion was done for 30 minutes. In each single experiment, the activity of RhoA or Rac1 in all the other samples are presented as percentages compared with the sample of normal control. The error bar in the column of normal control shows the standard deviation of RhoA or Rac1 activity around the average of 4 experiment repeats. The underlines (A, B, and C) are used to group samples. The data values of samples in different groups are significantly different from each other by statisctical analysis (two-way ANOVA).

Activation of AMPK inhibits RhoA activity and changes stress fiber morphology

In order to investigate whether AMPK activation is upstream of the signaling pathways that leads to the inhibition of Rho GTPases activity, we treated S3 cells with two different cell-permeable small molecule chemicals, AICAR and metformin, which were considered to activate AMPK *in vivo* by different mechanisms. We found that both AICAR (used at 2mM concentration in normal growth medium of S3 cells for 90 minutes continuous treatment) and metformin (used at 10mM concentration in normal growth medium of S3 cells for 4 hours continuous treatment) were able to activate AMPK in S3 cells as indicated by the increase of Thr172 phosphorylation level of the AMPK α subunit. Meanwhile, after AICAR activation of AMPK or metformin activation of AMPK, we also found that the GTPase activity of RhoA (but not Rac1) decreased as measured by the "pull-down" assay of GTP-bound, active RhoA (or Rac1) (Fig. 16 and Fig. 17), although

the decrease of the RhoA activity after metformin activation of AMPK was not statistically significant, which could be due to the small number of experiment repeats.

Figure 16. AMPK activation by AICAR inhibits RhoA activity, but not Rac1

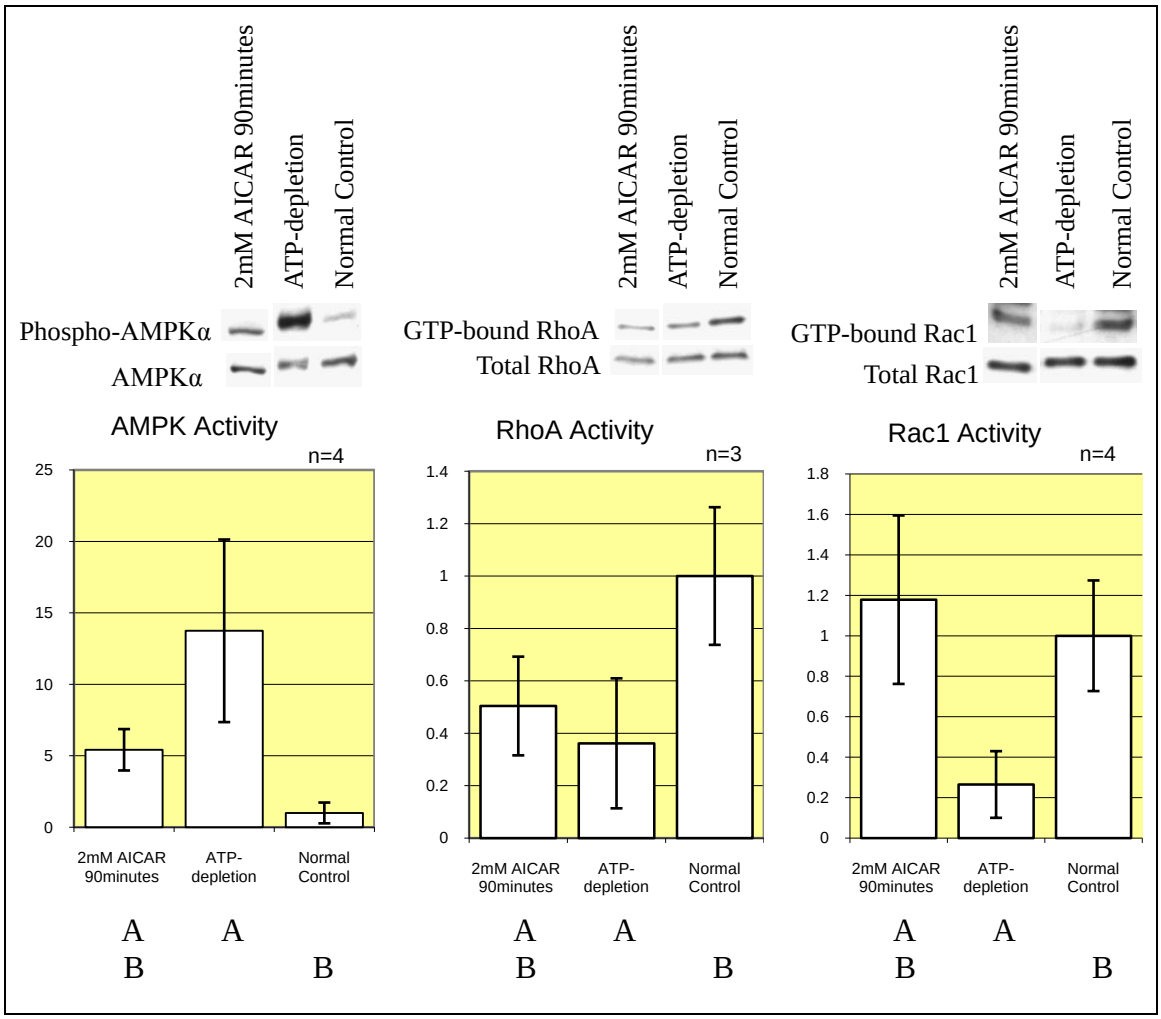

Fig. 16. AICAR treatment of S3 cells under normal growth conditions activated AMPK and suppressed RhoA activity, but had no significant effect on Rac1 activity. AICAR in aqueous stock solution was used at 2mM for 90 minutes treatment of S3 cells. The activity of AMPK, RhoA and Rac1 was measured respectively as previously described.

In each single experiment, the activity of AMPK, RhoA or Rac1 in all the other samples are presented as the ratios compared with the sample of normal control. The error bar in the column of normal control shows the standard deviation of the activity of AMPK, RhoA or Rac1 around the average of experiment repeats. The letters of A and B under the column charts label and group samples. The data values of samples in different groups are significantly different from each other by statisctical analysis (two-way ANOVA).

Figure 17. AMPK activation by metformin may inhibit RhoA activity, but not Rac1

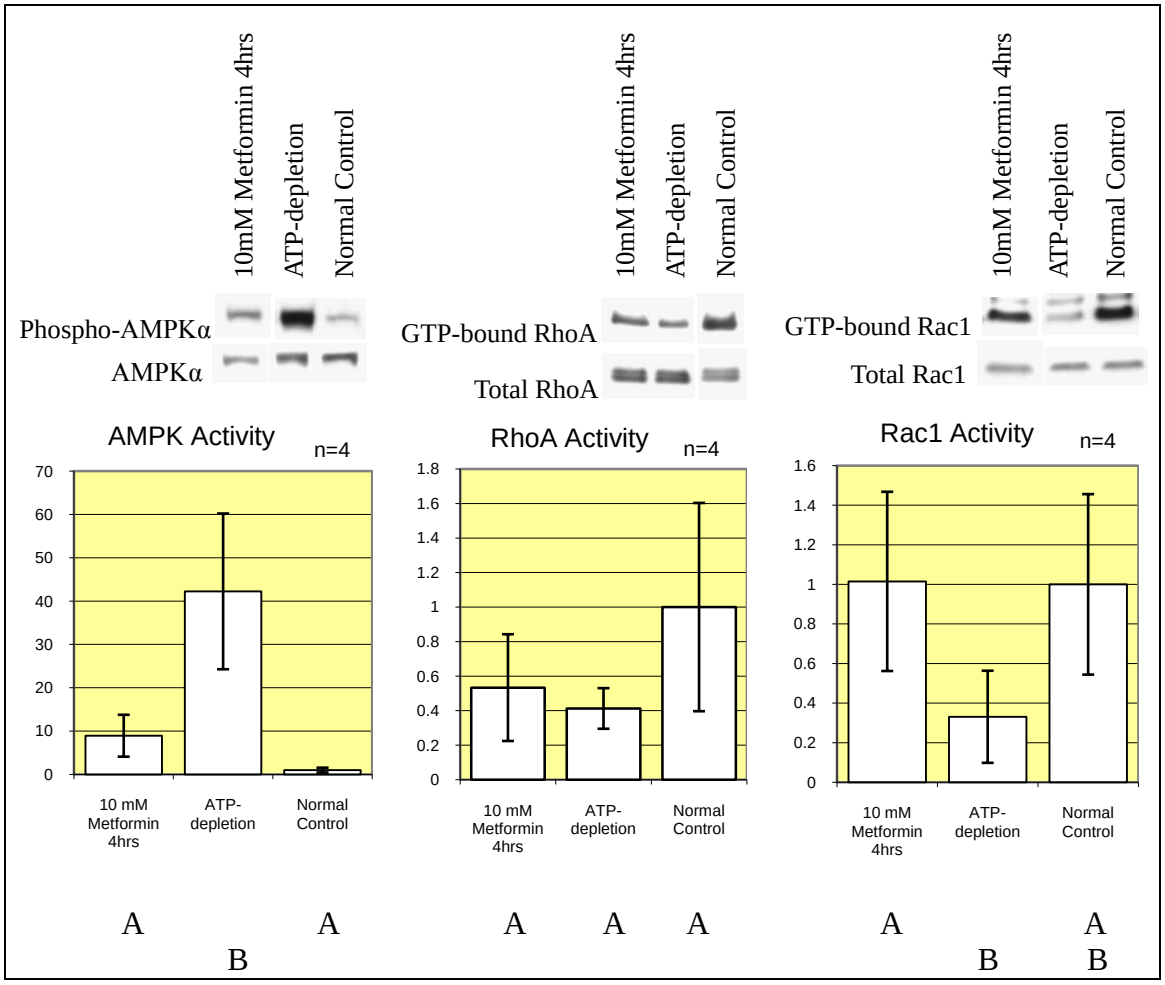

Fig. 17. Metformin treatment of S3 cells under normal growth conditions activated AMPK and might suppress RhoA activity, but had no significant effect on Rac1 activity. Metformin in aqueous stock solution was used at 10mM for 4 hours treatment of S3 cells. The activity of AMPK, RhoA and Rac1 was measured respectively as previously described. In each single experiment, the activity of AMPK, RhoA or Rac1 in all the other samples are presented as the ratios compared with the sample of normal control. The error bar in the column of normal control shows the standard deviation of the activity

of AMPK, RhoA or Rac1 around the average of experiment repeats. The letters of A and B under the column charts label and group samples. The data values of samples in different groups are significantly different from each other by statisctical analysis (two-way ANOVA).

We were also interested in the possible changes of actin cytoskeleton after AMPK activation. We labeled the F-actin in S3 cells with rhodamine-conjugated phalloidin. The results showed that the activation of AMPK with either AICAR or metformin induced similar morphological changes of stress fibers in S3 cells. After treating S3 cells with either AICAR or metformin, there was not such a global and total disruption of actin cytoskeleton in S3 cells as seen during ATP-depletion, instead the stress fibers appeared to be considerably thicker and more bundled in comparison with the control S3 cells under normal growth conditions (Fig. 18 and Fig. 19), which indicated that the actin cytoskeleton was affected by AMPK activation with AICAR or metformin treatment.

Figure 18. AMPK activation by AICAR induced morphological changes of stress fibers

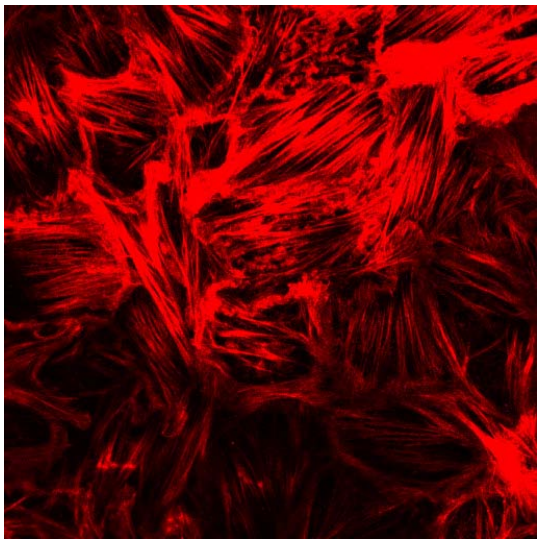

A. AICAR treatment

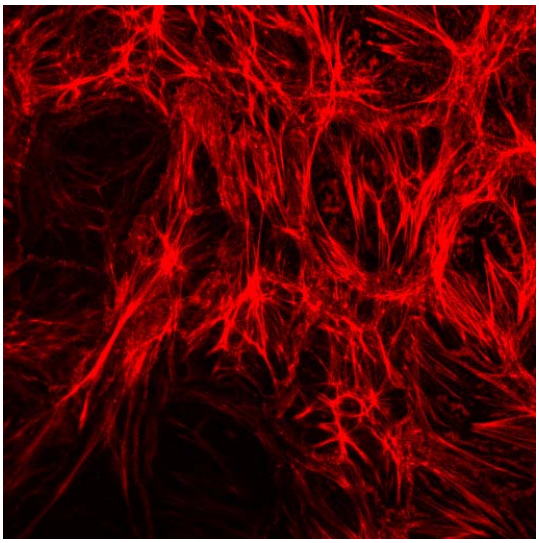

B. Normal control

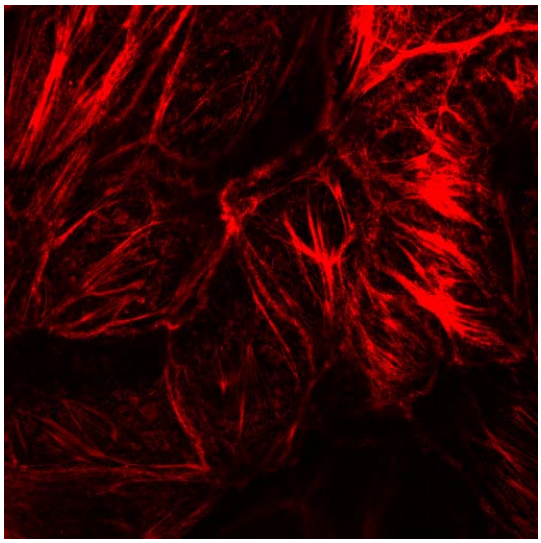

C. ATP-depletion

20 μm

Fig. 18. AMPK activation by AICAR induced morphological changes of stress fibers in S3 cells. The F-actin in S3 cells were labeled with rhodamine-phalloidin. The stress fibers in S3 cells after 90 minutes treatment with 2mM AICAR (Fig. 18A) appeared to be considerably thicker and more bundled in comparison with the control S3 cells (Fig. 18B) under normal growth conditions. C shows S3 cells after 30 minutes ATP-depletion for comparison.

Figure 19. AMPK activation by metformin induced morphological changes of stress fibers

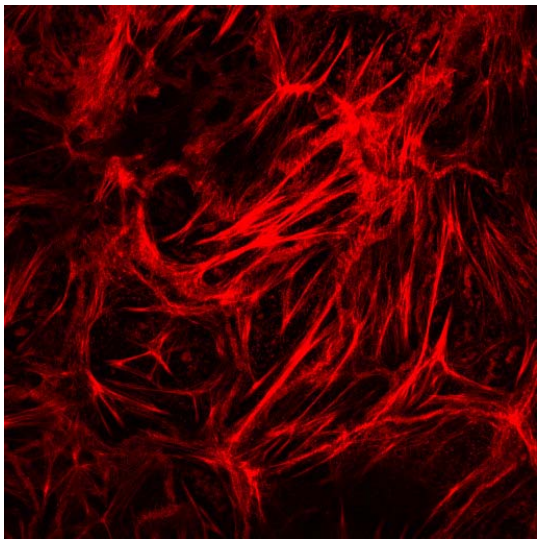

A. Metformin treatment

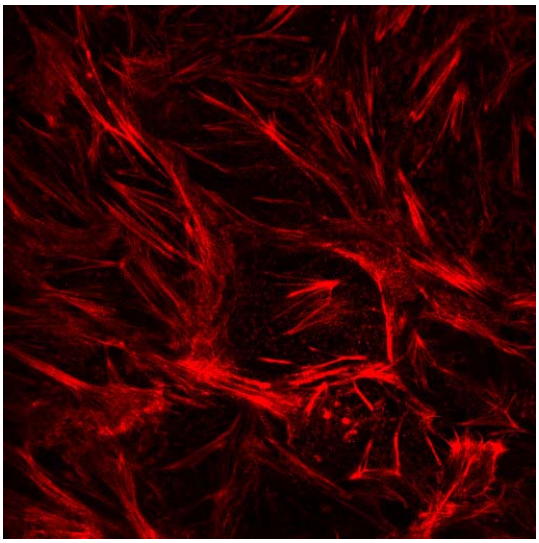

B. Normal control

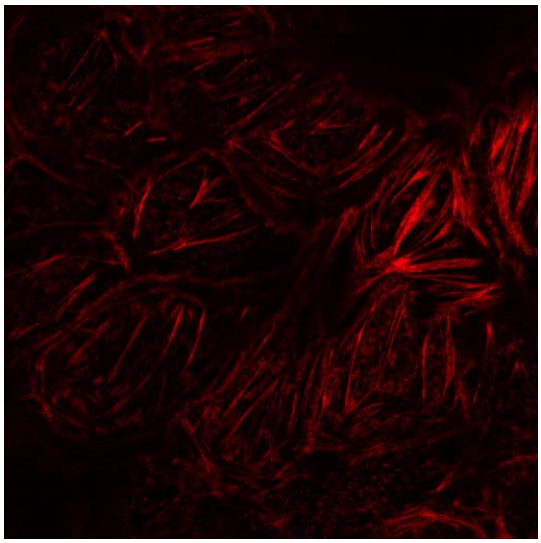

C. ATP-depletion

20 μm

Fig. 19. AMPK activation by metformin induced morphological changes of stress fibers in S3 cells. The F-actin in S3 cells were labeled with rhodamine-phalloidin. The stress fibers in S3 cells after 4 hours treatment with 10mM metformin (Fig. 19A) appeared to be considerably thicker and more bundled in comparison with the control S3 cells (Fig. 19B) under normal growth conditions. C shows S3 cells after 30 minutes ATP-depletion for comparison.

Inhibition of AMPK activation partially rescues stress fibers disruption during ATP-depletion

In order to further investigate how the activation of AMPK during ATP-depletion affects the Rho GTPases activity and actin cytoskeleton, we utilized the strategy of inhibiting AMPK activation during ATP-depletion. The Compound C, a cell-permeable small molecule chemical, is a selective, ATP-competitive inhibitor of AMPK. It has been frequently used to inhibit AMPK activity in previous studies related to AMPK. We pre-treated S3 cells with 100μM compound C for 4 hours before ATP-depletion and also added 100μM compound C into the medium during ATP-depletion. We found that the treatment with compound C inhibited activation of AMPK during ATP-depletion in S3 cells, as indicated by the decrease of Thr172 phosphorylation level of AMPK α subunit (Fig. 20); although we failed to detect significant change of GTPase activity of either RhoA or Rac1 as measured by the "pull-down" assay of GTP-bound, active RhoA (or Rac1) after inhibition of AMPK activation with compound C during ATP-depletion (data not shown here). However when we labeled the F-actin in S3 cells with rhodamine-conjugated phalloidin, we found some thin, continuous and longer stress fibers in the S3

cells after using compound C to inhibit AMPK activation during ATP-depletion (Fig. 21). Such stress fibers exist in S3 cells under normal growth condition, but not in S3 cells with severe actin cytoskeleton disruptions after ATP-depletion. Therefore our results showed that the inhibition of AMPK activation by the compound C treatment during ATP-depletion partially rescued the actin cytoskeleton dysregulation during ATP-depletion.

Figure 20. Compound C inhibited AMPK activation during ATP-depletion

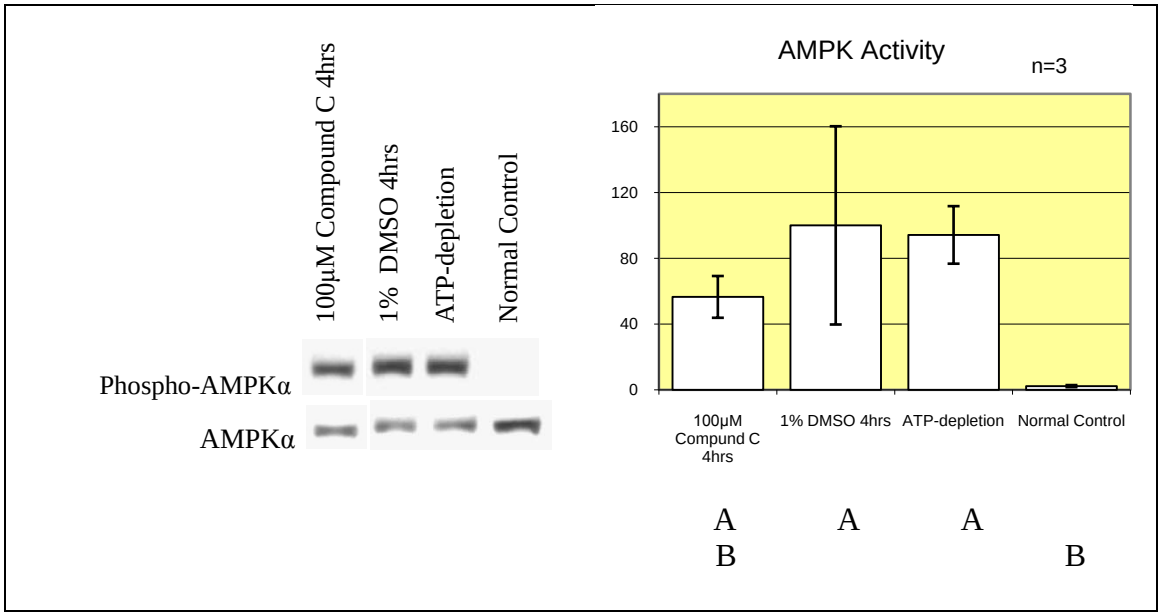

Fig. 20. Compound C treatment of S3 cells during ATP-depletion inhibited AMPK activation as indicated by the Thr172 phosphorylation level decrease of AMPK α subunit in comparison with S3 cells after only regular ATP-depletion or after ATP-depletion with DMSO (solvent of compound C) treatment. Compound C in DMSO stock solution was used at 100μM for 4 hours treatment of S3 cells immediately before ATP-depletion and

also used at 100μM during 30 minutes ATP-depletion. DMSO was used at 1% under the same treatment conditions as a control of compound C. In each single experiment, the activity of AMPK in all the other samples are presented as percentages compared with the sample of 1% DMSO treatment. The error bar in the column of 1% DMSO treatment shows the standard deviation of the activity of AMPK around the average of 3 experiment repeats. The letters of A and B under the column chart label and group samples. The data values of samples in different groups are significantly different from each other by statisctical analysis (two-way ANOVA).

Figure 21. Inhibition of AMPK activation partially rescued stress fiber disruption during ATP-depletion

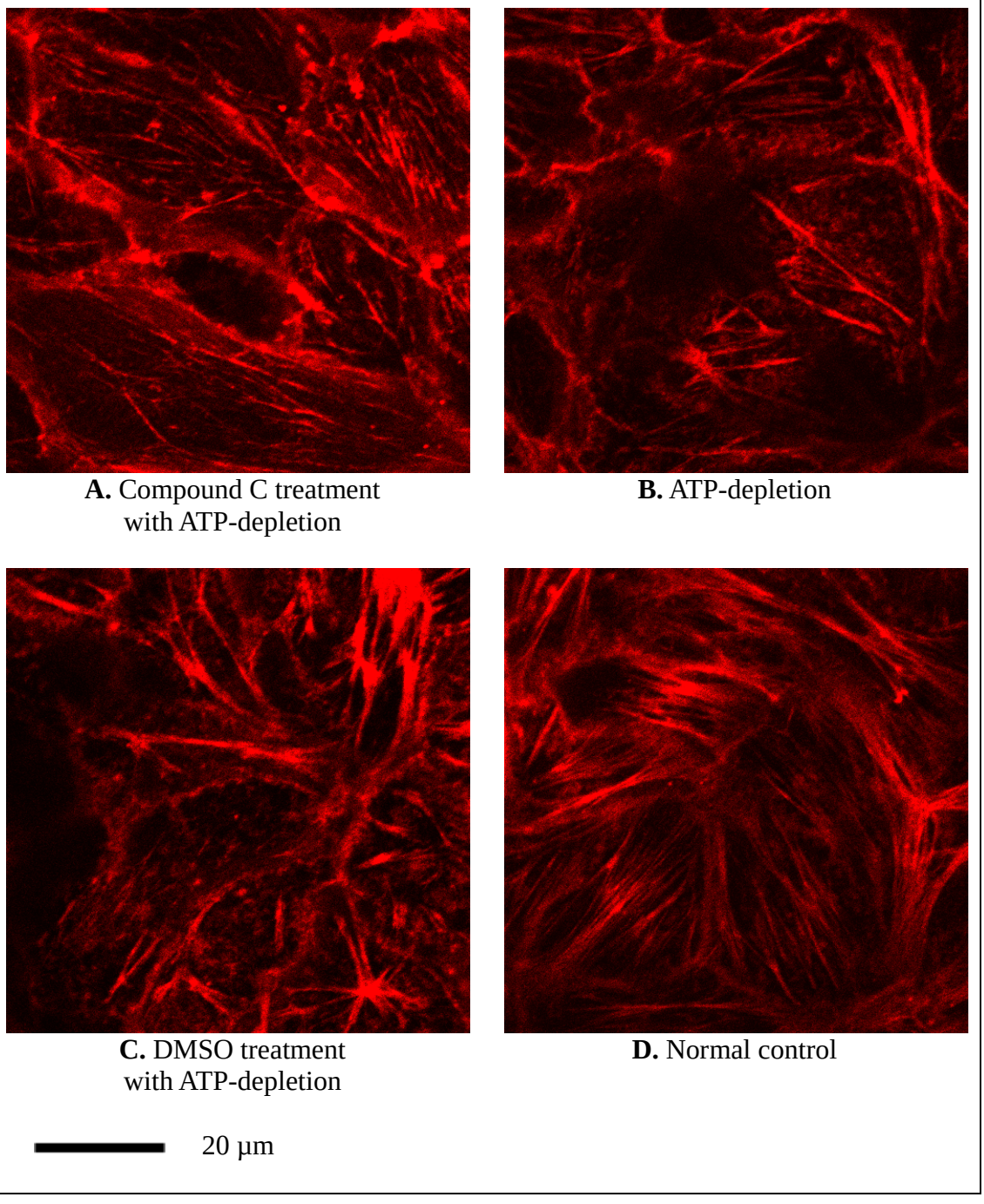

A. Compound C treatment with ATP-depletion

B. ATP-depletion

C. DMSO treatment with ATP-depletion

D. Normal control

20 µm

Fig. 21. The F-actin in S3 cells were labeled with rhodamine-phalloidin after different treatments. Some thin, continuous and longer stress fibers existed in the S3 cells after ATP-depletion with inhibition of AMPK activation by the compound C treatment (Fig. 21A), but not in either the S3 cells after only regular ATP-depletion (Fig. 21B) or after ATP-depletion with DMSO (solvent of Compound C) (Fig. 21C) treatment. Fig. 21D shows the F-actin staining (mostly stress fibers) in the S3 cells under normal growth conditions.

4. Discussion

Rho GTPases play a critical role in the regulation of actin cytoskeleton. In our previous study, we found that in kidney epithelial cells the activity of Rac and RhoA but not Cdc42 significantly and also very quickly decreased with ATP-depletion/ischemia. The GTP level decrease during ATP-depletion cannot fully explain the GTPase activity decrease of Rho and Rac, because the GTP level is still considerably higher than the Km for GTP of Rho and Rac during ATP-depletion [160], and also because the rate of RhoA inactivation during ischemia/ATP-depletion is so rapid that it cannot be explained by the intrinsic rate of nucleotide exchange or hydrolysis. Taken together, these point to upstream signaling pathways which are activated or inactivated during ischemia and lead to the downregulation of Rho GTPases activity. In this study we propose these signaling pathways are initiated through the activation of the ultra-sensitive cellular energy sensor AMP-activated protein kinase (AMPK). We found that within 5 minutes of ATP-depletion AMPK was strongly activated, which suggested that AMPK was extremely sensitive to the energy level change in kidney epithelial cells.

Since the ATP-depletion was achieved by antimycin A treatment of S3 cells in serum-free substrate-depleted medium, we tested whether AMPK responded to different ATP and energy levels, and if the rapid activation of AMPK during ATP-depletion was due to the antimycin A treatment instead. By supplementing the medium with different concentrations of glucose (500-2000mg/L) during ATP-depletion, we were able to induce intermediate ATP and energy levels (between the levels after regular ATP-depletion and under normal growth conditions). Even though the activity level of AMPK after ATP-depletion with lower concentrations of glucose supplementation did not appear to be

significantly different from after regular ATP-depletion with no glucose supplementation, we did find that the AMPK activity decreased when the glucose concentration increased with the overall energy/ATP level (as measured with HPLC) being closer to the level under normal growth conditions. The “pull-down” assays of GTP-bound active RhoA and Rac1 showed that they also exhibited intermediate levels of GTPase activity upon glucose supplementation. At lower concentrations of glucose supplementation, the activity of RhoA and Rac1 was still higher than after regular ATP-depletion without glucose supplementation. This may suggest that when the severity of ischemia and ATP-depletion reaches a certain level, upstream regulators other than AMPK further contribute to the inactivation of Rho GTPases. Overall these results confirm a correlation among energy/ATP level decrease, AMPK activation and Rho GTPases inactivation during ATP-depletion in kidney epithelial cells.

To further investigate the relationship between activation of AMPK and Rho GTPases inactivation, we attempted to manipulate the AMPK activity in S3 cells and expected to find a subsequent effect on Rho GTPases activity. AICAR and metformin are two drugs widely-used to activate AMPK in previous studies. The mechanism of metformin activating AMPK is still unclear. There was a report that metformin increased the cytosolic concentration of AMP in the heart, and therefore activated AMPK [161]. AICAR is metabolized into ZMP in cells, which is an AMP analogue and activates AMPK. After the treatment of S3 cells with either metformin or AICAR, there was an activation of AMPK as shown by the increase in Thr172 phosphorylation level of AMPK α subunit. We also detected a decrease of RhoA activity in S3 cells after treatment with AICAR and also after treatment with metformin (although the latter difference was not

statistically significant), in comparison with S3 cells under only normal growth conditions. Although there was a report showing that AMPK activation affected Rac1 activity in muscle cells [162], we did not find significant change of Rac1 activity upon AMPK activation by metformin or AICAR. This could be due to the activation of AMPK by these two drugs still not being strong enough to affect Rac1 activity in S3 epithelial cells, or possibly because other signaling pathways make major contributions to the inactivation of Rac1 during ATP-depletion and ischemia. When we treated S3 cells with either AICAR or metformin, we found that the stress fibers in S3 cells were considerably thicker and more bundled than under normal growth conditions. These results were different from our initial expectations since we expected that after AMPK activation and partial inhibition of RhoA activity with these drug treatments, the actin cytoskeleton would be dysregulated and exhibit morphology more resembling that after ATP-depletion. It is possible that in addition to AMPK activation, AICAR and metformin also affect other signaling pathways which have stronger effects on actin cytoskeleton and lead to these morphological changes. These findings indicate that AMPK activation does affect Rho GTPase signaling pathways and actin cytoskeleton, but the real mechanisms are more complex than our initial hypothesis, particularly in terms of its effect on the actin cytoskeleton.

In addition to activating AMPK with metformin and AICAR, we treated S3 cells with another drug, compound C which enabled us to inhibit partially the activation of AMPK caused by ATP-depletion. Such an inhibition partially rescued the drastic stress fibers disruption caused by ATP-depletion, but we did not find significant change of RhoA or Rac1 activity at the same time. One possible explanation is that the changes of

RhoA and/or Rac1 activity upon compound C treatment during ATP-depletion localized at the actin cytoskeleton and these fractions of RhoA and/or Rac1 were not fully recovered by the lysis buffer; therefore we were unable to detect the actual changes.

In addition to activating AMPK with metformin and AICAR, we also attempted to express different types of AMPK mutants (dominant negative mutant, constitutively active mutant, etc.) in S3 cells by transient transfection of plasmids encoding these mutants. For some unclear reasons, the transfection of these plasmids was not successful. We also attempted to manipulate AMPK activity in S3 cells by knocking down AMPK expression with siRNA targeting against the AMPK α subunit. After transfection of such siRNA into S3 cells, we were able to knock down the expression of AMPK α subunit by 60-70%, and there was a similar extent of AMPK activity decrease (as shown by the decrease of Thr172 phosphorylation level of AMPK α subunit) during ATP-depletion in these S3 cells with siRNA transfection. However we did not detect a significant change of either RhoA or Rac1 activity in the same experiment. Possibly the more significant knockdown of AMPK expression is necessary to induce the reversal of Rho GTPases inactivation during ATP-depletion and ischemia. In the future, we would like to construct lentiviral vectors or other viral vectors encoding different types of AMPK mutants or shRNA against AMPK α subunit in order to manipulate AMPK activity more significantly. Stronger changes of AMPK activity than what we have been able to achieve by drug treatment or SiRNA knock-down will probably enable us to investigate more informatively the relationship between AMPK activation and Rho GTPases inactivation.

In this study, we propose that ATP-depletion and ischemia activates AMPK which further depresses the activity of signaling pathways through TSC1/2, Rheb GTPase and mTOR kinase in mTOR complex, leading to disrupted Rho GTPase activity and eventually cytoskeletal dysregulation. There was also a study suggesting that independently from mTOR complex pathway, TSC1 inhibits Rac1 activity and activates Rho activity through the antagonism between Rac1 and Rho, and this effect of TSC1 is blocked upon TSC2 binding to form TSC1/2 complex [163].

Since the mTOR kinase exists *in vivo* in both mTOR complex 1 and mTOR complex 2 that have different components, the question arises as to which mTOR complex plays the major role in the signaling pathways proposed by us. Although mTOR complex 2 has been deemed to be an actin cytoskeleton regulator, and it may signal to actin cytoskeleton through Rho and Rac [151]; there has not been any evidence showing that its activity is regulated by Rheb GTPase as mTOR complex 1 is. A recent study actually suggested that TSC1/2 complex physically associated with mTOR complex 2 and was required for the proper activation of mTOR complex 2 kinase activity [164]. The same study also suggested that the ability of TSC1/2 complex to promote mTOR complex 2 kinase activity was separate from its GAP activity toward Rheb GTPase. Meanwhile some recent studies have confirmed that the kinase activity of mTOR complex 1 is indeed involved in the regulation of actin cytoskeleton [152, 153]. Another recent study showed that AMPK inhibited the kinase activity of mTOR complex 1 by phosphorylating one of its components, Raptor, directly [144]. Therefore it is highly possible that it is mTOR complex 1 instead of mTOR complex 2 that is directly involved in the signaling pathways from AMPK activation to Rho GTPases inactivation during

ATP-depletion and ischemia as proposed by us. As for the effect of mTOR complex 2 kinase activity on actin cytoskeleton regulation, it could be indirect through mTOR complex 1. MTOR complex 2 has been found to phosphorylate Ser473 of Akt/protein kinase B (PKB), which is critical for the activation of Akt/PKB [165, 166]. Akt/PKB directly phosphorylates TSC2 in TSC1/2 complex on multiple sites, and this phosphorylation inhibits the GAP activity of TSC1/2 complex, thus upregulating mTOR complex 1 activity. Akt/PKB can also phosphorylate PRAS40 (proline-rich Akt substrate 40 kDa) and this phosphorylation appears to release the inhibition of PRAS40 on kinase activity of mTOR complex1 possibly by disrupting its binding with mTOR complex 1 (whether it is a component of mTOR complex 1 remains to be determined) [167, 168]. Therefore the inactivation of mTOR complex 2 could lead to the inhibition of mTOR complex 1 through Akt/PKB with further downstream effects on Rho GTPases and actin cytoskeleton.

In order to determine which mTOR complex is involved in the signaling pathways that we proposed, one possible strategy in our future work will be to treat S3 cells with rapamycin and investigate the possible Rho GTPases activity changes and actin cytoskeleton disruptions since mTOR complex 2 is not sensitive to rapamycin (or at least not responding to acute rapamycin treatment as significantly as mTOR complex 1). We might also knock down the protein expression of Raptor (which is the component of mTOR complex 1 but not mTOR complex 2) with SiRNA as another strategy to resolve the question of “1 or 2”.

5. Summary

The dysregulation of Rho GTPase signaling pathways is a critical mediator of the effects of ATP depletion and ischemia on the actin cytoskeleton, but the mechanism by which ATP depletion leads to altered RhoA and Rac1 activity is unknown. The AMP-activated protein kinase (AMPK) is a key metabolic regulator that senses the cellular ATP/AMP ratio. Renal ischemia *in vivo* has been shown to activate AMPK. We propose that ischemia and ATP depletion result in activation of AMPK and that this affects Rho GTPase activity and cytoskeletal organization (possibly via TSC1/2 complex and/or mTOR complex). To test this hypothesis we used S3 epithelial cells derived from the proximal tubule in mouse kidney in a cell culture model of renal ischemia using antimycin A and substrate depletion to induce ATP depletion. We used the phosphorylation of Thr172 of the AMPK α-subunit as a measure of AMPK activation, and also used pull-down assays to measure the GTPase activity of RhoA and Rac1 proteins. AMPK was rapidly activated ($\leq$ 5 minutes) by ATP depletion, and there was a corresponding decrease in RhoA and Rac1 activity. We used graded concentrations of glucose in the nutrient-depleted growth medium containing antimycin A to achieve intermediate levels of ATP depletion, confirmed by HPLC analysis. We found intermediate levels of AMPK activity at these intermediate ATP levels while the activity of both RhoA and Rac1 correlated inversely with the activity of AMPK. AICAR or metformin treatment activated AMPK in S3 cells, and the RhoA activity was suppressed by AICAR or metformin activation of AMPK. This is consistent with our hypothesis. Meanwhile after either AICAR or metformin treatment the stress fibers of S3 cells exhibited morphological changes. We also found that treating S3 cells with the AMPK

inhibitor, compound C continuously before and during ATP-depletion partially inhibited the activation of AMPK caused by ATP-depletion, and also partially rescued the disruptions of stress fibers caused by ATP-depletion. Therefore our data support the hypothesis that the activation of AMPK is at the upstream of the signaling pathways downregulating RhoA activity during ATP depletion that eventually leads to the actin cytoskeletal disruptions. Further studies will be needed to elucidate the intermediary signaling pathways between AMPK activation and RhoA inactivation during kidney ischemia, which could be via TSC1/2 complex activation and/or Rheb GTPase inactivation leading to mTOR complex 1 kinase activity inhibition.

REFERENCES

1. Sutton TA, Molitoris BA 1998 Mechanism of Cellular Injury in Ischemic Acute Renal Failure *Seminars in Nephrology* 18(5): 490-497

2. Reddi AS *Essential of Renal Physiology* Chapter2 ©1999 by College Book Publishers, L.L.C.

3. Bonventre JV 1993 Mechanisms of Ischemic Acute Renal Failure *Kidney International* 43(5):1160-1178

4. Donohoe JF, Venkatachalam MA, Bernard DB, Levinsky NG 1978 Tubular Leakage and Obstruction after Renal Ischemia: Structural-functional Correlations *Kidney International* 13(3):208-222

5. Venkatachalam MA, Bernard DB, Donohoe JF, Levinsky NG 1978 Ischemic Damage and Repair in the Rat Proximal Tubule: Differences among the S1, S2, and S3 Segments *Kidney International* 14(1):31-49

6. Johnston PA, Rennke H, Levinsky NG 1984 Recovery of Proximal Tubular Function from Ischemic Injury *American Journal of Physiology* 246(2):F159-F166

7. Coudrier E, Kerjaschki D, Louvard D 1988 Cytoskeleton Organization and Submembranous Interactions in Intestinal and Renal Brush Borders *Kidney International* 34(3):309-320

8. Bretscher A 1991 Microfilament Structure and Function in the Cortical Cytoskeleton *Annual Review of Cell Biology* 7:337-74

9. Rodman JS, Mooseker M, Farquhar MG 1986 Cytoskeletal Proteins of the Rat Kidney Proximal Tubule Brush Border *European Journal of Cell Biology* 42(2):319-327

10. Brown D, Stow JL 1996 Protein Trafficking and Polarity in Kidney Epithelium: from Cell Biology to Physiology *Physiological Reviews* 76(1):245-297

11. Kerjaschki D, Noronha-Blob L, Sacktor B, Farquhar MG 1984 Microdomains of Distinctive Glycoprotein Composition in the Kidney Proximal Tubule Brush Border *The Journal of Cell Biology* 98(4):1505-1513

12. Rodman JS, Kerjaschki D, Merisko E, Farquhar MG 1984 Presence of an Extensive Clathrin Coat on the Apical Plasmalemma of the Rat Kidney Proximal Tubule Cell *The Journal of Cell Biology* 98(5):1630-1636

13. Wagner MC, Molitoris BA 1999 Renal Epithelial Polarity in Health and Disease *Pediatric Nephrology* 13(2):163-170

14. Verkman AS, Alpern RJ 1987 Kinetic Transport Model for Cellular Regulation of pH and Solute Concentration in the Renal Proximal Tubule *Biophysical Journal* 51(4):533-546

15. Christensen EI 1976 Rapid Protein Uptake and Digestion in Proximal Tubule Lysosomes *Kidney International* 10(4):301-310

16. Christensen EI 1982 Rapid Membrane Recycling in Renal Proximal Tubule Cells *European Journal of Cell Biology* 29(1):43-49

17. Brown D, Sabolic I, Gluck S 1991 Colchicine-induced Redistribution of Proton Pumps in Kidney Epithelial Cells *Kidney International Supplement* 33:S79-S83

18. Gutmann EJ, Niles JL, McCluskey RT, Brown D 1989 Colchicine-induced Redistribution of an Apical Membrane Glycoprotein (gp330) in Proximal Tubules *American Journal of Physiology* 257(2):C397-C407

19. Gottlieb TA, Ivanov IE, Adesnik M, Sabatini DD 1993 Actin Microfilaments Play a Critical Role in Endocytosis at the Apical but not the Basolateral Surface of Polarized Epithelial Cells *The Journal of Cell Biology* 120(3):695-710
20. Lutz KL, Siahaan TJ 1997 Molecular Structure of the Apical Junction Complex and its Contribution to the Paracellular Barrier *Journal of Pharmaceutical Sciences* 86(9):977-984
21. Clark EA, Brugge JS 1995 Integrins and Signal Transduction Pathways: the Road Taken *Science* 268(5208):233-239
22. Molitoris BA, Hoilien CA, Dahl R, Ahnen DJ, Wilson PD, Kim J 1988 Characterization of Ischemia-induced Loss of Epithelial Polarity *The Journal of Membrane Biology* 106(3):233-242
23. Molitoris BA, Wilson PD, Schrier RW, Simon FR 1985 Ischemia Induces Partial Loss of Surface Membrane Polarity and Accumulation of Putative Calcium Ionophores *The Journal of Clinical Investigation* 76(6):2097-2105
24. Molitoris BA 1991 Ischemia-induced Loss of Epithelial Polarity: Potential Role of the Actin Cytoskeleton *American Journal of Physiology. Renal Physiology* 260(6):F769-F778
25. Venkatachalam MA, Jones DB, Rennke HG, Sandstrom D, Patel Y 1981 Mechanism of Proximal Tubule Brush Border Loss and Regeneration Following Mild Renal Ischemia *Laboratory Investigation* 45(4):355-365
26. Kellerman PS, Clark RA, Hoilien CA, Linas SL, Molitoris BA 1990 Role of Microfilaments in Maintenance of Proximal Tubule Structural and Functional Integrity *American Journal of Physiology. Renal Physiology* 259(2):F279-F285
27. Kellerman PS, Bogusky RT 1992 Microfilament Disruption Occurs Very Early in Ischemic Proximal Tubule Cell Injury *Kidney International* 42(4):896-902
28. Goligorsky MS, Lieberthal W, Racusen L, Simon EE 1993 Integrin Receptors in Renal Tubular Epithelium: New Insights into Pathophysiology of Acute Renal Failure *American Journal of Physiology. Renal Physiology* 264(1):F1-F8
29. Gailit J, Colflesh D, Rabiner I, Simone J, Goligorsky MS 1993 Redistribution and Dysfunction of Integrins in Cultured Renal Epithelial Cells Exposed to Oxidative Stress *American Journal of Physiology. Renal Physiology* 264(1):F149-F157
30. Lieberthal W, McKenney JB, Kiefer CR, Snyder LM, Kroshian VM, Sjaastad MD 1996 β1 Integrin-Mediated Adhesion between Renal Tubular Cells after Anoxic Injury *Journal of the American Society of Nephrology* 8(2):175-183
31. Zuk A, Bonventre JV, Brown D, Matlin KS 1998 Polarity, Integrin, and Extracellular Matrix Dynamics in the Postischemic Rat Kidney *American Journal of Physiology. Cell Physiology* 275(3):C711-C731
32. Molitoris BA, Marrs J 1999 The Role of Cell Adhesion Molecules in Ischemic Acute Renal Failure *The American Journal of Medicine* 106(5):583-592
33. Mandel LJ, Bacallao R, Zampighi G 1993 Uncoupling of the Molecular 'Fence' and Paracellular 'Gate' Functions in Epithelial Tight Junctions *Nature* 361(6412):552-555
34. Atkinson JA, Molitoris BA *Acute Renal Failure: A Companion to Brenner & Rector's the Kidney* Chapter8 © 2001 by W.B. Saunders Company
35. Molitoris BA, Geerdes A, McIntosh JR 1991 Dissociation and Redistribution of Na^+,K^+-ATPase from its Surface Membrane Actin Cytoskeletal Complex during Cellular ATP Depletion *The Journal of Clinical Investigation* 88(2):462-469

36. Atkinson SJ, Hosford MA, Molitoris BA 2004 Mechanism of Actin Polymerization in Cellular ATP Depletion *The Journal of Biological Chemistry* 279(7):5194-5199
37. Gumbiner B 1988 Structure, Biochemistry, and Assembly of Epithelial Tight Junctions *American Journal of Physiology. Cell Physiology* 253(6 Pt 1):C749-C758
38. Molitoris BA, Falk SA, Dahl RH 1989 Ischemia-induced Loss of Epithelial Polarity. Role of the Tight Junction *The Journal of Clinical Investigation* 84(4):1334-1339
39. Rothman JE, Wieland FT 1996 Protein Sorting by Transport Vesicles *Science* 272(5259):227-234
40. Mukherjee S, Ghosh RN, Maxfield FR 1997 Endocytosis *Physiological Reviews* 77(3):759-803
41. Daly RJ 2004 Cortactin Signaling and Dynamic Actin Networks *Biochemical Journal* 382(1):13-25
42. Wu H, Reynolds AB, Kanner SB, Vines RR, Parsons JT 1991 Identification and Characterization of a Novel Cytoskeleton-Associated pp60^{src} Substrate *Molecular and Cellular Biology* 11(10):5113-5124
43. Wu H, Parsons JT 1993 Cortactin, an 80/85-Kilodalton pp60^{src} Substrate, is a Filamentous Actin-binding Protein Enriched in the Cell Cortex *The Journal of Cell Biology* 120(6):1417-1426
44. Du Y, Weed SA, Xiong WC, Marshall TD, Parsons JT 1998 Identification of a Novel Cortactin SH3 Domain-binding Protein and its Localization to Growth Cones of Cultured Neurons *Molecular and Cellular Biology* 18(10):5838-5851
45. Kaksonen M, Peng HB, Rauvala H 2000 Association of Cortactin with Dynamic Actin in Lamellipodia and on Endosomal Vesicles *Journal of Cell Science* 113(24):4421-4426
46. Patel AS, Schechter GL, Wasilenko WJ, Somers KD 1998 Overexpression of EMS1/Cortactin in NIH3T3 Fibroblasts Causes Increased Cell Motility and Invasion *in vivo Oncogene* 16(25):3227-3232
47. Katsube T, Takahisa M, Ueda R, Hashimoto N, Kobayashi M, Togashi S 1998 Cortactin Associates with the Cell-Cell Junction Protein ZO-1 in both *Drosophila* and Mouse *the Journal of Biological Chemistry* 273(45):29672-29677
48. Helwani FM, Kovacs EM, Paterson AD, Verma S, Ali RG, Fanning AS, Weed SA, Yap AS 2004 Cortactin is Necessary for E-cadherin-mediated Contact Formation and Actin Reorganization *the Journal of Cell Biology* 164(6):899-910
49. Cao H, Orth JD, Chen J, Weller SG, Heuser JE, McNiven MA 2003 Cortactin is a Component of Clathrin-coated Pits and Participates in Receptor-mediated Endocytosis *Molecular and Cellular Biology* 23(6):2162-2170
50. Sauvonnet N, Dujeancourt A, Dautry-Varsat A 2005 Cortactin and Dynamin are Required for the Clathrin-independent Endocytosis of γc Cytokine Receptor *the Journal of Cell Biology* 168(1):155-163
51. Zhu J, Zhou K, H J-J, Liu J, Smith N, Zhan X 2005 Regulation of Cortactin/Dynamin Interaction by Actin Polymerization during the Fission of Clathrin-coated Pits *Journal of Cell Science* 118(4):807-817
52. Cao H, Weller S, Orth JD, Chen J, Huang B, Chen JL, Stamnes M, McNiven MA 2005 Actin and Arf1-dependent Recruitment of a Cortactin-dynamin Complex to the Golgi Regulates Post-Golgi Transport *Nature Cell Biology* 7(5):483-492

53. Bougneres L, Girardin SE, Weed SA, Karginov AV, Olivo-Marin JC, Parsons JT, Sansonetti PJ, Van Nhieu GT 2004 Cortactin and Crk Cooperate to trigger Actin Polymerization during *Shigella* Invasion of Epithelial Cells *the Journal of Cell Biology* 166(2):225-235
54. Agerer F, Lux S, Michel A, Rohde M, Ohlsen K, Hauck CR 2005 Cellular Invasion by *Straphylococcus Aureus* Reveals a Functional Link between Focal Adhesion Kinase and Cortactin in Integrin-mediated Internalisation *Journal of Cell Science* 118(10):2189-2200
55. Schuuring E, Verhoeven E, Mooi WJ, Michalides RJ 1992 Identification and Cloning of Two Overexpressed Genes, U21B31/PRAD1 and EMS1, within the Amplified Chromosome 11q13 Region in Human Carcinomas *Oncogene* 7(2):355-361
56. Schuuring E, Verhoeven E, Litvinov S, Michalides RJ 1993 The Product of the EMS1 Gene, Amplified and Overexpressed in Human Carcinomas, is Homologous to a v-*src* Substrate and is Located in Cell-substratum Contact Sites *Molecular and Cellular Biology* 13(5):2891-2898
57. Li Y, Tondravi M, Liu J, Smith E, Haudenschild CC, Kaczmarek M, Zhan X 2001 Cortactin Potentiates Bone Metastasis of Breast Cancer Cells *Cancer Research* 61(18):6906-6911
58. Artym VV, Zhang Y, Seillier-Moiseiwitsch F, Yamada KM, Mueller SC 2006 Dynamic Interactions of Cortactin and Membrane Type 1 Matrix Metalloproteinase at Invadopodia: Defining the Stages of Invadopodia Formation and Function *Cancer Research* 66(6):3034-3043
59. Clark ES, Whigham AS, Yarbrough WG, Weaver AM 2007 Cortactin is an Essential Regulator of Matrix Metalloproteinase Secretion and Extracellular Matrix Degradation in Invadopodia *Cancer Research* 67(9):4227-4235
60. Wu H, Montone KT 1998 Cortactin Localization in Actin-containing Adult and Fetal Tissues *The Journal of Histochemistry and Cytochemistry* 46(10):1189-1191
61. Weed SA, Karginov AV, Schafer DA, Weaver AM, Kinley AW, Cooper JA, Parsons JT 2000 Cortactin Localization to Sites of Actin Assembly in Lamellipodia Requires Interactions with F-Actin and the Arp2/3 Complex *the Journal of Cell Biology* 151(1):29-40
62. Weaver AM, Karginov AV, Kinley AW, Weed SA, Li Y, Parsons JT, Cooper JA 2001 Cortactin Promotes and Stabilizes Arp2/3-induced Actin Filament Network Formation *Current Biology* 11(5):370-374
63. Weaver AM, Heuser JE, Karginov AV, Lee WL, Parsons JT, Cooper JA 2002 Interaction of Cortactin and N-WASP with Arp2/3 Complex *Current Biology* 12(15):1270-1278
64. McNiven MA, Kim L, Krueger EW, Orth JD, Cao H, Wong TW 2000 Regulated Interactions between Dynamin and the Actin-binding Protein Cortactin Modulate Cell Shape *The Journal of Cell Biology* 151(1):187-198
65. Martinez-Quiles N, Ho HY, Kirschner MW, Ramesh N, Geha RS 2004 Erk/Src Phosphorylation of Cortactin Acts as a Switch On-Switch off Mechanism that Controls its Ability to Activate N-WASP *Molecular and Cellular Biology* 24(12):5269-5280
66. Kinley AW, Weed SA, Weaver AM, Karginov AV, Bissonette E, Cooper JA, Parsons JT 2003 Cortactin Interacts with WIP in Regulating Arp2/3 Activation and Membrane Protrusion *Current Biology* 13(5):384-393

67. Huang C, Liu J, Haudenschild CC, Zhan X 1998 The Role of Tyrosine Phosphorylation of Cortactin in the Locomotion of Endothelial Cells *The Journal of Biological Chemistry* 273(40):25770-25776
68. Kim L, Wong TW 1998 Growth Factor-dependent Phosphorylation of the Actin-binding Protein Cortactin is Mediated by the Cytoplasmic Tyrosine Kinase FER *The Journal of Biological Chemistry* 273(36):23542-23548
69. Fan L, Di Ciano-Oliveira C, Weed SA, Craig AW, Greer PA, Rotstein OD, Kapus A 2004 Actin Depolymerization-induced Tyrosine Phosphorylation of Cortactin: the Role of Fer Kinase *The Biochemical Journal* 380(2):581-591
70. Lopez I, Duprez V, Melle J, Dreyfus F, Levy-Toledano S, Fontenay-Roupie M 2001 Thrombopoietin Stimulates Cortactin Translocation to the Cytoskeleton Independently of Tyrosine Phosphorylation *Biochemical Journal* 356(3):875-881
71. Campbell DH, Sutherland RL, Daly RJ 1999 Signaling Pathways and Structural Domains Required for Phosphorylation of EMS1/Cortactin *Cancer Research* 59(20):5376-5385
72. Martin KH, Jeffery ED, Grigera PR, Shabanowitz J, Hunt DF, Parsons JT 2006 Cortactin Phosphorylation Sites Mapped by Mass Spectrometry *Journal of Cell Science* 119(14):2851-2853
73. De Kimpe L, Janssens K, Derua R, Armacki M, Goicoechea S, Otey C, Waelkens E, Vandoninck S, Vandenheede JR, Seufferlein T, Van Lint J 2009 Characterization of Cortactin as an *in vivo* Protein Kinase D Substrate: Interdependence of Sites and Potentiation by Src *Cellular Signalling* 21(2):253-263
74. Head JA, Jiang D, Li M, Zorn LJ, Schaefer EM, Parsons JT, Weed SA 2003 Cortactin Tyrosine Phosphorylation Requires Rac1 Activity and Association with the Cortical Actin Cytoskeleton *Molecular Biology of the Cell* 14(8):3216-3229
75. Illes A, Enyedi B, Tamas P, Balazs A, Bogel G, Buday L 2006 Inducible Phosphorylation of Cortactin is not Necessary for Cortactin-mediated Actin Polymerization *Cell Signalling* 18(6):830-840
76. Huang C, Ni Y, Wang T, Gao Y, Haudenschild CC, Zhan X 1997 Down-regulation of the Filamentous Actin Cross-linking Activity of Cortactin by Src-mediated Tyrosine Phosphorylation *The Journal of Biological Chemistry* 272(21):13911-13915
77. Tehrani S, Tomasevic N, Weed S, Sakowicz R, Cooper JA 2007 Src Phosphorylation of Cortactin Enhances Actin Assembly *PNAS* 104(29):11933-11938
78. Tehrani S, Faccio R, Chandrasekar I, Ross FP, Cooper JA 2006 Cortactin Has an Essential and Specific Role in Osteoclast Actin Assembly *Molecular Biology of the Cell* 17(7):2882-2895
79. Webb BA, Jia L, Eves R, Mal AS 2007 Dissecting the Functional Domain Requirements of Cortactin in Invadopodia Formation *European Journal of Cell Biology* 86(4):189-206
80. Ayala I, Baldassarre M, Giacchetti G, Caldieri G, Tete S, Luini A, Buccione R 2007 Multiple Regulatory Inputs Converge on Cortactin to Control Invadopodia Biogenesis and Extracellular Matrix Degradation *Journal of Cell Science* 121(3):369-378
81. Williams MR, Jonathan C. Markey JC, Doczi MA, Morielli AD 2007 An Essential Role for Cortactin in the Modulation of the Potassium Channel Kv1.2 *PNAS* 104(44): 17412-17417

82. Tian L, McClafferty H, Chen L, Shipston MJ 2008 Reversible Tyrosine Protein Phosphorylation Regulates Large Conductance Voltage- and Calcium-activated Potassium Channels via Cortactin *The Journal of Biological Chemistry* 283(6):3067-3076
83. Zhu J, Yu D, Zeng XC, Zhou K, Zhan X 2007 Receptor-mediated Endocytosis Involves Tyrosine Phosphorylation of Cortactin *The Journal of Biological Chemistry* 282(22):16086-16094
84. El Sayegh TY, Arora PD, Laschinger CA, Lee W, Morrison C, Overall CM, Kapus A, McCulloch CA 2004 Cortactin Associates with N-cadherin Adhesions and Mediates Intercellular Adhesion Strengthening in Fibroblasts *Journal of Cell Science* 117(21): 5117-5131
85. Sayegh TY, Arora PD, Fan L, Laschinger CA, Greer PA, McCulloch CA, Kapus A 2005 Phosphorylation of N-cadherin-associated Cortactin by Fer Kinase Regulates N-cadherin Mobility and Intercellular Adhesion Strength *Molecular Biology of the Cell* 16(12):5514-5527
86. Gopalakrishnan S, Hallett MA, Atkinson SJ, Marrs JA 2007 aPKC-PAR Complex Dysfunction and Tight Junction Disassembly in Renal Epithelial Cells during ATP Depletion *American Journal of Physiology. Cell Physiology* 292(3):C1094-C1102
87. Chen G, Akintola AD, Catania JM, Covington MD, Dean DD, Trzeciakowski JP, Burghardt RC, Parrish AR 2007 Ischemia-induced Cleavage of Cadherins in NRK Cells is not Sufficient for β-catenin Transcriptional Activity *Cell Communication and Adhesion* 14(4):111-123
88. Orth JD, McNiven MA 2003 Dynamin at the Actin-membrane Interface *Current Opinion in Cell Biology* 15(1):31-39
89. Schafer DA, Weed SA, Binns D, Karginov AV, Parsons JT, Cooper JA 2002 Dynamin2 and Cortactin Regulate Actin Assembly and Filament Organization *Current Biology* 12(21):1852-1857
90. Hinshaw JE 2000 Dynamin and its Role in Membrane Fission *Annual Review of Cell and Developmental Biology* 16:483-519
91. McNiven MA, Cao H, Pitts KR, Yoon Y 2000 The Dynamin Family of Mechanoenzymes Pinching in New Places *Trends in Biochemical Sciences* 25(3):115-120
92. Shpetner HS, Vallee RB 1989 Identification of Dynamin, a Novel Mechanochemical Enzyme that Mediates Interaction between Microtubules *Cell* 59(3):421-432
93. van der Bliek AM, Meyerowitz EM 1991 Dynamin-like Protein Encoded by the *Drosophila Shibire* Gene Associated with Vesicular Traffic *Nature* 351(6325):411-414
94. Obar RA, Collins CA, Hammarback JA, Shpetner HS, Vallee RB 1990 Molecular Cloning of the Microtubule-associated Mechanochemical Enzyme Dynamin Reveals Homology with a New Family of GTP-binding Proteins *Nature* 347(6290):256-261
95. van der Bliek AM, Redelmeier TE, Damke H, Tisdale EJ, Meyerowitz EM, Schmid SL 1993 Mutations in Human Dynamin Block an Intermediate Stage in Coated Vesicle Formation *The Journal of Cell Biology* 122(3):553-563
96. Herskovits JS, Burgess CC, Obar RA, Vallee RB 1993 Effects of Mutant Rat Dynamin on Endocytosis *The Journal of Cell Biology* 122(3):565-578
97. Damke H, Baba T, Warnock DE, Schmid SL 1994 Induction of Mutant Dynamin Specifically Blocks Endocytic Coated Vesicle Formation *The Journal of Cell Biology* 127(4):915-934

98. Henley JR, Krueger EW, Oswald BJ, McNiven MA 1998 Dynamin-mediated Internalization of Caveolae *The Journal of Cell Biology* 141(1):85-99
99. Oh P, McIntosh DP, Schnitzer JE 1998 Dynamin at the Neck of Caveolae Mediates their Budding to Form Transport Vesicles by GTP-driven Fission from the Plasma Membrane of Endothelium *The Journal of Cell Biology* 141(1):101-114
100. Gold ES, Underhill DM, Morrissette NS, Guo J, McNiven MA, Aderem A 1999 Dynamin 2 is Required for Phagocytosis in Macrophages *The Journal of Experimental Medicine* 190(12):1849-1856
101. Maier O, Knoblich M, Westermann P 1996 Dynamin II Binds to the Trans-Golgi Network *Biochemical and Biophysical Research Communications* 223(2):229-233
102. Henley JR, McNiven MA 1996 Association of a Dynamin-like Protein with the Golgi Apparatus in Mammalian Cells *The Journal of Cell Biology* 133(4):761-775
103. Llorente A, Rapak A, Schmid SL, van Deurs B, Sandvig K 1998 Expression of Mutant Dynamin Inhibits Toxicity and Transport of Endocytosed Ricin to the Golgi Apparatus *The Journal of Cell Biology* 140(3):553-563
104. Cao H, Thompson HM, Krueger EW, McNiven MA 2000 Disruption of Golgi Structure and Function in Mammalian Cells Expressing a Mutant Dynamin *Journal of Cell Science* 113 (11):1993-2002
105. Kreitzer G, Marmorstein A, Okamoto P, Vallee R, Rodriguez-Boulan E 2000 Kinesin and Dynamin are Required for Post-Golgi Transport of a Plasma-membrane Protein *Nature Cell Biology* 2(2):125-127
106. Schlunck G, Damke H, Kiosses WB, Rusk N, Symons MH, Waterman-Storer CM, Schmid SL, Schwartz MA 2004 Modulation of Rac Localization and Function by Dynamin *Molecular Biology of the Cell* 15(1):256-267
107. Ochoa GC, Slepnev VI, Neff L, Ringstad N, Takei K, Daniell L, Kim W, Cao H, McNiven M, Baron R, De Camilli P 2000 A Functional Link between Dynamin and the Actin Cytoskeleton at Podosomes *The Journal of Cell Biology* 150(2):377-389
108. Baldassarre M, Pompeo A, Beznoussenko G, Castaldi C, Cortellino S, McNiven MA, Luini A, Buccione R 2003 Dynamin Participates in Focal Extracellular Matrix Degradation by Invasive Cells *Molecular Biology of the Cell* 14(3):1074-1084
109. Salim K, Bottomley MJ, Querfurth E, Zvelebil MJ, Gout I, Scaife R, Margolis RL, Gigg R, Smith CI, Driscoll PC, Waterfield MD, Panayotou G 1996 Distinct Specificity in the Recognition of Phosphoinositides by the Pleckstrin Homology Domains of Dynamin and Bruton's Tyrosine Kinase *the EMBO Journal* 15(22):6241-6250
110. Lee CS, Kim IS, Park JB, Lee MN, Lee HY, Suh PG, Ryu SH 2006 The Phox Homology Domain of Phospholipase D Activates Dynamin GTPase Activity and Accelerates EGFR Endocytosis *Nature Cell Biology* 8(5):477-484
111. Warnock DE, Hinshaw JE, Schmid SL 1996 Dynamin Self-assembly Stimulates its GTPase Activity *The Journal of Biological Chemistry* 271(37):22310-22314
112. Hinshaw JE, Schmid SL 1995 Dynamin Self-assembles into Rings Suggesting a Mechanism for Coated Vesicle Budding *Nature* 374(6518):190-192
113. Carr JF, Hinshaw JE 1997 Dynamin Assembles into Spirals under Physiological Salt Conditions upon the Addition of GDP and γ-phosphate Analogues *The Journal of Biological Chemistry* 272(44):28030-28035
114. Sweitzer SM, Hinshaw JE 1998 Dynamin Undergoes a GTP-dependent Conformational Change Causing Vesiculation *Cell* 93(6):1021-1029

115. Klein DE, Lee A, Frank DW, Marks MS, Lemmon MA 1998 The Pleckstrin Homology Domains of Dynamin Isoforms Require Oligomerization for High Affinity Phosphoinositide Binding *The Journal of Biological Chemistry* 273(42):27725-27733
116. Sever S, Muhlberg AB, Schmid SL 1999 Impairment of Dynamin's GAP Domain Stimulates Receptor-mediated Endocytosis *Nature* 398(6727):481-486
117. Foster-Barber A, Bishop JM 1998 Src Interacts with Dynamin and Synapsin in Neuronal Cells *PNAS* 95(8):4673-4677
118. Ahn S, Maudsley S, Luttrell LM, Lefkowitz RJ, Daaka Y 1999 Src-mediated Tyrosine Phosphorylation of Dynamin is Required for β2-Adrenergic Receptor Internalization and Mitogen-activated Protein Kinase Signaling *The Journal of Biological Chemistry* 274(3):1185-1188
119. Werbonat Y, Kleutges N, Jakobs KH, van Koppen CJ 2000 Essential Role of Dynamin in Internalization of M2 Muscarinic Acetylcholine and Angiotensin AT1A Receptors *The Journal of Biological Chemistry* 275(29):21969-21974
120. Shajahan AN, Timblin BK, Sandoval R, Tiruppathi C, Malik AB, Minshall RD 2004 Role of Src-induced Dynamin-2 Phosphorylation in Caveolae-mediated Endocytosis in Endothelial Cells *The Journal of Biological Chemistry* 279(19):20392-20400
121. Ahn S, Kim J, Lucaveche CL, Reedy MC, Luttrell LM, Lefkowitz RJ, Daaka Y 2002 Src-dependent Tyrosine Phosphorylation Regulates Dynamin Self-assembly and Ligand-induced Endocytosis of the Epidermal Growth Factor Receptor *The Journal of Biological Chemistry* 277(29):26642-26651
122. Hinshaw DB, Armstrong BC, Burger JM, Beals TF, Hyslop PA 1988 ATP and Microfilaments in Cellular Oxidant Injury *The American Journal of Pathology* 132(3):479-488
123. Bernstein BW, Chen H, Boyle JA, Bamburg JR 2006 Formation of Actin-ADF/cofilin Rods Transiently Retards Decline of Mitochondrial Potential and ATP in Stressed Neurons *American Journal of Physiology. Cell Physiology* 291(5):C828-C839.
124. Kobryn CE, Mandel LJ 1994 Decreased Protein Phosphorylation Induced by Anoxia in Proximal Renal Tubules *American Journal of Physiology. Cell Physiology* 267(4):C1073-C1079
125. Corton J M, Gillespie JG, Hardie DG 1994 Role of the AMP-activated Protein Kinase in the Cellular Stress Response *Current Biology* 4(4):315-324
126. Jaffe AB, Hall A 2005 Rho GTPases: Biochemistry and Biology *Annual Review of Cell and Developmental Biology* 21:247-269
127. Heasman SJ, Ridley AJ 2008 Mammalian Rho GTPases: New Insights into Their Functions from *in vivo* Studies *Nature Reviews Molecular Cell Biology* 9(9):690-701
128. Kroschewski R, Hall A, Mellman I 1999 Cdc42 Controls Secretory and Endocytic Transport to the Basolateral Plasma Membrane of MDCK Cells *Nature Cell Biology* 1(1):8-13
129. Hallett MA, Dagher PC, Atkinson SJ 2003 Rho GTPases Show Differential Sensitivity to Nucleotide Triphosphate Depletion in a Model of Ischemic Cell Injury *American Journal of Physiology. Cell Physiology* 285(1):C129-C138
130. Raman N, Atkinson SJ 1999 Rho Controls Actin Cytoskeletal Assembly in Renal Epithelial Cells during ATP Depletion and Recovery *American Journal of Physiology* 276(6):C1312-C1324.

131. Gopalakrishnan S, Hallett MA, Atkinson SJ, Marrs JA 2003 Differential Regulation of Junctional Complex Assembly in Renal Epithelial Cell Line *American Journal of Physiology. Cell Physiology* 285(1):C102-C111
132. Gopalakrishnan S, Raman N, Atkinson SJ, Marrs JA 1998 Rho GTPase Signaling Regulates Tight Junction Assembly and Protects Tight Junctions during ATP Depletion *American Journal of Physiology* 275(3):C798-C809
133. Zhang L, Young LH, Caplan MJ 2006 AMP-activated Protein Kinase Regulates the Assembly of Epithelial Tight Junctions *PNAS* 103(46):17272-17277
134. Zheng B, Cantley LC 2007 Regulation of Epithelial Tight Junction Assembly and Disassembly by AMP-activated Protein Kinase *PNAS* 104(3):819-822
135. Lee JH, Koh H, Kim M, Kim Y, Lee SY, Karess RE, Lee SH, Shong M, Kim JM, Kim J, Chung J 2007 Energy-dependent Regulation of Cell Structure by AMP-activated Protein Kinase *Nature* 447(7147):1017-1020
136. Hardie DG, Carling D, Sim AT 1989 The AMP-activated Protein Kinase: a Multisubstrate Regulator of Lipid Metabolism *Trends in Biochemical Sciences* 14(1):20-23
137. Hawley SA, Davison M, Woods A, Davies SP, Beri RK, Carling D, Hardie DG 1996 Characterization of the AMP-activated Protein Kinase Kinase from Rat Liver and Identification of Threonine 172 as the Major Site at which It Phosphorylates AMP-activated Protein Kinase *The Journal of Biological Chemistry* 271(44):27879-27887
138. Sanders MJ, Grondin PO, Hegarty BD, Snowden MA, Carling D 2007 Investigating the Mechanism for AMP Activation of the AMP-activated Protein Kinase Cascade *The Biochemical Journal* 403(1):139-148
139. Davies SP, Helps NR, Cohen PT, Hardie DG 1995 5'-AMP Inhibits Dephosphorylation, as well as Promoting Phosphorylation, of the AMP-activated Protein Kinase. Studies Using Bacterially Expressed Human Protein Phosphatase-2Cα and Native Bovine Protein Phosphatase-$2A_C$ *FEBS Letters* 377(3):421-425
140. Hardie DG 2007 AMP-activated/SNF1 Protein Kinases: Conserved Guardians of Cellular Energy *Nature Reviews Molecular Cell Biology* 8(10):774-785
141. Inoki K, Zhu T, Guan KL 2003 TSC2 Mediates Cellular Energy Response to Control Cell Growth and Survival *Cell* 115(5):577-590
142. Tee AR, Manning BD, Roux PP, Cantley LC, Blenis J 2003 Tuberous Sclerosis Complex Gene Products, Tuberin and Hamartin, Control mTOR Signaling by Acting as a GTPase-activating Protein Complex toward Rheb *Current Biology* 13(15):1259-1268
143. Long X, Lin Y, Ortiz-Vega S, Yonezawa K, Avruch J 2005 Rheb Binds and Regulates the mTOR kinase *Current Biology* 15(8):702-713
144. Gwinn DM, Shackelford DB, Egan DF, Mihaylova MM, Mery A, Vasquez DS, Turk BE, Shaw RJ 2008 AMPK Phosphorylation of Raptor Mediates a Metabolic Checkpoint *Molecular Cell* 30(2):214-226
145. Heitman J, Movva NR, Hall MN 1991 Targets for Cell Cycle Arrest by the Immunosuppressant Rapamycin in Yeast *Science* 253(5022):905-909
146. Kunz J, Henriquez R, Schneider U, Deuter-Reinhard M, Movva NR, Hall MN 1993 Target of Rapamycin in Yeast, TOR2, is an Essential Phosphatidylinositol Kinase Homolog Required for G1 Progression *Cell* 73(3):585-596
147. Yang Q, Guan KL 2007 Expanding mTOR Signaling *Cell Research* 17(8):666-681

148. Averous J, Proud CG 2006 When Translation Meets Transformation: the mTOR Story *Oncogene* 25(48):6423-6435
149. Sarbassov DD, Ali SM, Sengupta S, Sheen JH, Hsu PP, Bagley AF, Markhard AL, Sabatini DM 2006 Prolonged Rapamycin Treatment Inhibits mTORC2 Assembly and Akt/PKB *Molecular Cell* 22(2):159-168
150. Sarbassov DD, Ali SM, Kim DH, Guertin DA, Latek RR, Erdjument-Bromage H, Tempst P, Sabatini DM 2004 Rictor, a Novel Binding Partner of mTOR, Defines a Rapamycin-insensitive and Raptor-independent Pathway that Regulates the Cytoskeleton *Current Biology* 14(14):1296-1302
151. Jacinto E, Loewith R, Schmidt A, Lin S, Rüegg MA, Hall A, Hall MN 2004 Mammalian TOR Complex 2 Controls the Actin Cytoskeleton and is Rapamycin Insensitive *Nature Cell biology* 6(11):1122-1128
152. Liu L, Li F, Cardelli JA, Martin KA, Blenis J, Huang S 2006 Rapamycin Inhibits Cell Motility by Suppression of mTOR-mediated S6K1 and 4E-BP1 Pathways *Oncogene* 25(53):7029-7040
153. Liu L, Chen L, Chung J, Huang S 2008 Rapamycin Inhibits F-actin Reorganization and Phosphorylation of Focal Adhesion Proteins *Oncogene* 27(37):4998-5010
154. Mount PF, Hill RE, Fraser SA, Levidiotis V, Katsis F, Kemp BE, Power DA 2005 Acute Renal Ischemia Rapidly Activates the Energy Sensor AMPK but does not Increase Phosphorylation of eNOS-Ser1177 *American Journal of Physiology. Cell Physiology* 289(5):F1103-F1115
155. Sekulić A, Hudson CC, Homme JL, Yin P, Otterness DM, Karnitz LM, Abraham RT 2000 A Direct Linkage between the Phosphoinositide 3-kinase-AKT Signaling Pathway and the Mammalian Target of Rapamycin in Mitogen-stimulated and Transformed Cells *Cancer Research* 60(13):3504-3513
156. Sullivan JE, Brocklehurst KJ, Marley AE, Carey F, Carling D, Beri RK 1994 Inhibition of Lipolysis and Lipogenesis in Isolated Rat Adipocytes with AICAR, a Cell-permeable Activator of AMP-activated Protein Kinase *FEBS Letters* 353(1):33-36
157. Corton JM, Gillespie JG, Hawley SA, Hardie DG 1995 5-aminoimidazole-4-carboxamide Ribonucleoside. A Specific Method for Activating AMP-activated Protein Kinase in Intact Cells? *European Journal of Biochemistry* 229(2):558-565
158. Zhou G, Myers R, Li Y, Chen Y, Shen X, Fenyk-Melody J, Wu M, Ventre J, Doebber T, Fujii N, Musi N, Hirshman MF, Goodyear LJ, Moller DE 2001 Role of AMP-activated Protein Kinase in Mechanism of Metformin Action *The Journal of Clinical Investigation* 108(8):1167-1174
159. Fryer LG, Parbu-Patel A, Carling D 2002 Protein Kinase Inhibitors Block the Stimulation of the AMP-activated Protein Kinase by 5-amino-4-imidazolecarboxamide Riboside *FEBS Letters* 531(2):189-192
160. Zhang B, Zhang Y, Wang Z, Zheng Y 2000 The Role of Mg^{2+} Cofactor in the Guanine Nucleotide Exchange and GTP Hydrolysis Reactions of Rho Family GTP-binding Proteins *The Journal of Biological Chemistry* 275(33):25299-25307
161. Zhang L, He H, Balschi JA 2007 Metformin and Phenformin Activate AMP-activated Protein Kinase in the Heart by Increasing Cytosolic AMP Concentration *American Journal of Physiology. Heart and Circulatory Physiology* 293(1):H457-H466

162. Lee YM, Lee JO, Jung JH, Kim JH, Park SH, Park JM, Kim EK, Suh PG, Kim HS 2008 Retinoic Acid Leads to Cytoskeletal Rearrangement through AMPK-Rac1 and Stimulates Glucose Uptake through AMPK-p38 MAPK in Skeletal Muscle Cells *the Journal of Biological Chemistry* 283(49):33969-33974
163. Goncharova E, Goncharov D, Noonan D, Krymskaya VP 2004 TSC2 Modulates Actin Cytoskeleton and Focal Adhesion through TSC1-binding Domain and the Rac1 GTPase t*he Journal of Cell Biology* 167(6):1171-1182
164. Huang J, Dibble CC, Matsuzaki M, Manning BD 2008 The TSC1-TSC2 Complex is Required for Proper Activation of mTOR Complex 2 *Molecular and Cellular Biology* 28(12):4104-4115
165. Sarbassov DD, Guertin DA, Ali SM, Sabatini DM 2005 Phosphorylation and Regulation of Akt/PKB by the Rictor-mTOR Complex *Science* 307(5712):1098-1101
166. Bayascas JR, Alessi DR 2005 Regulation of Akt/PKB Ser473 Phosphorylation *Molecular Cell* 18(2):143-145
167. Kovacina KS, Park GY, Bae SS, Guzzetta AW, Schaefer E, Birnbaum MJ, Roth RA 2003 Identification of a Proline-rich Akt Substrate as a 14-3-3 Binding Partner *the Journal of Biological Chemistry* 278(12):10189-10194
168. Wang L, Harris TE, Roth RA, Lawrence JC Jr 2007 PRAS40 Regulates mTORC1 Kinase Activity by Functioning as a Direct Inhibitor of Substrate Binding *the Journal of Biological Chemistry* 282(27):20036-20044

CURRICULUM VITAE

Hao Zhang

Education:

1991 - 1995	Bachelor of Science Biochemical Engineering East China University of Science and Technology Shanghai, People's Republic of China
2002 - 2009	Doctor of Philosophy Biochemistry and Molecular Biology Indiana University Indianapolis, Indiana, U.S.A.

Honors, Awards, Memberships:

2008, 2009	Member of the American Society for Cell Biology

Research and Training Experience:

May 1996 - Jun. 1996	Completion of QA engineer training course with a QA engineer certificate from Shanghai Bureau of Drug Administration Shanghai, People's Republic of China
Oct. 2000 – May 2001	Participation in the human genome sequencing project Chinese National Human Genome Centre at Shanghai Shanghai, People's Republic of China

May 2001 - Apr. 2002 Participation in the research project of SNPs associated with human essential hypertension
Chinese National Human Genome Centre at Shanghai
Shanghai, People's Republic of China

Professional Experience:

Jul. 1995 - Nov. 1996 Process Engineer in QA Department
Shanghai Tongren Pharmaceuticals Co., Ltd.
Shanghai, People's Republic of China

Nov. 1996 - May 1997 Shift Supervisor in Spinning Section of Operations Department
DuPont Fibers (China), Ltd.
Shanghai, People's Republic of China

Nov. 1997 - Feb. 1999 Quality Engineer & Production Engineer
Production Department
Shanghai Danone Biscuits Co., Ltd.
Shanghai, People's Republic of China

Feb. 1999 - May 1999 Asset Leader
Facial Tissue Section of Converting Department
Shanghai Kimberly-Clark Papers Co., Ltd.
Shanghai, People's Republic of China

Sep. 1999 - Apr. 2000 Product Representative
Shanghai BMH Instruments Co., Ltd.
Shanghai, People's Republic of China

Oct. 2000 - May 2002	Research Intern & Research Assistant in Division of Genetics
	Chinese National Human Genome Centre at Shanghai
	Shanghai, People's Republic of China

Conferences Attended:

Dec. 2008	Poster Presented at
	Annual meeting of the American Society for Cell Biology

Publications:

1. Decrease of Cortactin Tyrosine Phosphorylation during ATP-Depletion in a Cell Culture Model of Ischemic Renal Injury and Its Effect on Cortactin's Cellular Function (In Preparation)

2. AMP-Activated Protein Kinase is an Upstream Regulator of Rho GTPases Activity and Cytoskeletal Organization during ATP-Depletion in a Cell Culture Model of Ischemic Renal Injury (In Preparation)